LAPPEENRANTA-LAHTI UNIVERSITY OF TECHNOLOGY LUT
School of Energy Systems
Degree Programme in Electrical Engineering

Vesa Mäki

FEASIBILITY EVALUATION OF LPWAN TECHNOLOGIES – CASE STUDY FOR A WEATHER STATION

Examiners: Associate Professor, D.Sc. (Tech.) Pedro Juliano Nardelli
Junior Researcher, M.Sc. Dick Carrillo Melgarejo

Supervisors: SW Manager Panu Kilponen

TIIVISTELMÄ

Lappeenrannan-Lahden teknillinen yliopisto LUT
School of Energy Systems
Sähkötekniikan koulutusohjelma

Vesa Mäki

Feasibility Evaluation of LPWAN Technologies – Case Study for a Weather Station
Diplomityö
2021

135 sivua, 31 kuvaa, 32 taulukkoa, 3 liitettä
Työn tarkastajat: Apulaisprofessori, TkT. Pedro Juliano Nardelli
Nuorempi tutkija, DI. Dick Carrillo Melgarejo
Hakusanat: NB-IoT, LoRaWAN, TS-UNB, Telegram Splitting, LPWAN, Sääasema

Tämän työn tarkoitus on arvioda langattomien tiedonsiirtoteknologioiden soveltuvuutta sääasemille. Työssä esitellään käyttötapauksena Vaisalan sääasema, sekä siihen liittyvät vaatimukset ja arvioitavat tekijät ja osa-alueet. Lisäksi esitellään arvioinnin kohteena olevat langattomat teknologiat ja argumentoidaan niiden valinta. Jokainen teknologia esitellään tarkemmin niin syvällisesti kuin soveltuvuusarvion tekijäosa-alueiden analysointi vaatii. Soveltuvuustekijöitä ovat kantama, lähetysintervalli, tiedonsiirtonopeus, energian kulutus ja kustannukset. Jokaisen soveltuvuus arvioidaan joko itsenäisesti, tai jatkona edellisille tekijöille, sisältäen laskennat, mallinnukset ja simulaatiot. Lopulta esitellään tekijäkohtaiset tulokset ja teknologioiden soveltuvuus arvioidaan käyttötavan vaatimuksia vastaan sekä luokittelemalla ne arvojärjestykseen havaitun suorituskyvyn mukaan. Lopullisena tuloksena todetaan, että NB-IoT on kandidaateista soveltuvin teknologia sääaseman käyttötapaukselle.

ABSTRACT

Lappeenranta-Lahti University of Technology LUT
School of Energy Systems
Degree Programme in Electrical Engineering

Vesa Mäki

Feasibility Evaluation of LPWAN Technologies – Case Study for a Weather Station
Master's Thesis
2021

135 pages, 31 figures, 32 tables, 3 appendices
Examiners: Associate Professor, D.Sc. (Tech.) Pedro Juliano Nardelli
Junior Researcher, M.Sc. Dick Carrillo Melgarejo
Keywords: NB-IoT, LoRaWAN, TS-UNB, Telegram Splitting, LPWAN, Weather Station

The purpose of this work is to evaluate the feasibility of wireless transmission technologies for weather stations. A use-case was presented and related requirements and factors to be evaluated in the study were defined in accordance to a weather station model from Vaisala. The evaluated technologies were chosen based on their functionality, which was presented to the degree needed to evaluate against feasibility factors. The evaluated factors are coverage, message interval, data rate, energy consumption and cost. The evaluation was performed independently or as continuation to preceding factors, and included performing calculations, models, and simulations. Finally, numerical results were presented, and the feasibility of different options was evaluated in respect to their applicability to requirements and ranking of observed performance. The work finally concludes that NB-IoT is chosen as the most feasible technology for the use-case of a Vaisala weather station.

PREFACE

This work was commissioned by Vaisala Oyj and was conducted during the second half of 2020 and the first half of 2021, the two years marked in history with the Covid-19 pandemic. For me, this was the "remote Thesis", a heavy mental burden I was to face mostly in the solitary confines of social distancing imposed by the pandemic.

I want to thank everyone who supported me through all the small video frames and chat box windows on my screen, as well as through the audio of my headphones. Big thanks to my thesis supervisor Ass. Professor Pedro Nardelli at LUT University, technical supervisor Panu Kilponen at Vaisala, and especially to Junior Researcher Dick Carrillo Melgarejo at LUT University. Many thanks to all other colleagues at Vaisala, who contributed their time and keyboards in answering my questions.

Special thanks to my line managers Sabit Nasretdin and Hannu Valo at Vaisala for allowing me this thesis opportunity and your flexibility when I overshot the deadline.

Lastly, I want to thank my wife Piia for the unwavering support and patience throughout this effort and all my studies. Without you I would not be on this road.

TABLE OF CONTENTS

Appendix 1 Comparison table of wireless technologies

Appendix 2 Link to original calculations and simulations

Appendix 3 Summary of feasibility evaluation

LIST OF FIGURES

LIST OF TABLES

LIST OF ABBREVIATIONS

2G	Second Generation
3G	Third Generation
4G	Fourth Generation
5G	Fifth Generation
ACK	Acknowledgement
ADR	Adaptive Data Rate
APL	Allowed Path Loss
ARQ	Automatic Repeat Request
AWGN	Additive White Gaussian Noise
BDU	Burst Data Unit
BER	Bit-Error Rate
BLER	Block Error Rate
BPSK	Binary Phase Shift Keying
CDMA	Code Division Multiple Access
C-DRX	Connected-mode DRX
CE	Coverage Extension
C-eDRX	Connected-mode enhanced DRX
CMAC	Cipher-based Message Authentication Code
CoAP	Constrained Application Protocol
CR	Code Rate
CRC	Cyclic Redundancy Check
CSS	Chirp Spread Spectrum
dB	Desibel
DC	Duty cycle
DCI	Downlink Control Indicator
DL	Downlink
DMRS	Demodulation Reference Signal
DNS	Domain Name System
DR	Data Rate

DRX	Discontinuous reception
DSSS	Direct-sequence Spread Spectrum
DTLS	Datagram Transport Layer Security
ECC	Error-Correcting Code
EIRP	Equivalent Isotropically Radiated Power
eNB	E-UTRAN Node B, also Evolved Node B
ETSI	European Telecommunications Standards Institute
E-UTRAN	Evolved Universal Terrestrial Radio Access Network
FCC	Federal Communications Commission
FEC	Forward Error Coding
FSPL	Free Space Path Loss
GFSK	Gaussian Frequency-Shift Keying
GMSK	Gaussian MSK
GSM	Global System for Mobile
H2M	Human-to-Machine
HARQ	Hybrid ARQ
HDR	Header
H-RF	Hyper Radio Frame
HTTP	Hypertext Transfer Protocol
Hz	Hertz
I-DRX	Idle-mode DRX
I-eDRX	Idle-mode enhance DRX
IEEE	Institute of Electrical and Electronics Engineers
IoT	Internet-of-Things
IPv4 / -6	Internet Protocol version 4 / 6
LCC	Life-Cycle Cost
LoRa	Long Range
LPWAN	Low-Power Wide Area Network
LTE	Long Term Evolution
LTE-M	LTE-MTC
LwM2M	Lightweight M2M

M2M	Machine-to-Machine
MAC	Media Access
MCL	Maximum Coupling Loss
MCS	Modulation and Coding Scheme
MIB	Master Information Block
mMTC	massive Machine-Type-Connections
MPF	MAC-payload Format
MPL	Maximum Path Loss
MSK	Minimum Shift Keying
MTBF	Mean Time Between Failures
NB-IoT	Narrowband-IoT
NF	Noise Figure
NPBCH	Narrowband Physical Broadcast Channel
NPDCCH	Narrowband Physical Downlink Control Channel
NPDSCH	Narrowband Physical Downlink Shared Channel
NPRACH	Narrowband Physical Random Access Channel
NPSS	Narrowband Primary Synchronization Signal
NPUSCH	Narrowband Physical Uplink Shared Channel
NRS	Narrowband Reference Signal
NSSS	Narrowband Secondary Synchronization Signal
NTP	Network Time Protocol
OaT	On-air Time
OFDMA	Orthogonal Frequency Division Multiple Access
OS	Operating System
OVH	Overhead
P1	Profile 1
P2	Profile 2
PDCP	Packet Data Convergence Protocol
PDU	Protocol Data Unit
PER	Packet Error Rate
PF	Paging Frame

PH	Paging H-RF
PHR	Power Head Room
PHY	Physical
PL	Path Loss
PLD	Payload
PO	Paging Occasion
PSM	Power Saving Mode
PTW	Paging Time Window
QCI	Quality Class Indicator
QoS	Quality-of-Service
QPSK	Quadrature Phase Shift Keying
RAI	Release Assistance Indicator
RB	Radio Burst
RF	Radio Frame, Radio Frequency
RLC	Radio Link Control
ROHC	Robust Header Compression
RRC	Radio Resource Control
RU	Resource Unit
RX	Reception
S1	Scenario 1
S2	Scenario 2
SC	Subcarrier
SC-FDMA	Single Carrier – Frequency Division Multiple Access
SCS	Subcarrier spacing
SDU	Service Data Unit
SF	Spreading Factor, Subframe
SIR	Signal-to-Interference-Ratio
SNR	Signal-to-Noise-Ratio
TAU	Tracking Area Update
TB(S)	Transport Block (Size)
TBCC	Tail Biting Convolutional Coding

TCP/IP	Transmission Control Protocol / Internet Protocol
TLS	Transport Layer Security
TS	Technical Specification
TSMA	Telegram Splitting Multiple Access
TS-UNB	Telegram Splitting Ultra Narrow Band
TX	Transmission
UDP	User Datagrap Protocol
UL	Uplink
WLAN	Wireless Local Area Network
WPAN	Wireless Personal Area Network

LIST OF SYMBOLS

Δt	Symbol duration
β	Hata/COST 231 model fitting coefficient
λ	Wave length, constant failure rate
τ	Failure rate
$a(x)$	Hata/COST 231 model environment fitting parameter
B	Bandwidth
B_{SC}	Subcarrier bandwidth
c	Speed of light
C	Capacity
C_{bat}	Battery capacity
C_{BS}	Cost of base station
C_{BSkit}	Cost of base station installation hardware kit
C_{BSsub}	Cost of base station data plan per MB
C_{item}	Cost item
C_{mod}	Cost of module
C_{Mrent}	Cost of mast rent
C_{msub}	Cost of module data plan per MB
C_{work}	Cost of labor
CR_{ind}	Code Rate index
d	Distance
$D_{L(i)}$	Data at layer of index i
d_{km}	Distance in kilometers
E	Energy
E_B	Bit energy
$E_{byte}^{D_{L(i)}}$	Energy per byte of data
E_{total}^{module}	Total energy consumption of module
f_C	Carrier frequency
F_{total}	Expected number of failed devices

G_{RX}	Gain of receiving antenna
G_{TX}	Gain of transmitting antenna
h_{RX}	Effective height of receiving antenna
h_{TX}	Effective height of transmitting antenna
i	Index
I	Current
i_{SF}	Resource assignment index
i_{MCS}	MCS indication
i_{PO}	PO subframe index
i_{Rep}	Repetition index
i_{RU}	RU index
i_{SC}	Subcarrier index
i_{TBS}	Transport Block Size index
k	Boltzmann's constant
L_{AP}	Antenna pointing loss
L_{bat}	Battery lifetime
L_{Body}	Body loss
L_C	Cable loss
LCC_{decom}	Decommissioning component of LCCs
LCC_{depl}	Deploying component of LCCs
$LCC_{S1-P1/2}^{LoRaWAN/TS-UNB}$	LCC for LoRaWAN or TS-UNB for S1 with P1 or P2
$LCC_{S2-P2}^{LoRaWAN/TS-UNB}$	LCC for LoRaWAN or TS-UNB for S2 with P2
LCC_{maint}	Maintaining component of LCCs
LCC_{oper}	Operating component of LCCs
LCC_{pur}	Purchasing component of LCCs
$LCC_{S1-P1/2}^{NB-IoT}$	LCC of NB-IoT for S1 with P1 or P2
LCC_{total}	Total LCC
L_i	Layer hierarchy index
L_k	Loss by index k
L_{Pen}	Penetration loss

L_{Total}	Total losses
m	Number of base stations
M_I	Interference margin
M_{SCF}	Small scale fading margin
M_{SF}	Shadow fading margin
M_{Total}	Total margin
n	Number of modules
N	Noise power
N_0	Noise power spectral density
n_{IeDRX}	Number of I-eDRX cycles
n_{IDRX}	Number of I-DRX cycles
$n_{payload}$	Number of payload symbols
$n_{preamble}$	Preamble lenght
$n_{RB,core}$	Number of RBs in core frame
$n_{RB,ext}$	Number of RBs in extension frame
n_{Rep}	Number of repetitions
n_{RU}	Number of RUs
n_{SC}^{RU}	Number of allocated subcarriers to RU
n_{SF}	Number of subframes
n_{slots}^{UL}	Number of slots in uplink
n_{symb}^{UL}	Number of symbols per slot in uplink
p	Pattern number
P	Power
P_{avg}^{device}	Average power consumption by end-device
P_{avg}^{module}	Average power consumption by module
$P_{avg}^{charging}$	Average charging power
P_{Idle}	Power consumed in Idle-state
$PL_{Open}^{Hata/COST\ 231}$	Path Loss in Hata/COST 231 Open/rural model
$PL_{Suburban}^{Hata/COST\ 231}$	Path Loss in Hata/COST 231 Suburban model

$PL_{Urban}^{Hata/COST\ 231}$	Path Loss in Hata/COST 231 Urban model
P_{PSM}	Power consumed in PSM-state
P_{RX}	Power consumed in RX-state
$P_{RX,min}$	Receiver sensitivity
P_{sd}^{bat}	Battery self-discharge power
P_{Sleep}	Power consumed in Sleep-state
P_{TX}	Power consumed in TX-state
Q_m	Modulation order
R_b	Bitrate
$R_{PeakPhy}$	Peak physical data rate
R_s	Symbol rate
s	RB index
S	Signal power
SF_{bat}	Battery safety factor
SNR_c	SNR after combining repeated transmissions
SNR_{reqd}	SNR threshold to reach defined reliability target
t	Time
T	Temperature
t_{3324}	Active Timer
t_{3412}	TAU Timer
t_b	Bit time
t_{core}	Core frame transmission time
t_{ext}	Extension frame transmission time
t_{Idle}	Time in Idle-state
t_{IDRX}	I-DRX cycle duration
t_{IeDRX}	I-eDRX cycle duration
t_{obs}	Observation period
t_{OFF}	Time between RBs, while not transmitting
t_{PSM}	Time in PSM-state
t_{PW}	Paging Window Timer

t_{RB}	Time between RBs
$t_{RB,avg}$	Average time between RBs
t_{RF}	Full radio frame transmission time
t_{RRC-IA}	RRC Inactivity Timer
t_{RU}	Transmission time or RU
t_{RX}	Time in RX-state
t_{Sleep}	Time in Sleep-state
t_{Total}	Total time of message transmission
t_{TX}	Time in TX-state
U	Voltage

1 INTRODUCTION

Vaisala has a long history in designing weather stations and in utilization of wireless access technologies. Installation locations are sometimes exotic or otherwise out of reach of telecommunication lines, which means that a wireless link may be the only option. In addition to satellite-based systems, for the choice wireless link technology, two categories are available which differ in their use of radio spectrum. The first is cellular technologies, standardized by 3GPP, which operate on licensed spectrum. The second is the many radio technologies operating on unlicensed spectrum, which come based to either an open standard or proprietary technology.

Particularly for the latter category, the last decade has sprung up a multitude of choices along with the rise (or the expectation) of concepts such as Internet of Things (IoT) and Industry 4.0. In the IoT, sensory devices and connectivity is embedded to all the "things" around us in our homes, city streets, cars and even clothing, bringing about an internet where machines talk to machines (M2M). This in a sense is nothing new. M2M communication has existed for decades. The difference is in the volume of information which arises from connecting massive amounts of devices to the internet. With the use management platforms, big data analysis, machine learning and smart algorithms IoT then promises to enable a "smart world". [34; 43]

During the first half of 2010s, it became apparent, that 3GPP and progression of cellular technologies was late to the game of IoT, so to say. At that time, cellular technologies of 2G, 3G and Long Term Evolution (LTE / 4G) where mainly focused to provide connectivity and capability to Human-to-Machine (H2M) type of communications, as in video calls and smartphone web surfing, and not well suitable for the resource constrained small sensors as characterized by the IoT. As a consequence, many new technologies were developed to fill-in that niece, such as Zig-Bee, LoRaWAN, SigFox, TS-UNB and Weightless to name a few. Generally, these were designed from the ground up to cater IoT devices and aim to favor low energy consumption and simple and low-cost hardware design with the expense of data rate and reliability or coverage. [5; 12]

However, IoT covers a wide range of use-cases, and here lies an issue. Due to laws of nature, some use-case requirements are contrary to others. For example, achieving minimal energy consumption with very long communication range and high data rate. Emphasis for one side of a coin means a sacrifice for the other. Because of this fact, most of the current IoT focused wireless technologies are aimed at specific use-cases that come with a set of specific requirements, as stated in [5]. To add to the mix, 3GPP also eventually noticed the IoT, and has since developed new IoT specific cellular technologies under the umbrella of 5G, of which LTE-M, short for LTE-Machine-Type-Connections (LTE-MTC), and Narrowband-IoT (NB-IoT) are currently in adoption. The question thus is: "Which wireless technology is best suited for my use-case?"

1.1 Background

Traditionally, Vaisala's customers for weather stations are national meteorological organizations, research centers, airports and other publicly funded entities, as well as larger corporations. A common factor is the requirement of top tier measurement accuracy, quality, and reliability. On the other hand, another common trait for these customers is that they traditionally are not very avid in hopping on with the latest technology trends but tend to stick to established ones (even until forced to move on due to components reaching end-of-life -status).

Thereof, it is not surprising to find the many weather stations and instruments of this field equipped with serial line output telemetry based on TIA-485/422/232 standards. They are still considered as industry standard output telemetry options, and many customers request support of these "legacy" interfaces. The landscape is changing however, and perhaps due to the media hype around 5G and the IoT during the past decade, a growing voice in the market is asking for modern communication options. The fact that many people increasingly have cheap wirelessly connected smart sensors at their homes may also play a role in shifting attitudes on a personal level.

Wirelessly connected sensors have the advantage of offering greater diversity with regards to installation location, since the location is not bound by the availability of wired

communication medium. Particularly, when coupled with some form of energy harvesting and storage technology. A weather station commonly includes sensor elements, but can additionally act as a base station, to which other sensors connect to from further afield. This is illustrated in the example of Figure 1. Generally, there is more freedom to choose the installation location to get the most accurate and representative measurement. Material and labor costs may be reduced due as no cabling work is required.

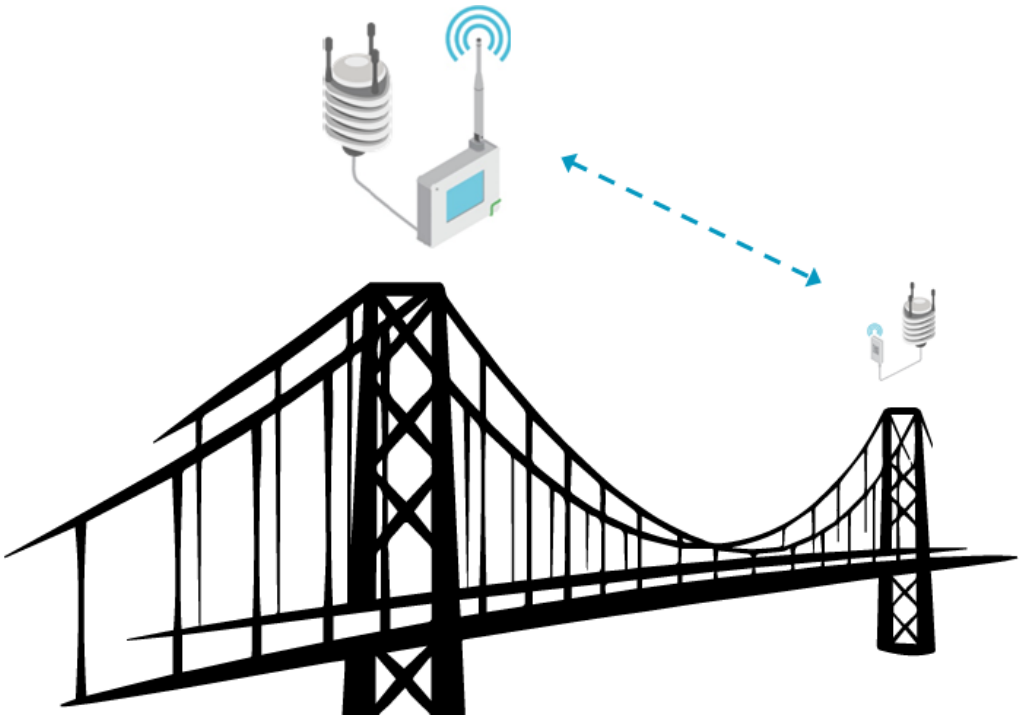

Figure 1. Example weather station use-case setup.

The aspiration is that the weather station would be simple to deploy with freedom to choose a location that is not bound by access to wired communications and mains-power. However, lack of mains power necessitates reliance on batteries and energy harvesting, commonly with solar panels, and imposes a requirement to focus on minimizing energy consumption. Battery operation demands emphasis on the communication technology choice and on the design of the weather station and its communication module to minimize energy consumption to prevent or at least minimize any down time

This background provides the motivation for this work. The purpose of this work is to research the feasibility of a few chosen wireless technologies in the context of a weather station and its specific requirements.

1.2 Regarding Terminology

There are a multitude of different terms used in literature, whilst discussing the area of wireless IoT. Cellular terminology largely comes from 3GPP nomenclature and specifications, which are riddled with abbreviations. In example, common terms as end-device and base station are referred to as User Equipment or eNB. Some terms have also changed over the course of specification evolution, such as NB-IoT and LTE-M. In example, the 3GPP Technical Specification (TS) 36.306 discusses about device categories such as category NB1, which in other specifications, such as TS 36.300, refers to NB-IoT. Commonly, specifications may use different terms, than what industry and marketing use, as is the case with IEEE 802.11 / WiFi. Then there are industry use-case terms, which are sometimes used as umbrellas for multiple technologies. An example being massive MTC (mMTC). As a reaction to this, and in an attempt to introduce clarity, this thesis aims to mention the many terms used for each technology, but use the term most commonly given in academia.

As explained in [3], in telecommunications different functions and behavior of data transactions are governed by sets of rules universally called protocols. They can be thought of as software modules with each performing some specific function, which may be, in example, internet addressing or data encryption. Each protocol has an input interface and an output product, and they are arranged as layers in what is called a protocol stack. At the top is what is called an application layer, and at the bottom is the physical layer where data actually takes the form of ones and zeros on the wire / radio waves. When discussing protocol layers, the layer in question is often referred to as $\boldsymbol{L_{(i)}}$, where $\boldsymbol{i}$ is the layer number starting from one at the physical layer. In layer numbering, this work refers to the TCP/IP protocol layer model.

1.3 Research Questions, Goals and Delimitations

This work sets out to answer the question "*What is the most feasible wireless technology for the use-case of a weather station?*" To get to the bottom of this topic there are many prior questions to answer. Since there are a multitude of different technologies introduced in the industry, both proprietary and open standard, as well established and newly emerging, to keep this report at reasonable length, it is necessary to define which technologies to include in our more detailed analysis. More specifically, the wireless technologies in question here are categorized as Low-Power Wide Area Network (LPWAN) technologies. The choice of technologies in this work is further discussed in Chapter 3.

Generally, this work mainly relies on information and works available in industry and academia. Most analyses presented here base on theory and any derived information through calculation or simulation. No empirical analyses were conducted for any technology by the author but references to empirical results of analyses conducted by others may be given.

It is very difficult or possibly even impossible to do general comparisons between technologies. This is because each tech has their unique behavior (which may be dynamic and beyond user's control), which is heavily affected by the specific use-case. Technologies may also face operational restrictions such as duty cycle and packet size limits.

For example as given in [35], LoRaWAN has maximum supported MAC-payload sizes of 51, 115 and 222 bytes depending on the spreading factor (SF) used. SF is dynamically adjusted based on observed signal conditions. As explained in more detail under Chapter 3.1, NB-IoT on the other hand is not bound by duty cycle limits and has a completely different link adaption scheme and payload limits. Is it fair to make the comparison with a payload the size of 300 Bytes, which would cause fragmentation with LoRaWAN, but not necessarily with NB-IoT? But selecting a smaller payload may not reflect the optimal situation for NB-IoT.

While it may be technically possible to perform direct simulation-based analysis and comparison by fixing enough of the variables involved according to a specific use-case, how

confident can one be on the representativeness of the results to real deployments, because of the highly dynamic behavior and environment? How useful will any information gained for this sort of analysis ultimately be?

Of course, the feasibility of the entire weather station including the communication module is subject to meeting many other requirements, of which one of the greatest is the overall energy consumption. This work limits the focus to the aspects of the communication technology, and purposely does not consider of the device as a complete system, its measurement interval, processing, or other such points. Transmission interval is included in the analysis. In addition, to limit the scope, this work will mainly focus on uplink.

Finally, IoT connectivity is a very broad subject, and the choice wireless communication technology is only a small part of getting data from the IoT device to the end user. This work will concentrate mainly on the physical and data link layers of data communication. Aspects regarding higher layers will only be addressed where appropriate for the reader's convenience, like, in example, for the subject of packet sizes and amount of traffic generated.

1.4 Methodology and Structure of the Thesis

Feasibility can be determined through an evaluation of capabilities versus requirements. Factors to be used in the evaluation must be defined, such as upstream/downstream data rate, range, transmission interval etc. from the use-case requirements. A key sub-topic of interest for this work in conjunction with other capabilities, is the energy consumption characteristics of each wireless technology. Consequently, the work flows on towards an analysis of energy consumption, while defining and setting prerequisite factors along the way. The factors used in this evaluation can mostly be straightforwardly derived numerical values.

The analysis starts with Chapter 2, where the specific use-case at the focus of this study – Vaisala weather station – is defined along with its requirements as factors of feasibility in discrete measurable values.

Chapter 3 covers the wireless technologies analyzed in this work, which identify themselves as IoT specific and low-power/energy. Because the array of technologies in the LPWAN category is relatively large, the author conducted a pre-study and compared technologies by their "data sheet figures" against the use-case requirements. The purpose was to narrow down candidates to three most potential ones for a more detailed analysis in this work. Focus was in an overview of each technology and details of lower layers of the protocol stack, mainly physical (PHY) and media-access (MAC) layers, L1 and L2.

After presenting the technologies, Chapter 4 proceed with the feasibility analysis. Each factor is analyzed consecutively and in a chain-like order, which results from relationships the factors have to each other. Each factor analysis requires making assumptions on values to input parameter and produce results based on those assumptions. Subsequent factors in the relationship chain then use the results for their input parameters, as applicable. This chapter also covers the basic understanding and theoretical basis of each factor, and presents calculations or simulations used to derive results. Any further presumptions or other limitations are also given.

Chapter 5 presents results of each factor's feasibility analysis and discusses the implications of findings individually. Chapter 6 then draws up the findings together for final conclusions on feasibility of each technology for the use-case. Topics of potential and interesting future work are also presented.

2 WEATHER STATION AS A USE-CASE

This chapter introduces three weather station IoT use-case profiles. Use-case for Profile 1 (P1) is for an end-device, which has direct connectivity to a cloud-service. Generally, the message transmitted over the wireless link includes the application payload and full stack protocol overhead, such as IP-addressing, as applicable to the technology. Profile 2 (P2) represents a device, which connects to a local gateway. In example, an auxiliary sensor element connected wirelessly to a larger station. Here the application layer payload is smaller, and the wireless link is burdened only with its inherent protocol overhead. Figure 2 illustrates both use-cases.

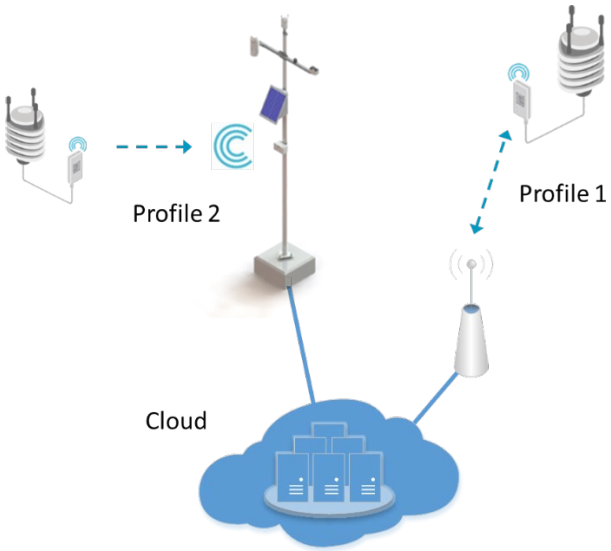

Figure 2. Wireless connectivity use-case representations.

The two profiles feature their own set of requirements, which are presented in more detail in the following subchapters. For each, the weather station only assumes the role of end-device.

The same weather station hardware is assumed in both profiles. As given in the datasheet [57] of the weather station, it is a compact instrument, which provides measurement of multiple weather related parameters: temperature, humidity, air pressure, rainfall, wind speed and direction. Various configurations of the station are offered, as shown in Figure 3, but this case-study expects a hardware configuration with broadest set of measurements.

Figure 3. Various configurations of the weather station. [57]

The following chapters present the weather station use-case further and define its requirements and evaluation factors. For energy consumption and cost factors there is no requirement but are still ranked.

2.1 Message Size and Format

The weather station is highly configurable and has many types of output messages available. In this work we consider two types of messaging. The message type used with P1 is an LwM2M application framework implementation.

In short, LwM2M (abbreviated from lightweight M2M) defines a framework with a protocol stack to enable communication between client and server. As a framework, it also includes various supporting services (interfaces), such as device bootstrapping, client registration, device management and information reporting. It is optimized to be used with resource constrained IoT devices and minimizes overhead data through the use of a protocol called Constrained Application Protocol (CoAP). CoAP may be described as a simplified version of Hypertext Transfer Protocol (HTTP). A CoAP header is only 4 bytes and it is usually used over User Datagram Protocol (UDP), while supporting Datagram Transport Layer Security (DTLS). [33]

The LwM2M-message amounts to about 1 KB in size for the weather station. In this work LwM2M application framework is assumed to use CoAP with UDP and DTLS encryption. Further, technology specific lower layer headering (from L1 to L3) must be added to get the total figure for frame size. For LwM2M they are approximated in Table 1 down to the network layer.

Table 1. LwM2M protocol stack overhead down to network-layer.

Layer		**LwM2M Size [Byte]**
Application	L5	1000
Transfer		CoAP: 4
Transport	L4	DTLS: 13
		UDP: 8
Network	L3	IPv4/-6: 20/40
Total		1045

For P2 the message is based on a commonly used lightweight ASCII string message, called composite message. For example:

1R0,Dm=169D,Sm=0.9M,Ta=16.0C,Ua=81.3P,Pa=1005.5H,Rc=40.15M,Ri=0.0M,Hc=0.0M,Hi=0.0M,Th=16.3C,Vh=25.6N<CR><LF>

The composite message amounts to 102 characters (and 102 Bytes), where both carriage-return <*CR*> and linefeed <*LF*> signify one character each. For P2, it is assumed that L4 headering is included (without DTLS), amounting to at least 110 Bytes in total. Whether L3 headering is included with either profile message depends on the technology.

2.2 Transmission Intervals

The weather station can be individually configured for different measurement and transmission intervals. The configuration options are presented in detail in the User's Guide [58]. This case-study uses four different transmission intervals: 3 seconds, 15 seconds, 1

minute and 10 minute. These figures are selected to reflect the most common reporting intervals among customers by Vaisala's experience as a manufacturer of weather stations. The interval of 3 seconds is required for support of wind gust reporting.

2.3 Data Rate

According to measurements at Vaisala, an end-device for Profile 1 transmits approximately 743374 Bytes and receives 10602 Bytes over a period of 2717 seconds for observation transmission interval of 60 seconds. This consists of about 45 observation data packets plus general network overhead of Network Time Protocol (NTP) and Domain Name System (DNS) -queries, broadcasts and the like. These values provide approximations of the generated data volumes and may be used as requirements for the MAC-layer data rate. Extrapolated rate requirements for both profiles are recorded in Table 2. Similarly, Table 3 gives the monthly cumulative amount of data generated. With P2, MAC-layer data rate requirement are taken directly from the payload size defined in the previous chapter and transmit intervals.

Table 2. Uplink MAC-layer data rate requirements.

Interval	**Data rate (bps)**	
	P1	**P2**
3 seconds	1555.4	293.3
15 seconds	311.1	58.7
60 seconds	77.8	14.7
600 seconds	7.8	1.5

It should be noted, that the derived values for 3, 15 and 600 second intervals are biased due to linear scaling of network overhead included in the measurement. For 3 and 15 second intervals the portion of overhead is overemphasized, while for 600 second interval the portion is underemphasized. Unfortunately, the ratio between payload data and overhead is not known for the measurements to allow estimation of compensation factor. For

technologies, which include no L3 headering in their message, the values are also further slightly overemphasized.

Table 3. Generated monthly cumulative data in MB per month.

Interval		**P1**	**P2**
3 seconds	UL	504.0	95.0
	DL	202.3	
15 seconds	UL	100.8	19.0
	DL	40.5	
60 seconds	UL	25.2	4.8
	DL	10.1	
600 seconds	UL	2.5	0.5
	DL	1.0	95.0

2.4 Reliability

Most of Vaisala's customers for weather stations are industrial or enterprise customers. High reliability and availability is of great importance to these sectors, since the weather station data is used as part of many customers' business processes. Reliable packet delivery is essential.

The fastest transmission interval of 3 seconds results in $60/3 * 60 * 24 = 28800$ messages per day. Missing one message per day comes down to a Packet Error Rate (PER) of 10^{-5} or better. The reliability requirement can also be defined through industry standards and a good representation is given by the 3GPP Quality Class Indicator (QCI) level as expressed in TS 23.203 Ch. 6.1.7, here applicably abbreviated to Table 4. With cellular technologies reliability is commonly given as Block Error Rate (BLER) and here the requirement is set to 10% BLER. [34]

Table 4. 3GPP Standardized QCI characteristics, level 6.

QCI level	PER	Example Services
6	10^{-6}	TCP-based (e.g., www, e-mail, chat, ftp, p2p file sharing, progressive video, etc.)

Additionally, for both profiles, bidirectional data transmission capability is required in order for the higher layers to acknowledge transmissions and to request retransmissions.

2.5 Communication Range

There is a broad range of application areas where localized weather observation data is utilized. This translates directly as a very broad range of installation locations and from the connectivity perspective, encompasses the dense connectivity of cities to sparser in rural areas, or even “remote islands” on offshore platforms and ships. This work specifies 1000 meters as the minimum required communication distance between weather station transmitter and gateway / base station. The required reliability and transmission intervals need to be maintained over the distance.

2.6 Battery Capacity

The weather station is expected to use include batteries, but some differences between use-case profiles are suspected. The battery capacity and current consumption for the minimum operation of the weather station as presented in Table 5.

Table 5. Profile current consumption and battery capacity.

	P1	P2
Battery capacity	8000.0 mAh	3600.0 mAh
Self-discharge	0.03 mA	0.01 mA
Weather station	16.06 mA	

The weather station power consumption comprises of base consumption of 1.5 mA and measurements for wind (4.5 mA), pressure-temperature-humidity (0.9 mA) and continuous precipitation (0.4 mA) for a 12 V supply. The total is adjusted to 3.6 V with a factor of 2.2. In general, the overall power consumption is highly dependent on the wind measurement, as much as 61%. According to the WXT User's Guide [58], for wind the default is a sampling rate of 4 Hz and continuous measurement, but much lower consumption may be achieved by selecting a lower sampling rate and including measurement averaging.

3 WIRELESS LPWAN TECHNOLOGIES

This chapter presents the technology options evaluated by this work. As explained in Chapter 1, the expected boom of the IoT market has sprung up a multitude wireless technologies over the years, all aiming for different niches, while striving to gain popularity and market share. This presents a challenge for a designer to figure out the most suitable for their use-case. The available technologies include short-range radio protocols (such as ZigBee, Bluetooth and IEEE 802.11 Wi-Fi); longer-range radio protocols (such as LoRaWAN, SigFox and TS-UNB); or mobile networks with LTE-M, NB-IoT, legacy 2G and 3G, LTE 4G and 5G. There are also many others, often proprietary in nature at least in part. An indicative presentation of different technologies capability with respect to range is given in Figure 4 below.

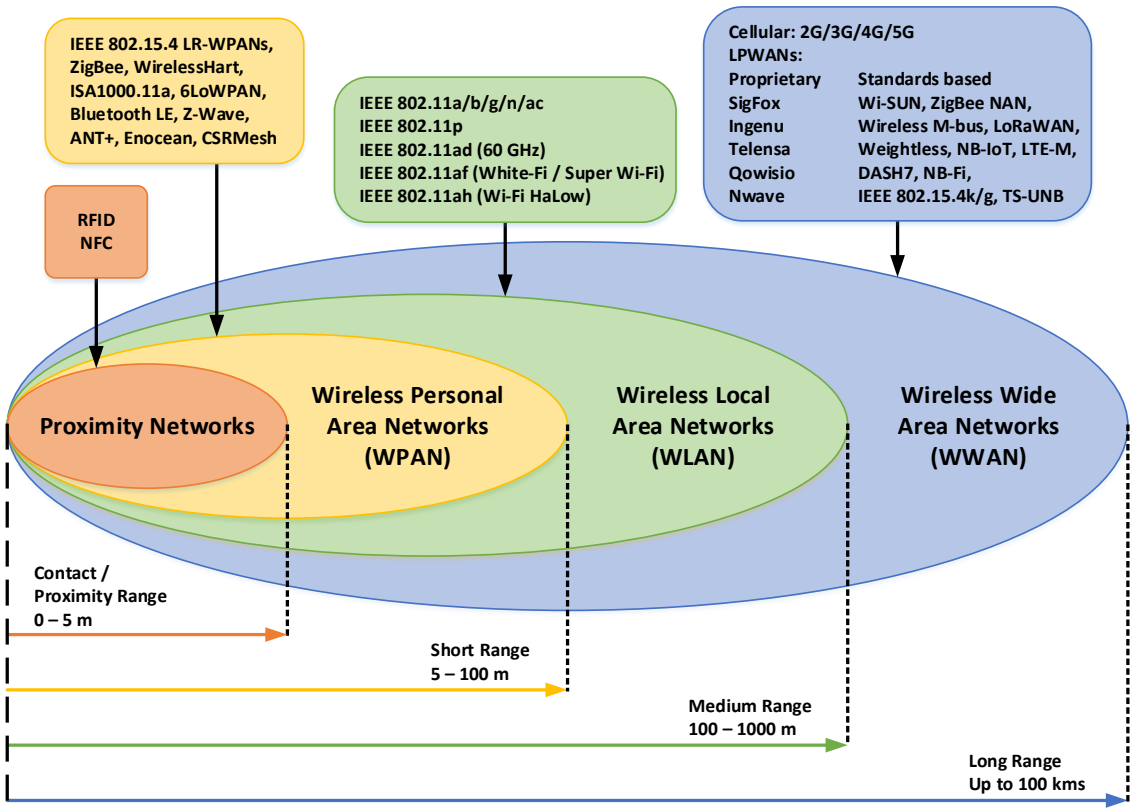

Figure 4. Various wireless access technologies presented with relation to maximum range, adapted from [12].

To reduce complexity of this work, technologies were filtered by a pre-selection step based on qualitative high-level evaluation of technology capability factors against use-case

requirements. The original list of technologies considered for the evaluation is given in Table 6, while arguments for the filtering of different technologies are given in the following paragraphs.

Table 6. List of IoT aimed wireless technologies.

WPANs	Bluetooth Low Energy, Z-Wave (ITU G.9959), IEEE 802.15.4 (ZigBee, Thread, WirelessHart)
WLANs	IEEE 802.11ah (WiFi HaLow)
LPWANs	LoRaWAN, SigFox, TS-UNB, Telensa, Ingenu, Weightless standards, DASH7, Wireless M-Bus
Cellular	LTE-M, NB-IoT, EC-GSM-IoT, Legacy 2G, 3G and LTE

A factor with a high limiting effect is communication range, for which, a minimum limit was defined in Chapter 2.5. This prunes many of the WPAN-labeled technologies such as Bluetooth Low Energy, Z-Wave, and IEEE 802.15.4 based ZigBee, Thread and WirelessHART, which are mainly rated for range of max. 100 meters. As stated by [50], utilization of the 2.4 GHz unlicensed band is in practice only applicable in short range communication of some tens of meters at best.

In the face of the argument of lack of range, advocates of WPAN-technologies will mention that many feature mesh-networking capability to reach greater coverage. In a mesh-topology, a node may communicate with any other node in the network either directly or by routing through other nodes. A mesh-network is also at best self-organizing and self-healing [6]. However, meshing requires well planned networks and high node density to achieve adequate levels of reliability and low outage probability. The node density needed for a mesh-network to cover our required range may be available cities, but it is not conceivable to expect such in rural or even suburban areas. Yet, authors in [5] also note, that real-life deployments, such as the ZigBee enabled smart meter example of Barcelona, can experience unforeseen problems with reliability. That system commonly experienced outages and high latency in the order of minutes at the worst due to the dynamically changing environment's effect on channel conditions of the multi-hop natured network. A weather station with the

ability to connect to a meshing network in itself is an attractive concept from a sales point-of-view. However, there are again multiple technologies to choose from and the reliability concerns alone are worth their own dedicated investigation.

SigFox is widely promoted by industry and has also been the subject of much academic work. All in all, it provides an easily approachable service for a narrow range of use-cases. However, our use-case does not fit in to this range simply due to SigFox's limits in maximum payload size of 12 Bytes and amount of allowed daily packets, 140, on the uplink. [49]

This work will not consider any legacy cellular technologies (2G/3G/4G), even though they have been widely used in the past for similar use-cases – by Vaisala as well. They offer great coverage and adequate data rates, as well as being standardized and mature technologies with world-wide network deployments. Still, their greatest short coming is energy consumption, of which improvement aspirations have led to the development todays NB-IoT, LTE-M and EC-GSM-IoT standards in the first place.

Neither EC-GSM-IoT nor IEEE 802.11ah will be considered as both lack in popularity by the industry. Lastly, technologies such as Telensa, Ingenu, Weightless, DASH7 etc. will not be considered due to not having enough information available regarding their inner workings. Further feasibility study will conducted for NB-IoT, LoRaWAN and TS-UNB.

For reference, Appendix 1 presents a comparison table of above mention technologies. Data was sourced from various standards and academic and industry literary sources such as [11; 16; 20; 27; 30; 34; 35; 40; 41; 45; 46; 55].

3.1 NB-IoT

The second technology proposed in 3GPP Release 13 for M2M communications is NB-IoT. It is sometimes also referred to as Cat-NB1 and was originally proposed as a clean-slate approach called NB-CIoT by Huawei [29]. Release 14, introduced a second device category, referenced as Cat-NB2, which introduced performance improvements and higher peak data rates. In Release 15, 3GPP performed an evaluation of NB-IoT against a set performance

requirements, which were agreed and defined for the 5G mMTC use-case concept. According to [34], NB-IoT qualifies as a member under the 5G mMTC umbrella by meeting those requirements in all fronts with margins to spare. This work specifically refers to Cat-NB2, when discussing about NB-IoT.

Bandwidth-wise NB-IoT requires 180 kHz of spectrum for both up- and downlink, respectively. It's designed to be relatively simple to deploy as a direct replacement of an LTE or Global System for Mobile (GSM) sub carrier. Alternatively an LTE guard-band may be used for deployment. NB-IoT deployments are referred to as stand-alone, in-band or guard-band deployments in 3GPP nomenclature. Also, any new hardware is not required by the network operator as deployment requires only a software update to existing equipment. [34]

NB-IoT builds upon the same radio frame structure as LTE. For uplink, Single Carrier – Frequency Division Multiple Access (SC-FDMA) is used, while Orthogonal Frequency Division Multiple Access (OFDMA) is for downlink. For the uplink, the 180 kHz bandwidth is divided to either 12 or 48 subcarriers (SCs) with correspondingly 15 kHz or 3.75 kHz spacing. The downlink always uses 15 kHz spacing. In the downlink a cycle of 1024 time domain hyper radio frames (H-RFs) is repeated, where each H-RF contains 1024 radio frames (RFs). One frame is made of 10 subframes (SFs), each lasting 1 ms. A subframe is further divided to two 0.5 ms slots, both carrying seven OFDM symbols. If 3.75 kHz spacing is used on the uplink, then slot duration expands to 2 ms. This is illustrated in in Figure 5 and Figure 8. The uplink can be further chosen to use either single or multi-carrier transmissions, which in NB-IoT are referred to as tones. For multi-tone transmission, subcarrier spacing (SCS) is always 15 kHz and 3, 6 or 12 subcarriers can be used. [30; 34; 37]

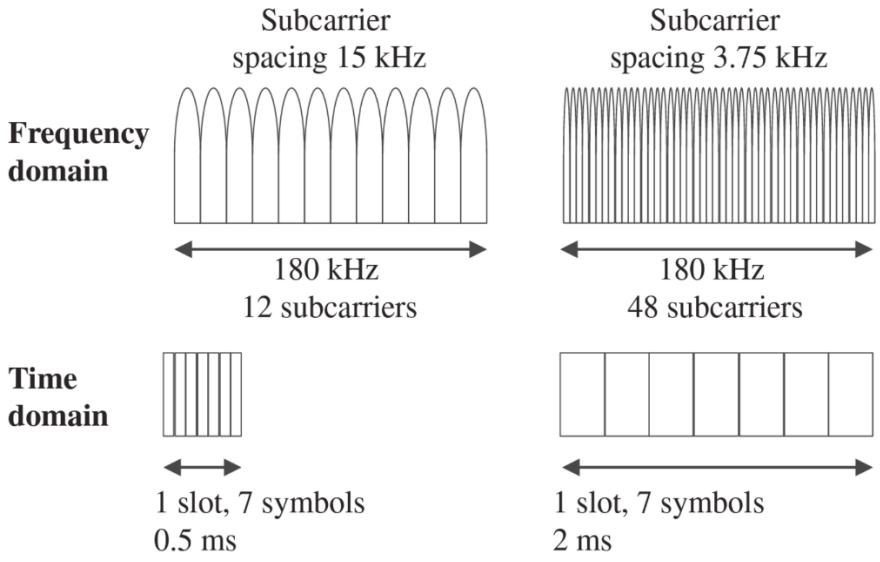

Figure 5. NB-IoT subcarrier spacing [30].

In contrast to LTE, NB-IoT brings along a new type of resource mapping scheme in the uplink, called the Resource Unit (RU). The RU, illustrated in Figure 6, results from the combination of the number of subcarriers and the number of subframes. The way the RU is used is explained in the following chapter. [37]

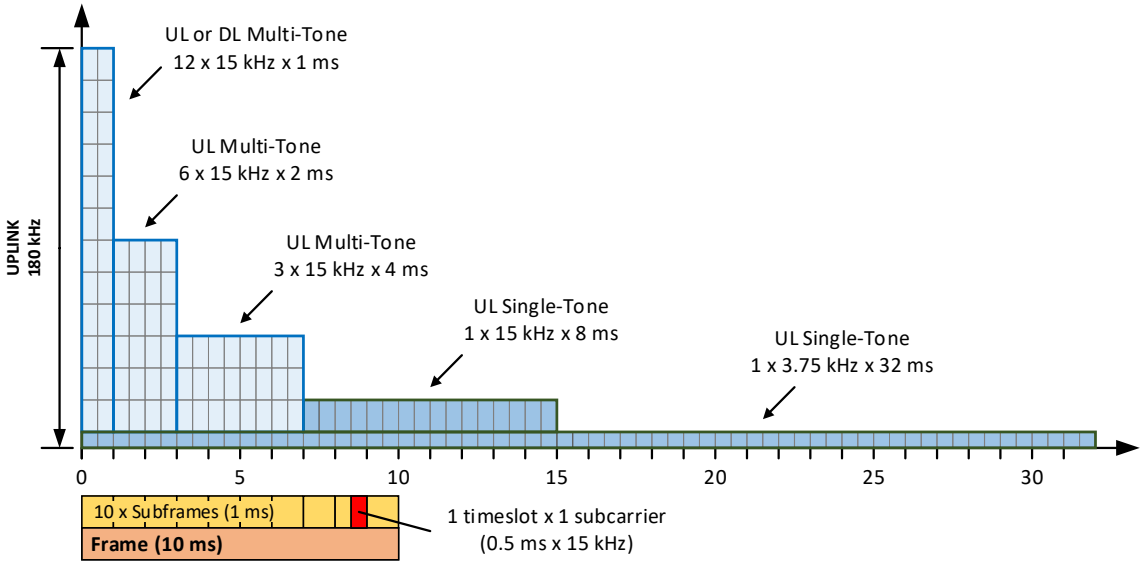

Figure 6. NB-IoT UL Resource Unit assignment combinations [37].

Like LTE, the up- and downlink carry information over a number of different signals and channels, which are listed in Figure 7.

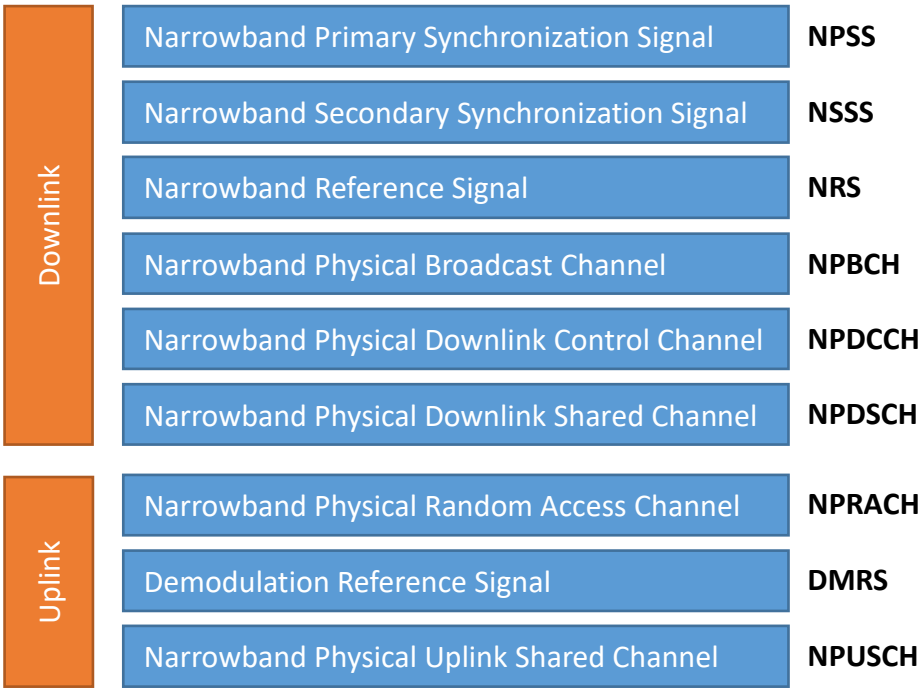

Figure 7. NB-IoT physical signals and channels [30].

NPRACH channel has three main uses. Over this channel the end-device performs the initial connection procedure to the network, requests radio resources when they wish to transmit, and reconnects to the network in case of link failure. During initial network access, end-devices acquire the network's information by listening for the Master Information Block (MIB) and System Information Blocks (SIBs), which are transmitted periodically by the base station, called Evolved Node B (eNB) in 3GPP nomenclature, from channels NPBCH and NPDCCH, respectively. The NRS channel's purpose is with cell search and initial system acquisition, where as NPSS and NSSS handle frequency and timing synchronization for the end-device with the eNB. Actual user data is transmitted over the NPDSCH and NPUSCH channels. It should also be noted, that in contrast with LTE, NB-IoT utilizes no control channel for uplink, and any control data is transmitted over NPUSCH. [30]

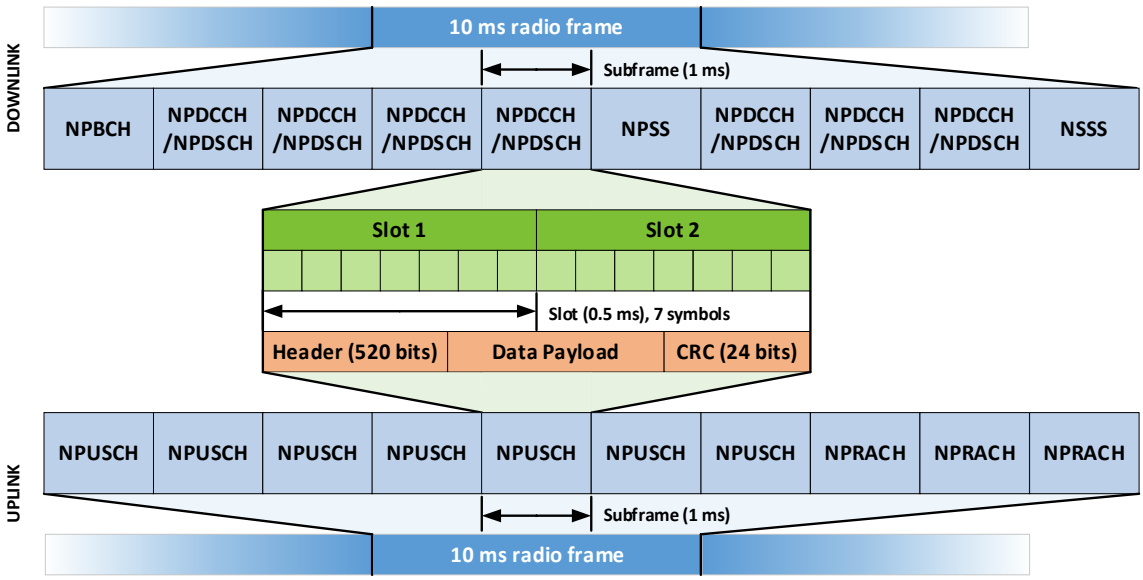

Figure 8. Generalization of NB-IoT DL and UL frame structure with 15 kHz subcarrier spacing [37].

When the end-device has data to send upstream, it first makes a request to the network for scheduled resources. The request is made over the NPARCH procedure, and the eNB responds with Downlink Control Indicator (DCI) report containing the scheduling and resource info. According to this information, the end-device sets its parameters and transmits the data. Similar procedure happens on the downlink. However, this time there is no request, but instead the end-device tunes-in to the downlink data on the NPDSCH according to the DCI information received on the NPDCCH. The contents of DCIs and resourcing in general is explained in Chapter 3.1.2 in more detail. Chapter 3.1.3 also shed further light on how the end-device is informed to expect downlink data. [30; 39]

3GPP defines three CE levels for NB-IoT operation: normal, robust and extreme, through which dynamic service is provided for devices in varying levels of network coverage. The extreme CE is expected for devices located indoors or underground. The coverage level is dynamically adjusted through control signaling and it dictates the type of channel coding, modulation, amount of repetitions, and such measures used. Data rates are poorer with robust and extreme CE levels, but perceived receiver sensitivity is increased. Repetitions can be applied individually per channel and count up to 2048. NB-IoT incorporates MAC-layer reliability mechanisms, which do ensure message delivery. However, in the worst case, latencies potentially measured in the order of seconds may be experienced. [30; 39]

On paper, NB-IoT is capable of an instantaneous peak physical data rate of 250 kbps on the uplink and 170 kbps on the downlink. The instantaneous peak physical data rate is often the performance metric included in data sheets. However, it does not account for signaling and data scheduling overhead present overall for a transmission. Actual sustained rates are much lower and highly dependent on the channel conditions and determined CE level. NB-IoT offers no Quality-of-Service (QoS) concept and thus cannot guarantee any minimum data rate. Peak MAC-layer data rates, which include all the physical layer overhead of signaling and data scheduling may be in the range of 26 kbps (depends on deployment type) for downlink and 62 kbps for uplink [30; 34; 41].

NB-IoT is secured with LTE type encryption on the link. However, TCP/UDP payloads crossing over to the Internet should be further encrypted at the Transport layer with Transport Layer Security (TLS) or DTLS. Essentially, NB-IoT exposes devices with direct TCP/IP connectivity to the Internet, and therefore should be secured with appropriate measures.

End-devices transmission power is set by an open-loop power control as defined in [34], when the number of used repetitions is less than three. Furthermore, three power classes are given in Release 13 and 14 specifications: 14, 20 or 23 dBm for the maximum transmit power level. Lastly, NB-IoT employs power saving features, which affect end-devices' behavior in the network, as further explained in Chapter 3.1.3. [39]

3.1.1 Protocol Stack

The maximum payload size for each transmission (allocated resources in one grant) is 1600 bytes. In other words, this is the maximum supported size of the Packet Data Convergence Protocol (PDCP) Service Data Unit (SDU) payload, which is the protocol just below the Network-layer on the protocol stack. PDCP-protocol is responsible of functions such as transfer of user data, sequence numbering, Robust Header Compression (ROHC) function, ciphering and integrity protection. It adds a header to the data before it is passed down to the

Radio Link Control (RLC) protocol as an RLC SDU. The NB-IoT protocol stack for user data is given in Figure 9 for reference. [25]

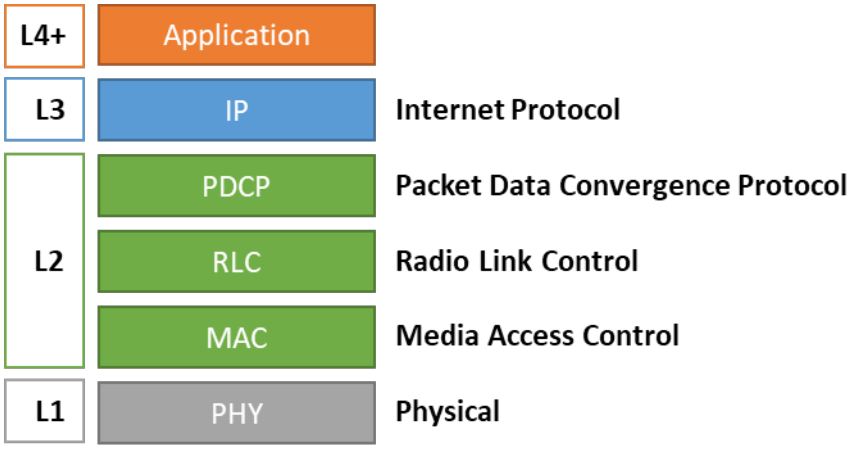

Figure 9. NB-IoT user data protocol stack.

The RLC protocol is a complex layer, and its main duty is to fit higher layer payloads into lower layer segments (RLC Protocol Data Units, PDUs) of a size indicated by the MAC layer as the chosen Transport Block Size (TBS) for the transmission. The RLC is also responsible for functions such as error correction through automatic repeat requests (ARQs), duplicate detection, protocol error detection and recovery, and more. [24]

3.1.2 Link Adaptation

In NB-IoT, the end-device and the eNB determine the link parameters based on a derived estimation of the channel state. Essentially, the idea is to choose the appropriate number of RUs, the modulation, code rate, transport block size and repetitions to accommodate a BLER of 10 % or less. The eNB informs the end-device over NPDCCH with a DCI report on what resources the end-device can use, what modulation and coding scheme (MCS) is to be utilized for the transmission and demodulation of received data, and the number of repetitions to use. There are different formats of the DCI for various circumstances. Generally, format 0 is used to define parameters for UL and formats 1A-D and 2A-C are for DL. [22]

On the downlink NPDSCH, for user data the DCI informs the end-device of the number of subframes ($\boldsymbol{n_{SF}}$) in the resource assignment index field ($\boldsymbol{i_{SF}}$). Repetition count ($\boldsymbol{n_{Rep}}$) is given in the DCI repetition number indication field ($\boldsymbol{i_{Rep}}$). Modulation order for downlink is always $\boldsymbol{Q_m = 2}$. To determine the MCS, the end-device must read the 4-bit MCS index field ($\boldsymbol{i_{MCS}}$) on the DCI. The TBS in bits is then given by associating $\boldsymbol{i_{MCS} = i_{TBS}}$ for the assigned number of subframes. This is summarized in Table 7. The downlink is always modulated with QPSK and uses Tail Biting Convolutional Coding (TBCC) with a code rate of 1/3 [21; 22].

Table 7. Combined tables for NB-IoT DL DCI information [22].

i_{Rep}	n_{Rep}
0	1
1	2
2	4
3	8
4	16
5	32
6	64
7	128
8	192
9	256
10	384
11	512
12	768
13	1024
14	1536
15	2048

i_{SF}	n_{SF}
0	1
1	2
2	3
3	4
4	5
5	6
6	8
7	10

i_{MCS} / i_{TBS}	i_{SF}							
	0	1	2	3	4	5	6	7
0	16	32	56	88	120	152	208	256
1	24	56	88	144	176	208	256	344
2	32	72	144	176	208	256	328	424
3	40	104	176	208	256	328	440	568
4	56	120	208	256	328	408	552	680
5	72	144	224	328	424	504	680	872
6	88	176	256	392	504	600	808	1032
7	104	224	328	472	584	680	968	1224
8	120	256	392	536	680	808	1096	1352
9	136	296	456	616	776	936	1256	1544
10	144	328	504	680	872	1032	1384	1736
11	176	376	584	776	1000	1192	1608	2024
12	208	440	680	904	1128	1352	1800	2280
13	224	488	744	1032	1256	1544	2024	2536

On the uplink, for NPUSCH channel, the DCI includes similar information. First there is the subcarrier indication field ($\boldsymbol{i_{SC}}$), which determines how many subcarriers $\left(\boldsymbol{n_{SC}^{RU}}\right)$, and at which frequencies, are allocated for an RU. Then, in the DCI, the resource assignment indication field ($\boldsymbol{i_{RU}}$) gives the number of resource units ($\boldsymbol{n_{RU}}$), and $\boldsymbol{n_{Rep}}$ is given by the repetition number indication field ($\boldsymbol{i_{Rep}}$).

MCS is determined by the MCS indication field ($\boldsymbol{i_{MCS}}$) in the DCI. Modulation order (the modulation technique) is dependent on the used subcarrier spacing and number of allocated subcarriers for the RU.

- If $\boldsymbol{n_{SC}^{RU} = 1}$, the modulation order $\boldsymbol{Q_m}$ and TBS indication $\boldsymbol{i_{TBS}}$ are given by table 16.5.1.2-1 of [23] and as given in Table 9.
- If $\boldsymbol{n_{SC}^{RU} > 1}$, then modulation order $\boldsymbol{Q_m = 2}$ and $\boldsymbol{i_{MCS} = i_{TBS}}$.

Allowed values for $\boldsymbol{n_{SC}^{RU}}$ are listed in Table 8. [21; 23]

Table 8. Supported combinations of $\boldsymbol{n_{SC}^{RU}}$, $\boldsymbol{n_{slots}^{UL}}$ and $\boldsymbol{n_{symb}^{UL}}$ for frame structure type 1 used to carry uplink user data [21].

NPUSCH format	$\boldsymbol{SCS}$	$\boldsymbol{n_{SC}^{RU}}$	$\boldsymbol{n_{slots}^{UL}}$	$\boldsymbol{n_{symb}^{UL}}$
1	3.75 kHz	1	16	7
	15 kHz	1	16	
		3	8	
		6	4	
		12	2	
2	3.75 kHz	1	4	
	15 kHz	12	4	

Finally, TBS is derived according to $\boldsymbol{i_{MCS}}$ and $\boldsymbol{i_{RU}}$. The above details are summarized below in Table 9. The uplink is modulated with either Binary Phase Shift Keying (BPSK) or Quadrature Phase Shift Keying (QPSK), and uses Turbo coding with a code rate of 1/3. Lower coding redundancy is achieved on higher MCS levels, which means greater TB sizes for equal number of RUs. [21; 22; 40]

Table 9. Combined tables for NB-IoT UL DCI information [23].

				$n_{sc}^{RU} = 1$			
i_{Rep}	n_{Rep}	i_{RU}	n_{RU}	i_{MCS}	Q_m	i_{TBS}	Modulation
0	1	0	1	0	1	0	BPSK
1	2	1	2	1	1	2	BPSK
2	4	2	3	2	2	1	QPSK
3	8	3	4	3	2	3	QPSK
4	16	4	5	4	2	4	QPSK
5	32	5	6	5	2	5	QPSK
6	64	6	8	6	2	6	QPSK
7	128	7	10	7	2	7	QPSK
				8	2	8	QPSK
				9	2	9	QPSK
				10	2	10	QPSK

i_{TBS}	i_{RU}							
	0	1	2	3	4	5	6	7
0	16	32	56	88	120	152	208	256
1	24	56	88	144	176	208	256	344
2	32	72	144	176	208	256	328	424
3	40	104	176	208	256	328	440	568
4	56	120	208	256	328	408	552	680
5	72	144	224	328	424	504	680	872
6	88	176	256	392	504	600	808	1032
7	104	224	328	472	584	680	968	1224
8	120	256	392	536	680	808	1096	1352
9	136	296	456	616	776	936	1256	1544
10	144	328	504	680	872	1032	1384	1736
11	176	376	584	776	1000	1192	1608	2024
12	208	440	680	904	1128	1352	1800	2280
13	224	488	744	1032	1256	1544	2024	2536

NB-IoT is designed to be usable also in fringe areas of coverage (such as basements) and the main tool to achieve this is use of transmission repetitions. For NPRACH and NPUSCH, $\boldsymbol{n_{rep}}$ can be chosen from the range defined by $\mathbf{2}^{\boldsymbol{x}}$, where $\boldsymbol{x} \in \{\mathbf{1}, \dots, \mathbf{7}\}$. For NPDSCH the number of repetition reaches up to 2048. Repetitions increase the probability of successful

decoding by increasing the perceived Signal-to-Noise-Ratio (SNR) at the receiver. In general, repeated copies of the transmission at the receiver can be combined, and the resulting SNR ($\boldsymbol{SNR_c}$) can be thought as the sum of SNRs of each transmission copy. This can be expressed as

$$\boldsymbol{SNR_c} = \sum_{\boldsymbol{i=1}}^{\boldsymbol{n_{rep}}} \boldsymbol{SNR(i)} = \boldsymbol{n_{rep}} * \boldsymbol{SNR}\,. \tag{1}$$

This assumes that the channel conditions do not change between transmissions of each repetition. [6; 34]

3.1.3 Power Saving Features

NB-IoT incorporates many power saving features, of which aim is to lengthen the battery life of end-devices. In NB-IoT, the Radio Resource Control (RRC) is the function, similar as in LTE, which handles many of the logical connectivity procedures. RRC has two states: Idle and Connected. These include connection establishment and release, broadcast of control information, paging notifications and such. An end-device starts in RRC-Idle state, and transits to RRC-Connected after it has established connection. In RRC-Connected, the end-device may request communication resources from the network. [39; 43]

Discontinuous reception (DRX) is a feature specified in 3GPP cellular technologies, which allows IoT devices to conserve energy. In general, to receive downlink data, the end-device needs to know of pending transmission, and thus when to turn on its receiver. The information of pending downlink data is informed by the network through a paging procedure similar to LTE, in specific subframes called Paging Occasions (POs). The procedure specifies which subframe, within specific radio frames called Paging Frames (PFs), to listen to. What results is cycles of alternating periods of active reception and idling. Hence it's called discontinuous reception, and the feature is available for both RRC-Connected and RRC-Idle -modes. End-devices may also transfer into a sleep-state during this idle period for further energy conservation. Energy saving are further optimized by the fact that during idling or sleeping both the network and the end-device maintain device

context. This reduces signaling needs as well as need to renegotiate security in the case that the end-device transitions back to RRC-Connected state for new up- or downlink data. [34; 39; 49; 53]

When the end-device transitions to RRC-Connected state, it communicates any up- and downlink data with the network, and two timers, referred to as the DRX Inactivity Timer and the RRC Inactivity Timer, are started. Overall, the time the end-device spends in RRC Connected state depends on the RRC Inactivity Timer, which length is determined by the network. DRX Inactivity Timer on the other hand is a duration while the end-device is actively receiving. It can have values in $\mathbf{2}^{\boldsymbol{x}}$ ms, where $\boldsymbol{x} \in \{\mathbf{0}, \dots, \mathbf{14}\}$, and value zero disables the timer. If any downlink scheduling or an uplink grant is received in the NPDCCH, both timers are restarted. [34; 39; 49; 53]

There are some differences in how DRX functions in both RRC states. Below are the definitions and naming used in this work:

- Connected-DRX (C-DRX) cycle. In RRC-Connected state.
- C-eDRX cycle. Alternative enhanced-DRX cycle in RRC-Connected state.
- Idle-DRX (I-DRX) cycle. In RRC-Idle state. Also used within an I-eDRX cycle.
- I-eDRX cycle. Alternative enhanced-DRX cycle in RRC-Idle state.

After DRX Inactivity Timer expires, the end-device can start with C-DRX cycles until RRC Release. After RRC Inactivity Timer expires, the end-device takes action for the RRC Release and transitions to RRC-Idle state. If no further data is to be sent or is received, then the length of RRC-Idle state is determined by the Tracking Area Update (TAU) timer. A TAU may be thought of as an ultimate “Hello, I’m still here” message to the network, if no other communication is performed by the end-device. [34; 39; 53]

In LTE, C-DRX has to types: a short or a long cycle. For IoT-applications, based on [49], the short cycle is optional and hardly used. Thus, the long cycle is only discussed here. The long C-DRX cycle can range from 10 to 2560 ms and consists of two periods: a period of continuous active listening for notification of pending downlink data through NPDCCH,

called OnDuration; and an opportunity for a period of idle/sleep throughout the rest of the cycle. The OnDuration may range from 1 to 100 SFs (1 - 100 ms).

Alternatively, the end-device may request use of extended DRX cycle in RRC-Connected state, but it is only applicable for the long cycle. Essentially, C-eDRX modifies the parameter values to NB-IoT specific values, while the functionality is the same as with C-DRX. DRX Inactivity Timer and OnDuration can range up to 32 SFs, while DRX-cycle is extended to 9216 SFs. Figure 10 presents the behavior an end-device goes through and the different DRX cycles while transitioning between RRC states, including DRX Inactivity Timer. [49]

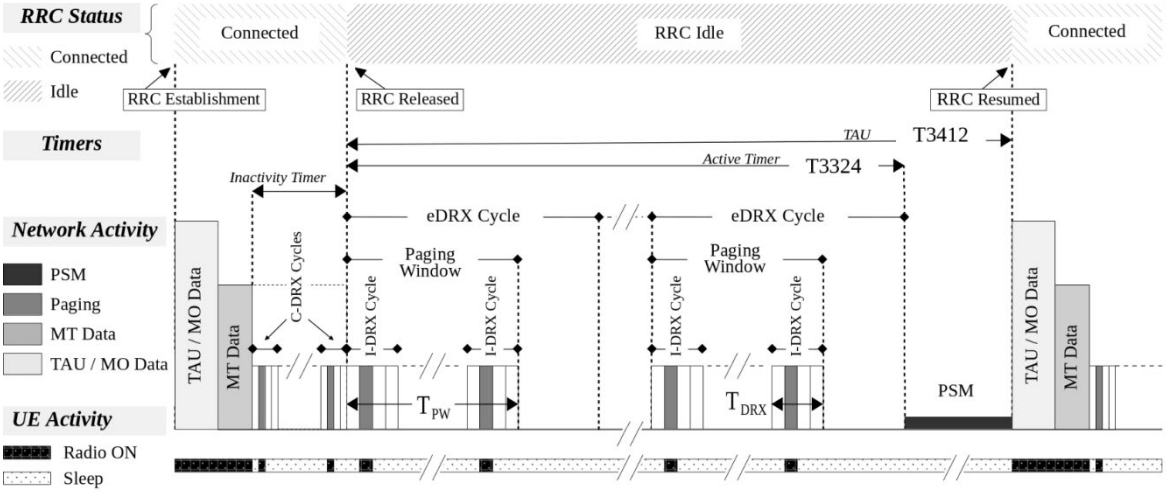

Figure 10. End-device behavior between transmission events [39].

If C-DRX/-eDRX is used, an end-device may also set a flag called Release Assistance Indicator (RAI), while communicating with the network before an uplink data transmission. The RAI flag indicates to the eNB that the end-device expects to: send another uplink transmission; receive a downlink transmission; or neither. Based on the flag information, the eNB has the opportunity to perform RRC Release ahead of time of the RRC Inactivity Timer, which allows the end-device to reduce time spent in C-DRX. [42]

As mentioned, within RRC-Idle, the end-device may employ the I-DRX paging procedure to check for any downlink data. The paging is controlled by several timers. In general, the time during which the end-device is reachable from the network is determined by the Active Timer T3324. The timer's length is determined by the number of I-DRX/-eDRX cycles

performed by the end-device and is in the range of 0 to 11160 seconds. I-DRX paging cycle is similar to LTE, as explained in a previous paragraph. PFs occur at periods of either 128, 256, 512 or 1024 RFs. Within a PF, up to 4 specific SFs may be assigned as POs. The end-device needs to listen to only one PO. Which PO the end-device listens to is controlled by the network through a calculation process. [49]

Alternatively, the end-device may request use of I-eDRX cycle in RRC-Idle state, which adds an extra layer to the process. An I-eDRX cycle is counted in Paging Hyper Radio Frames (PHs) with one hyper RF equaling 1024 radio frames. Valid values between PHs follow the formula $\mathbf{1}\,\boldsymbol{HF} * \mathbf{2}^{\boldsymbol{x}}$, where $\boldsymbol{x} = \{\mathbf{11}, \ldots, \mathbf{20}\}$, which allows for the maximum period of a little less than three hours. Within a PH, there is a further Paging Time Window (PTW, $\boldsymbol{t_{PW}}$), during which I-DRX cycles are performed (PFs observed). Valid values for PTW start from 256 RFs and go up to 4096. Figure 11 presents the above functionality. [34; 39; 49; 53]

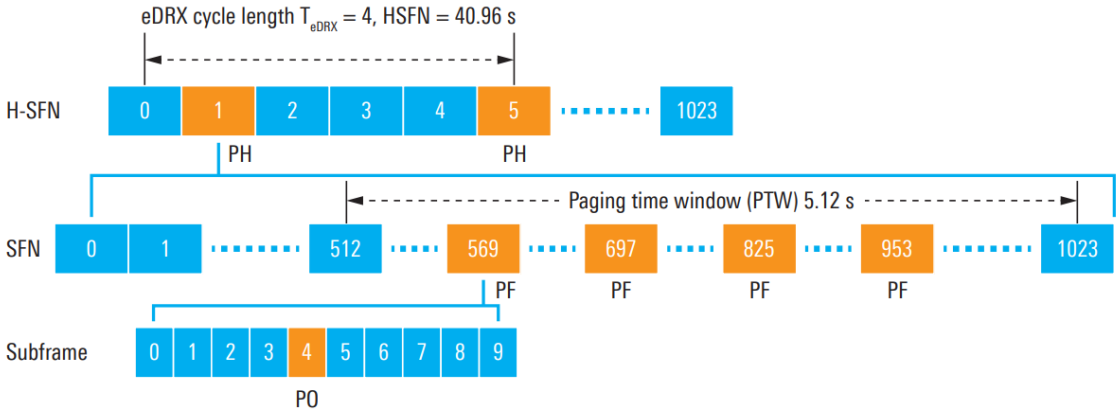

Figure 11. RRC-Idle state eDRX example as given by [49].

Power Saving Mode (PSM) is specifically named as a concept by 3GPP in Release 12/13 to decrease device power consumption. Generally, in PSM, an end-device or its communication module assumes a sleep-state, where various hardware components are powered down. The end-device is waken from sleep-state either when the TAU timer expires or when it has data to send. The maximum value for the TAU timer is 1 year. Overall, as mentioned, some of the timers, such as RRC Inactivity Timer or PTW, are mandatory and set by the network.

Others may be controlled by the end-device to the limits set by the network operator, if any. [32; 34; 39]

Another function of NB-IoT to save energy, is Power Head Room (PHR). It is a report, which an end-device may include in its uplink transmissions. The purpose of the report is to provide an indication of what is the difference between the estimated required transmit power level for a user data message and the device's configured maximum power level, with respect to nominal CE level and NPUSCH bandwidth. With this information, the eNB can adjust scheduling and resource allocation as in the chosen MCS and the number of SCs. [34]

3.2 LoRaWAN

LoRaWAN is a wireless technology traditionally used in the license-exempt spectrum. At its heart is LoRa, short for "Long Range", a patented proprietary physical layer technology from Semtech. While the physical layer is proprietary, the higher layers are part of the open standard LoRaWAN, managed by The LoRa Alliance™.

LoRaWAN is utilized in different deployments. There are free and public networks, which may be used for non-commercial activities, such as The Things Network. Additionally, many telecom operators have deployed their own networks and offer subscription based connectivity. Finally, users may acquire their own LoRaWAN gateways to deploy private networks. [11]

The physical layer part, LoRa, works on the sub-1 GHz industrial, scientific and medical (ISM) bands. LoRa is commonly distinguished and remembered by its use of the Chirp Spread Spectrum (CSS) modulation technique. In CSS, a narrow-band signal is spread to a wider bandwidth in pulses of finite length of increasing or decreasing frequency. These are called up or down "chirps". The waterfall graph of Figure 13 gives examples of these chirps in domains of frequency and time. CSS is also termed as a wideband linear frequency modulation technique. As common with spread spectrum techniques, the resulting modulated signal has high resilience against interference and is difficult to detect or jam.

Alternatively, specifically in Europe, LoRa may also utilize Gaussian Frequency-Shift Keying (GFSK) modulation. [12; 17; 33; 38; 40]

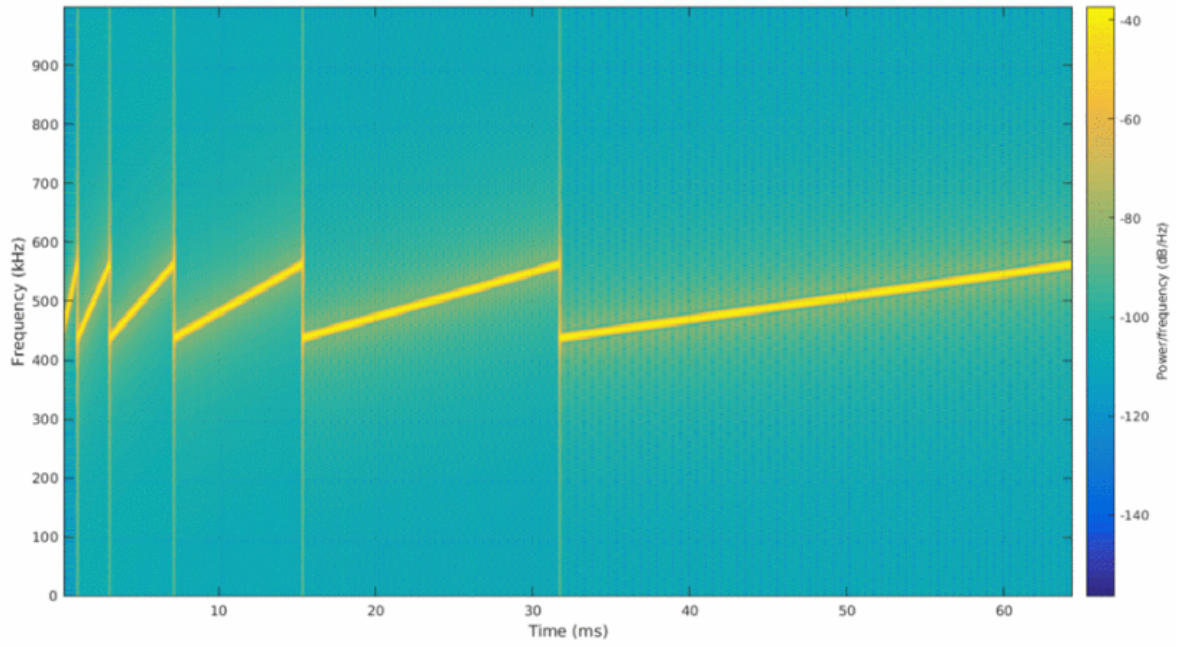

Figure 12. Examples of LoRa up-"chirps" for different spreading factors. [17].

Channel access of LoRa is based on ALOHA. This means, that LoRa end-devices do not follow any channel access protocol, but always immediately transmit any new data. LoRaWAN networks are star of star topologies, where LoRa gateways act as hubs, and listen-in for messages. The gateways are then responsible of further relaying of the messages to a central-server, often through a higher capacity wired medium. In LoRaWAN, end-devices are not tied to any specific gateway, and the same message may be received (and relayed) by multiple gateways. In this situation, it is up to the central server to filter out the duplicates. [12; 17; 40]

LoRaWAN employs three different device classes regarding downlink data transmissions. Class-A is for power-constrained end-devices and applications, which require no, or only minimal, downlink communications (i.e. acknowledgements). End-devices in this class often utilize sleep-state extensively between transmission events, and thus the downlink communication is only possible during windows after uplink transmissions. After each uplink transmission, the end-device will listen for short periods for any incoming downlink

messages as shown in Figure 13. If a downlink transmission is initiated during either periods, the end-device will continue to receive until the end of the transmission. [40]

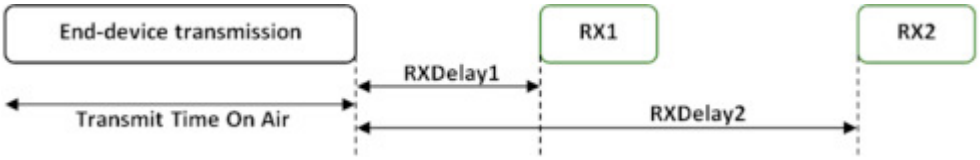

Figure 13. LoRa Class A downlink slots [40].

Class-B builds on top of Class-A uplink receive slots by opening an additional receive window at scheduled times regardless of uplink events. Scheduling on the other hand requires the end-device to synchronize with a gateway beacon so that the gateway knows when the end-device is in receive state. Finally, Class-C is for devices, essentially gateways, which are connected to a constant power source. In Class-C, the device is listening for incoming messages at all times except while transmitting. [40]

3.2.1 Link Adaptation

LoRa transmissions employ a concept named spreading factor (SF) to combat varying channel conditions. SF is the ratio between symbol rate and chip rate. In spread spectrum techniques, such as CSS, Direct-sequence Spread Spectrum (DSSS) or Code Division Multiple Access (CDMA), data bits are added with pseudorandom sequences, which result in pulses known as chips. The chip rate is always greater than the data rate. An increased SNR may be achieved with a higher SF, but with the expense of greater On-air Time (OaT) of the message. Indeed, each step in SF results with double the OaT for the same message payload size. This is illustrated in Figure 12. There are seven levels for the spreading factor, and the value of SF configuration parameter ranges from 6 to 12. SFs are orthogonal with respect to each other, which allows separation between networks utilizing different SFs. [9]

LoRa can operate on different channel bandwidths ranging from 7.8 kHz to 500 kHz. Still, many commercial implementations distinguish only three options: 125, 250 or 500 kHz. Additionally, the specification [35] of LoRaWAN lists region specific sets of channels,

which end-devices may use. In example, in Europe there are six 125 kHz channels listed for the 864.10 – 864.50 and 868.10 – 868.50 MHz frequency ranges.

LoRa is reported to be able to provide bitrates from 250 bps to 50 kbps. The actual rate much depends on modulation, SF, code rate (CR), channel bandwidth configuration and country/region specific ISM band uses. The bitrate $\boldsymbol{R_b}$ achievable with LoRa using CSS follows the equation

$$\boldsymbol{R_b = SF * \frac{B}{2^{SF}} * CR,} \tag{2}$$

where $\boldsymbol{SF}$ is the spreading factor, $\boldsymbol{B}$ the used bandwidth and $\boldsymbol{CR}$ the coding rate. [3; 12; 40]

The LoRaWAN specification [35] defines pre-calculated bitrates (DR) for various regions, such as Europe, US, China, etc. Not all are covered here, and instead the DRs for region of Europe are given in Table 10 as reference.

Table 10. EU863-870 Data Rate and end-device output power [35].

DR	Configuration	Indicative PHY bitrate (bit/s)	CR
0	LoRa: SF12 / 125 kHz	250	4/6
1	LoRa: SF11 / 125 kHz	440	4/6
2	LoRa: SF10 / 125 kHz	980	4/5
3	LoRa: SF9 / 125 kHz	1 760	4/5
4	LoRa: SF8 / 125 kHz	3 125	4/5
5	LoRa: SF7 / 125 kHz	5 470	4/5
6	LoRa: SF7 / 250 kHz	11 000	4/5
7	FSK: 50 kbps	50 000	

P_{TX} level	Configuration
0	20 dBm (if sup.)
1	14 dBm
2	11 dBm
3	8 dBm
4	5 dBm
5	2 dBm

LoRa also employs a feature called Adaptive Data Rate (ADR), which allows it to adapt and optimize the data rate according to changes in channel conditions.

To increase sensitivity, LoRa employs Forward Error Coding (FEC). The CR used to encode the message payload may be set to either 4/5, 4/6, 4/7 or 4/8 ratios. With regard to LoRa, the CR is often expressed as a parameter in literature, and the coding rate is given by $\mathbf{4}/(\mathbf{4}+\boldsymbol{CR_{ind}})$, where $\boldsymbol{CR_{ind}} = \{\mathbf{1},\mathbf{2},\mathbf{3},\mathbf{4}\}$. [9]

3.2.2 Frame Structure

LoRaWAN end-devices can be connected to the internet via the gateway. More specifically, the LoRa message does not include L3-headering, but relies on an assigned device-address, which allows gateways to identify each device. Upon receiving a message, the gateway then appends L3 and other headers in order to forward the message to a data collection platform.

The frame structure up to L2 with header fields and sizes are depicted in Figure 14. The fields indicating values starting from zero are optional, and may be omitted if the frame is only used to transmit commands to the receiver with no FRM Payload. Acknowledgements are transmitted as a bit in the Frame header's (FHDR) Frame Control (FCtrl) byte. [36]

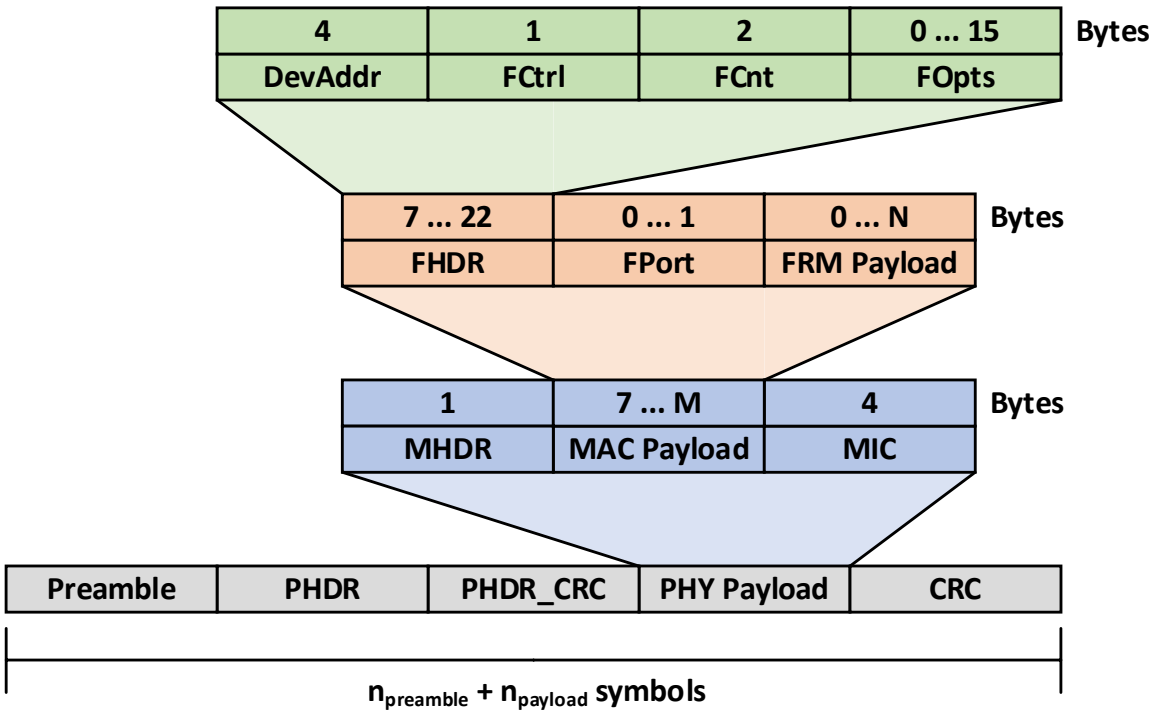

Figure 14. LoRa frame structure [36].

The physical LoRa frame transmission always starts with a preamble, which is by default 12 symbols long. The preamble is used for synchronization, but also is encoded with a sync word to be used to differentiate LoRa networks from each other if they utilize the same frequency band. The preamble length, denoted by $\boldsymbol{n_{preamble}}$, is configurable up-to 65535 symbols. The LoRa frame may optionally include a physical header (PHDR) and a header Cyclic Redundancy Check (CRC) field. The PHDR and PHDR CRC are always coded with $\boldsymbol{CR_{ind} = 4}$ and the CR used for the payload is stored in the header. This allows communication between radios using different CR. Such is the case for a gateway receiving messages from end-devices operating in various noise and interference environments. The PHDR also includes information such as payload length (1 byte) and if a payload CRC is included. It can be noted, that setting the payload length field to just 1 byte by definition restricts the maximum payload size per frame to 255 bytes. [6; 36; 54]

3.3 Telegram Splitting

Telegram Splitting Ultra Narrow Band (TS-UNB) is the name given for the ETSI TS 103 357 standard, which is to supersede an older standard called Wireless M-Bus. TS-UNB was originally developed by the Fraunhofer Institute for Integrate Circuits and currently the most prominent implementation is the MIoTy® protocol by the Canadian company BerhTech.

The main idea of the technology is to split higher layer data packets into small subpackets (radio bursts) at the physical layer, which are transmitted pseudo-randomly over frequency and time. The receiver (base station) listens to the whole spectrum and reassembles the subpackets to a coherent packet. The main idea is to give each radio burst (RB) a short on-air period, and thus avoid one interfering transmission from corrupting the entire message. The name given to this method is Telegram Splitting Multiple Access (TSMA) in the specification and illustrated in Figure 15. [20]

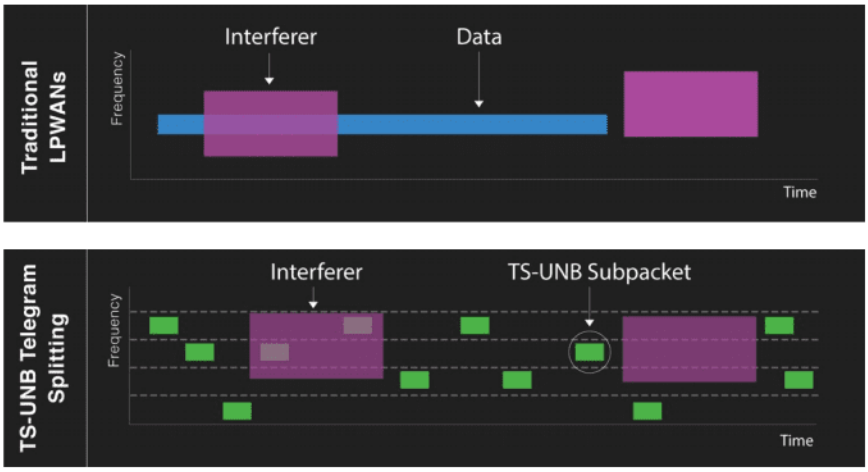

Figure 15. TSMA benefit against interference, as expressed by [8].

TS-UNB communication is asynchronous and initiated by the end-device. The protocol supports two communication classes, A and Z. Class A is for uplink data only and class Z is for bidirectional transmissions, which are supported with downlink having a defined transmission window after any uplink transmissions. Acknowledgements may be used in both links as a bit-flag in the MAC header. Channel coding is used in the RBs to increase receiver sensitivity (down to -139 dBm) and, as advertised by BehrTech, up-to 50% of RBs may be lost while still allowing for successful reassembly. Transmission are modulated with coherent Minimum Shift Keying (MSK) or Gaussian MSK (GMSK) techniques. TS-UNB may be operated on license-exempt bands with channel bandwidths of 25, 100 or 725 kHz. These are respectively referred to as Narrow, Standard and Wide TSMA modes in the specification. [20]

3.3.1 Frame Structure

TS-UNB end-devices can be connected to the internet via the gateway. More specifically, the sent message does not include L3-headering, but relies on an assigned device-address, which allows a gateway to identify each end-device. Upon receiving a message, the gateway then appends L3 and other headers in order to forward the message to a data collection platform.

Higher layer data payload size may be up to 245 bytes in uplink and 250 bytes in downlink. The payload is first encrypted with AES128 before arriving to the MAC-layer. On the uplink

the MAC-layer PDU (MPDU) includes the application payload and max. 15 bytes of headering including the fields: header, address, packet counter, MAC-payload format indicator (MPF) and a cipher-based message authentication code (CMAC). At the physical layer, the MPDU is taken as input for the physical payload data unit (PSDU), which may be minimum 20 and maximum 255 bytes in size. If the MPDU is less than 20 bytes, then zero padding is to fill the PSDU to 20 bytes. Then a further 26 bits are added including a Cyclic Redundancy Check (CRC) and MAC-mode fields.

The radio transmission of the packet, called the radio frame, consists of a core-frame and an optional extension frame. On the uplink, the technology is optimized for payload size of 10 bytes, which builds the core-frame. The extension frame is used in addition to the core frame with payloads larger than 8 bytes. The uplink core frame consists of 24 RBs.

Finally, before subpacketizing, the physical layer payload is whitened and encoded with 1/3 FEC of convolutional code. Each RB, or also called Burst Data Unit (BDU) at this point, make up from two data parts (A and B) of 12 bits. During the subpacketizing process a pilot sequence of 12 bits is placed between the data parts. After modulation with MSK, the symbol rate given for both uplink (UL-ULP mode) and downlink is 2 380.371 sym/s. [20]

3.3.2 TSMA

The TSMA procedure is where the radio frame is split into RBs, which are then spread over 24 subcarriers at different transmission times pseudo-randomly in what is called a TSMA pattern, as illustrated in Figure 16.

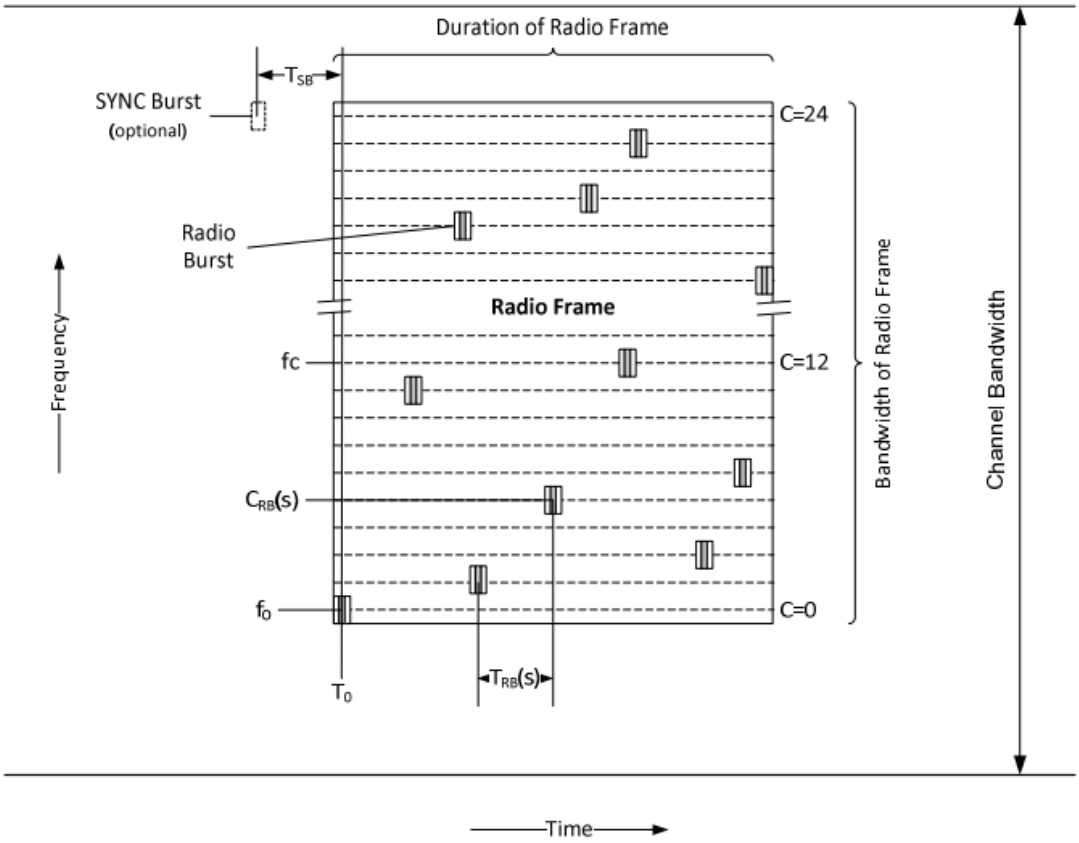

Figure 16. TSMA operation. [20]

For uplink, there are three groups specified for the patterns (UPG1-3), and one for downlink (DPG). UPG1 is used for single transmission, UPG2 when the radio frame is repeated and UPG3 is only used for frames with low latency requirements. The time between RBs is the Radio-burst Time $\boldsymbol{t_{RB}}$, measured between the middle points of pilot sequences of consecutive RBs in the number of symbols with duration $\Delta\boldsymbol{t}$. The tables 6-50, 6-52 and 6-54 of [20] give $\boldsymbol{t_{RB}}$ for each combination of pattern number $\boldsymbol{p}$ and RBs index $\boldsymbol{s}$ in the uplink. Table 6-57 gives the same for downlink.

As mentioned previously, the pilot sequence is placed between two data sections. As such, between middle points of two RBs lie the equivalent of two data sections and one pilot section in the amount of symbols. Thereof the separation between two RBs, denoted as $\boldsymbol{t_{OFF}}$, is

$$t_{OFF}(s,p) = \left(t_{RB}(s,p) - 2\left(data\ section + \frac{pilot\ seq}{2} \right) \right) * \Delta t \quad (3)$$

$$t_{OFF}(s,p) = (t_{RB}(s,p) - 32) * \Delta t. \quad (4)$$

This is illustrated in Figure 17. [20]

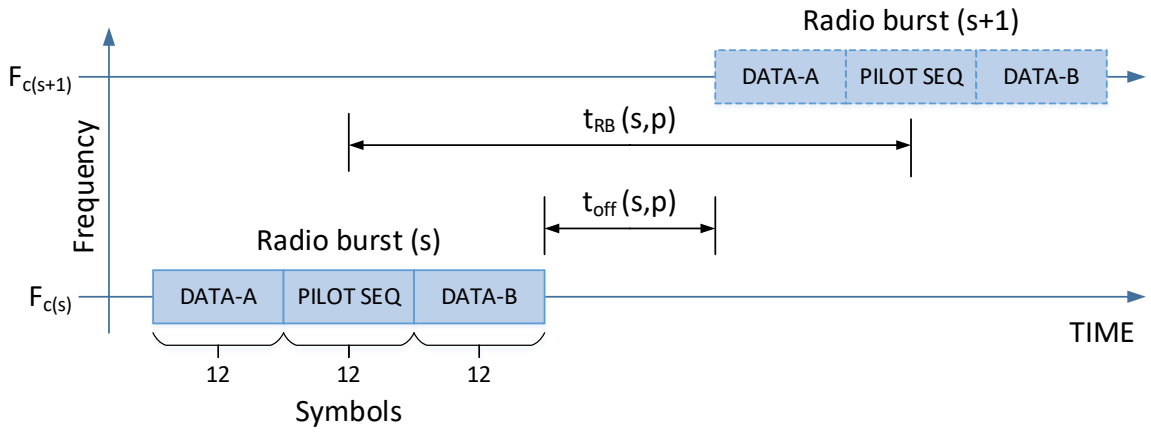

Figure 17. Determining time between radio bursts for TS-UNB uplink [20].

Given the previously mentioned symbol rate, the symbol duration $\Delta t = 1/2380.371\ Sym/s = 0.42\ ms$. The average for the number of symbols, $t_{RB,avg}$ for each pattern group are as follows:

- UPG1: 379
- UPG2: 378
- UPG3: 82
- DPG: 507

The radio frame transmission times are in Table 6-59 of [20], and show below in Table 11.

Table 11. TS-UNB radio frame transmission times [20].

Mode	RB duration	Core Frame on-air time	Ext. frame on-air time
UL-ULP	15.14 ms	362.97 ms	15.14 ms per add. Byte in MPDU
UL-ER	90.74 ms	2 177.81 ms	90.74 ms per add. Byte in MPDU
DL-TS	11.76 … 21.43 ms	105.57 ms	211.73 … 383.13 ms per add. ext. frame block

4 FEASIBILITY STUDIES

This chapter presents all factors evaluated for feasibility. First, relevant background information and theory is given for each factor and what values are used for relevant parameters. Any assumptions made and limitations are acknowledged. Further details all calculations and simulations used to evaluate each factor are provided in Appendix 2.

As mentioned in Chapter 1, a wireless link is always compromise between spatial coverage, data rate and reliability. This chapter will explore the relationships between each of them. Claude Shannon described that all electronic communication can be described by a system, which comprises of three basic parts, a transmitter, a receiver and a communications channel, as shown in Figure 18. A modulated signal is emitted by the transmitter and the receiver attempts to receive and decode it. It may not always succeed, since the communication channel imparts detrimental effects upon the signal's reception.

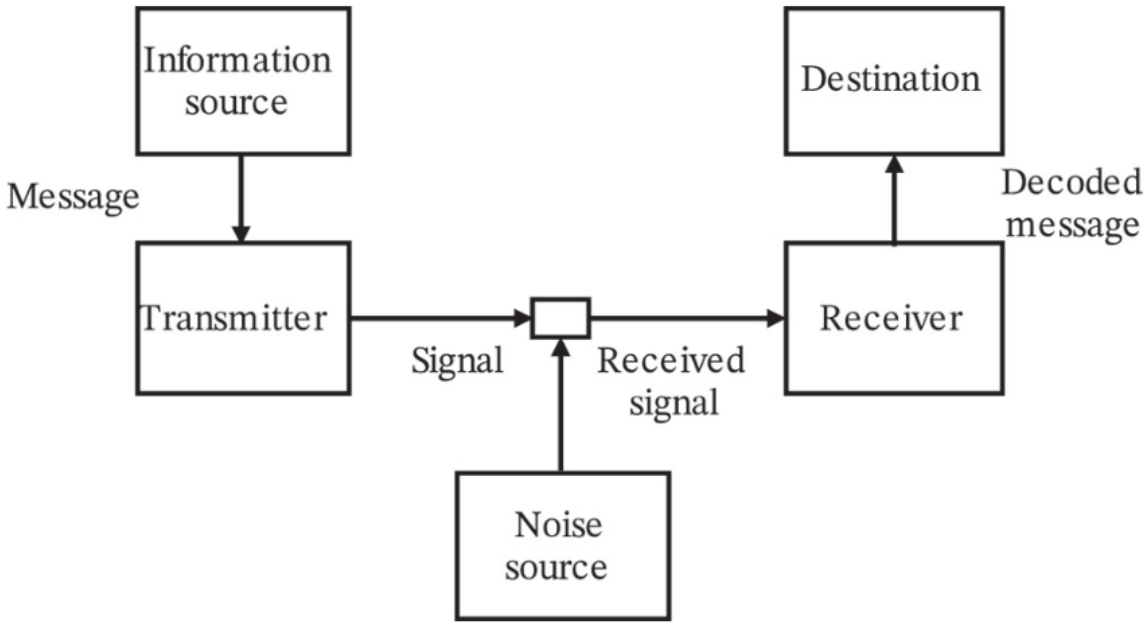

Figure 18. Communication system model [48].

The signal loses intensity over distance and, especially in the case of wireless transmission, there may be absorption and other signals or reflections, which cause interference at the receiver. The mechanic is combined in the SNR, which is the ratio of received average signal

power and average noise power. The higher the value of SNR, the more likely is a successful reception. [13, 48, 52]

Radio frequency (RF) band usage is a limited resource and subsequently heavily regulated by laws of nation states around the world, as well by laws of nature. Without regulation, it is likely that devices would be "polluting" the airways with overpowered transmitters just to get their message "heard" over others more easily. To avoid utter cacophony, the power of transmissions is limited in most parts of the world.

Since transmission power is being capped, to achieve greater spatial coverage, the industry has turned to narrowing bandwidth. This is why we see many "narrow-band" technologies being developed. A good intuition can be gained from the Shannon-Hartley theorem in an Additive White Gaussian Noise (AWGN) channel

$$\boldsymbol{C = Blog_2\left(1 + \frac{S}{N}\right)}, \tag{5}$$

where $\boldsymbol{C}$ is capacity in bits per second (bps) of the channel, $\boldsymbol{B}$ is the bandwidth in hertz, $\boldsymbol{S}$ and $\boldsymbol{N}$ accounts for the average signal and noise power over the bandwidth in watts as a linear power ratio. The theorem dictates, that for a fixed SNR, narrowing/decreasing bandwidth has a decreasing effect to capacity. On the other hand, if bitrate requirement is fixed low, better SNR can be achieved by lowering the bandwidth.

Data rate is related to modulation technique. If transmission power is fixed, usage of low modulation rate techniques such as BPSK, QPSK or GMSK means putting more energy for each transmitted bit, which increases the perceived SNR at the receiver and increases the probability of successful decoding. In other words, communication range can be increased. Or if the range is fixed, then transmission power may be decreased, resulting in lower energy consumption. Using lower modulation rate techniques also commonly means simpler hardware design, which potentially lowers costs and provides further energy savings. [12]

4.1 Coverage

The communication between a transmitter and receiver is possible only if the receiver is able to successfully decode the transmitted signal. More specifically, coverage area is defined as all spatial positions around the transmitter where the SNR perceived at the receiver is larger than a threshold for successful decoding. This point is also called the receiver sensitivity. At which physical distance this threshold is crossed depends on the degrading effects of loss and interference (noise and fading) imposed on the channel. [48]

A basic tool of wireless communication engineering is link budgeting. It is used to estimate the propagation loss and signal power level at the receiver of a link. It is required in estimating achievable user data rates in both up- and downlink, and the ultimate communication range, where this rate is still achievable. The link budget is indeed called a budget because it is much like a book-keeping of the gains and losses related to the transmitter, communication medium (wireless channel) and the receiver, as illustrated in Figure 19.

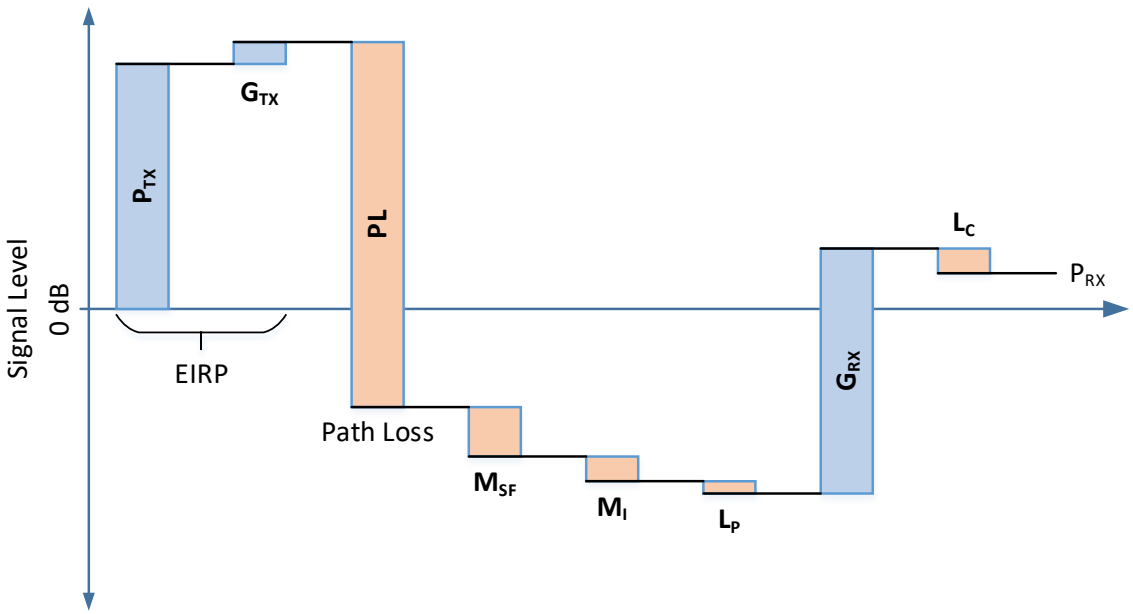

Figure 19. Gains and losses affecting signal level of a transmission.

Since link budget involves characterization of the link, it relies on a propagation model. The model's purpose is to estimate link characteristics as close to real life conditions as possible. It typically may account for distance-dependent path loss and spatio-temporal random effects caused by shadowing and Doppler-effect, as well as interfere from multipath propagation of the signal and other transmissions. [56]

In the budget, gains come from transmission power and antenna directivity, while losses are caused by the radio environment, attenuation and inefficiencies in cables and circuitry, and noise level at the receiver. The end result of the link budget is the allowed path-loss (***APL***) in the link, which is an indication of communication range. The general link budget formula is

$$\boldsymbol{APL = EIRP + G_{RX} - P_{RX,min} - M_{Total} - L_{Total}} \quad (\boldsymbol{dB}). \tag{6}$$

These parameters can be further broken down to a finer grained set of items contributing to the overall budget. The following paragraphs explain some of these parameters. [31]

The equivalent isotropically radiated power (**EIRP**) is an often used figure in link budgets, which combines the transmit power $\boldsymbol{P_{TX}}$ with transmit antenna's equivalent isotropic gain $\boldsymbol{G_{TX}}$. This is expressed as

$$\boldsymbol{EIRP = P_{TX} + G_{TX}} \quad (\boldsymbol{dBi}). \tag{7}$$

The receiver side antenna also has a gain, denoted as $\boldsymbol{G_{RX}}$. Gain is a coefficient, which describes the physical directional ability of the antenna to induce current with response electromagnetic radiation, mostly for the frequency the antenna is tuned for.

As explained in [52], the net effect of both loss and noise contribute to the degradation of average SNR, as losses decreased the perceived signal power, while interference sources accumulate the perceived noise power. For digital communications, SNR may be substituted by $\boldsymbol{E_B/N_0}$, which is a bit-normalized version of SNR. Bit energy is denoted by $\boldsymbol{E_B}$ in joules and it equals to $\boldsymbol{S \times t_b}$, where $\boldsymbol{S}$ is signal power in watts and $\boldsymbol{t_b}$ is bit time in seconds. $\boldsymbol{N_0}$

denotes noise power spectral density in watts per Hz (thermal noise), which equals to $\boldsymbol{N/B}$, where $\boldsymbol{N}$ is noise power and $\boldsymbol{B}$ is bandwidth. Because $\boldsymbol{t_b}$ is reciprocal with data rate $\boldsymbol{R_b}$ in bits/s, we can instead write $\boldsymbol{E_b = S \times 1/R_b}$. Finally, $\boldsymbol{E_B/N_0}$ relation to $\boldsymbol{S/N}$ can be expressed as

$$\frac{\boldsymbol{E_b}}{\boldsymbol{N_0}} = \frac{\boldsymbol{S\, t_b}}{\boldsymbol{N/B}} = \frac{\boldsymbol{S/R_b}}{\boldsymbol{N/B}} = \frac{\boldsymbol{S}}{\boldsymbol{N}}\left(\frac{\boldsymbol{B}}{\boldsymbol{R_b}}\right) \tag{8}$$

Receiver sensitivity, expressed as $\boldsymbol{P_{Rx,min}}$ and often given in dBm, is the minimum required power level at the receiver, which allows successful identification and processing of the transmitted signal. Sensitivity can expressed as

$$\boldsymbol{P_{RX,min} = N_0 + 10 * log_{10}(B) + NF + SNR_{reqd}} \quad \boldsymbol{(dB)}, \tag{9}$$

where $\boldsymbol{NF}$ is the Noise Figure, and $\boldsymbol{SNR_{reqd}}$ the SNR required to reach a predefined reliability in decoding of information. [15]

Reliability is an important angle in modeling communication links. Generally, this may be thought of as the probability of successfully transmitting one bit over the communication channel. On the flip-side, a common parameter is Bit-Error Rate (BER), which defines that how many transmitted bits may be expected to be erroneously decoded at the receiver. BER is a simple metric, but often times not enough, since information is commonly transmitted in terms of packets. In cellular communication transmitted information is referred to as blocks. PER and BLER are a much more complex topics than BER, because in addition to the communication channel characteristics, they are subject to protocol mechanics and other techniques, which aspire to enhance successful decoding of blocks and packets. For example, in modern communications, the transmitted information is usually coded with error-correcting code (ECC). As stated in [27], this allows detection or correction of bit errors by the receiver's decoder, which were introduced to the modulated signal as it was transmitted through the channel.

Link budgets are always conducted with a target reliability in mind, which links back to $\boldsymbol{SNR_{reqd}}$. It sets the threshold of $\boldsymbol{P_{RX,min}}$, at which one may expect to reach the reliability target. The value of $\boldsymbol{SNR_{reqd}}$ depends on characteristics of the technology in question and the desired data rate. It is commonly derived through various methods such as analytical calculation or statistical analysis from simulations or empirical measurements.

Thermal noise $\boldsymbol{N_0}$ is ever present noise perceived by the receiver circuits, which is caused by the thermal vibrations of atoms. It is commonly tied to temperature via the Boltzmann's constant $\boldsymbol{k = 1.38064852 * 10^{-23}\ m^2\ kg\ s^{-2}\ K^{-1}}$:

$$\boldsymbol{N_0 = 10 * log_{10}(kT) \quad (dB)}. \tag{10}$$

The temperature used in calculations for terrestrial systems is commonly $\boldsymbol{T = 290\ K = 16.85}$ ℃. [47]

Noise figure $\boldsymbol{NF}$ is the decibel equivalent of the absolute valued noise factor, which in turn is the ratio of SNR measured at the input of a system (i.e. a receiver component) to the SNR measured at the output. Any amplification (gain) by the component will affect both the input signal and noise, which will introduce additional noise at the output. The Noise Figure is a value commonly included in link budgeting, which is meant to account for various imperfections in the receiver circuitry. [47]

The transmitted signal can experience absorption, scattering, diversion, or reflection on its path to the receiver, which are also considered losses – part of the signal energy is lost. $\boldsymbol{M_{Total}}$ and $\boldsymbol{L_{Total}}$ are the sums of all margins and losses, respectively. The margins include parameters such as, small scale fading ($\boldsymbol{M_{SCF}}$), shadow fading ($\boldsymbol{M_{SF}}$) and interference ($\boldsymbol{M_I}$) margin, so that

$$\boldsymbol{M_{Total} = M_{SCF} + M_{SF} + M_I \quad (dB)} \tag{11}$$

Interference on the other hand is perceived at the receiver. It is like another conversation at the neighboring table making it harder for you to understand what your friend is talking to you. Noise and interference consist of mechanisms and sources such as thermal noise, atmospheric noise, galaxy noise, intermodulation noise, switching transients, and other interfering signal transmissions. Link budgeting commonly uses margins to counter these degrading effects to the signal. [31; 52]

Parameters marked explicitly as losses, which are more statistical in nature, are clumped in the $\boldsymbol{L_{Total}}$ parameter. These include, for example, feeder cable loss ($\boldsymbol{L_C}$), antenna pointing loss ($\boldsymbol{L_{AP}}$), wall penetration loss ($\boldsymbol{L_{Pen}}$), body loss ($\boldsymbol{L_{Body}}$), etc. Generally, the sum of all applicable loss components $\boldsymbol{L_k}$, as in

$$\boldsymbol{L_{Total}} = \sum_{\boldsymbol{k=1}}^{\boldsymbol{K}} \boldsymbol{L_k} \quad (\boldsymbol{dB}). \tag{12}$$

Maximum Coupling Loss (MCL) is another common way to which the industry and literature refer when discussing about coverage. MCL is defined as the difference in the conducted power level, when measuring at the antenna ports of the transmitter and receiver. The gains of transmitting or receiving antennas are not included, because the antenna connector is used as the reference point. MCL is essentially the maximum loss in the conducted power level required for operation. Figure 20 shows a visualization of the concept. [34]

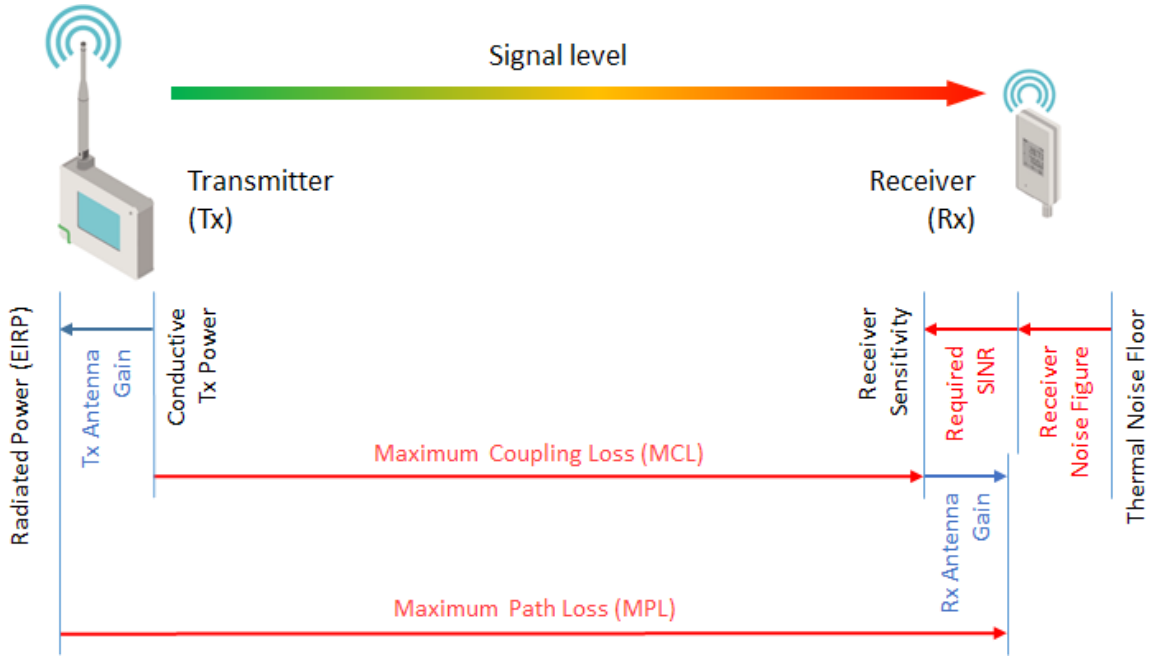

Figure 20. MCL and MPL.

In terms of the link budget, for a given SNR, MCL is expressed as:

$$\boldsymbol{MCL = P_{TX} - (N_0 + 10log_{10}(B) + NF + SNR)} \quad \boldsymbol{(dB)}. \tag{13}$$

On the other hand, $\boldsymbol{SNR_{reqd}}$ can also be calculated as a function of MCL:

$$\boldsymbol{SNR_{reqd} = P_{TX} + N_0 - NF - 10log_{10}(B) - MCL} \quad \boldsymbol{(dB)}. \tag{14}$$

Furthermore, the term Maximum Path Loss (MPL) is also sometimes used as a measure of coverage. It can be thought of as the maximum APL in terms of link budget that a technology can support. As also depicted in Figure 20, MPL is measured as the difference in radiated power levels at the transmitting and receiving antennas, and as such incorporates the gains of the transmitting and receiving antennas. [34]

MPL may be expressed as

$$\boldsymbol{MPL = MCL + G_{TX} + G_{RX}} \quad \boldsymbol{(dB)}. \tag{15}$$

4.1.1 Regarding Propagation Models

The link budget will provided the APL for the link in question, or how much signal power (in dBs) drop may occur between transmitter and receiver. However, to find out how much this drop is in distance over the land (or space), we must turn to propagation models.

The purpose of propagation models is to serve as tools in predicting the detrimental effects to the signal on its path to a receiver. The major component in models of path loss over a distance is Free Space Path Loss (FSPL), which is covered in the next chapter. Also, as previously mentioned, a signal is affected by a number of variables, which come from the physical environment such as the atmosphere and physical objects, as well as the signal itself and other signals. Part of these effects are categorized as small scale fading, which accounts for short time variations in signal level due to Doppler shifts and constructive or destructive multipath propagation. Fading due to multipath propagation can also be frequency specific, which means that in a multichannel system, such as cellular systems, subcarriers are not evenly affected. Another part for effects is from large scale fading, also called shadowing, which refers to attenuation of signal level from obstacles in the direct transmission path. Common values for shadowing range from 6 to 10 dB [31]. Shadowing affects the signal in longer time scales. FSPL is sometimes also included, when discussing about large scale fading. Figure 21 gives an illustration on signal attenuation over distance along with small- and large-scale variations. [13; 15; 52]

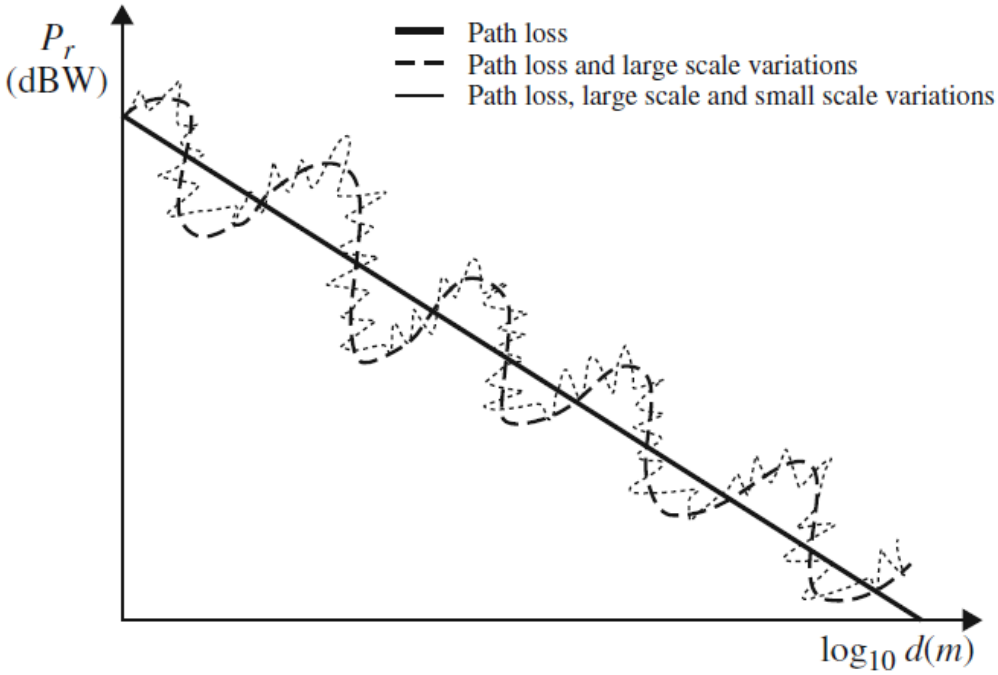

Figure 21. Path-loss and effects of large-scale and small-scale variations as a function of distance to signal power [15].

Propagation models cannot accurately provide predictions of the nature of any particular link, but instead provide in most cases a statistical average of the path loss. Also, no one model can provide accuracy in all environments and situation, and thus multiple models have been created to account for the many situations (i.e. urban or rural, flat or mountainous) where wireless links are used. In the following chapter, two models are presented, and of which the Hata/COST 213 is used in this work. [56]

4.1.2 Free Space Path Loss Model

The FSPL model sets the theoretical lower bounds for signal propagation based geometric properties and distance. It is often used as a benchmark for wireless channel model performance studies. The intensity of electromagnetic waves propagating from a single point in ideal free space decreases by the inverse-square of the distance from the source. FSPL does not take into account any attenuations, atmospheric effects, obstructions, reflections or intrusions to the radio path. Thus, of course, in practice the scenario where this model could apply accurately is deep space communications. FSPL is still a component of the total path

loss in all wireless communication and can be combined with other path loss models developed for practical purposes. [56]

FSPL is expressed as

$$\boldsymbol{PL} = \left(\frac{\boldsymbol{4\pi d}}{\boldsymbol{\lambda}}\right)^{\boldsymbol{2}} \tag{16}$$

where $\boldsymbol{d}$ is the distance between the receiver and transmitter in meters and $\boldsymbol{\lambda}$ the wave length. Since $\boldsymbol{\lambda = c/f_C}$ where $\boldsymbol{c}$ is the speed of light and $\boldsymbol{f_C}$ the carrier frequency in Hz, we can write

$$\boldsymbol{FSPL} = \left(\frac{\boldsymbol{4\pi d}}{\frac{\boldsymbol{c^2}}{\boldsymbol{f_C}^{\boldsymbol{2}}}}\right)^{\boldsymbol{2}} = \frac{\boldsymbol{(4\pi d f_C)^2}}{\boldsymbol{c^2}} \tag{17}$$

In decibels this is

$$\boldsymbol{FSPL = 10\, log_{10}\left(\frac{(4\pi d f_C)^2}{c^2}\right) \quad (dB)}, \tag{18}$$

which is commonly expressed in form

$$\boldsymbol{FSPL = 32.45 + 20\, log_{10}(d) + 20\, log_{10}(f_C) \quad (dB)}. \tag{19}$$

4.1.3 Hata/COST 231 Model

Hata/COST 231 model has its roots in the empirical measurements performed by Okumura et. al. in city of Tokyo, Japan, published in 1968. These measurements where further defined as a series of empirical relationships by Hata et. al., which are more commonly known as the Okumura-Hata model. Since then, the model has undergone further refining development

steps and the latest iteration was introduced in the European Conference of Postal and Telecommunications Administrations and European Radiocommunications Committee Report 68. [47]

The Hata/COST 213 model is based on curve matching to measurements of path loss done in environments categorized as urban, suburban or open/rural. It's defined for frequencies between 30 MHz and 3 GHz and between 1 and 100 km. Antenna heights are expected within range of 1 to 200 meters. The model accounts for fading as shadowing, which follows a Gaussian distribution with a mean of 0 dB and standard deviation of 5 dB. The model is best used for generic studies with an interest in average path loss over distance. [47]

According to [31; 47], the urban environment specifies the core of the Hata/COST 213 model, and is expressed as

$$\begin{aligned} PL_{Urban}^{Hata/COST\ 231} &= 69.55 + 26.16 * log_{10}(f_{C,MHz}) - 13.82 * log_{10}(h_{TX}) \\ &- a(h_{RX}) + [44.9 - 6.55 * log_{10}(h_{TX})] * log_{10}(d_{km})^{\beta}, \end{aligned} \tag{20}$$

where $f_{C,MHz}$ is the carrier frequency in megahertz, h_{TX} and h_{RX} are the effective heights of the transmitting and receiving antennas and d_{km} the distance between transmitter (TX) and receiver (RX) antennas in kilometers. The parameters β is used to fit the model for distance between 20 and 100 km, and is defined as

$$\beta = \begin{cases} 1, & d_{km} \leq 20km \\ 1 + \left(0.14 + 1.87 * 10^{-4} * f_{C,MHz} + 0.00107 * h_{TX}\right) & \\ * \left(log_{10}\left(\frac{d_{km}}{20}\right)\right)^{0.8}, & 20km < d_{km} \leq 100km \end{cases} \tag{21}$$

The effective antenna height is the height of the antenna with respect to the average terrain height between link end-points. The model can be adapted with regards to city size and

carrier frequency through the term $\boldsymbol{a(h_{rx})}$. For small and medium sized cities it is expressed as

$$\begin{aligned} \boldsymbol{a_{town}(h_{RX}) = \left[1.1 * log_{10}(f_{C,MHz}) - 0.7\right] * h_{RX}} \\ \boldsymbol{- \left[1.56 * log_{10}(f_{C,MHz}) - 0.8\right]} \end{aligned} \tag{22}$$

For a large city and carrier frequencies below 300 MHz, it is

$$\boldsymbol{a_{urbanLF}(h_{RX}) = 8.29 * [log_{10}(1.54 * h_{RX})]^2 - 1.1,} \tag{23}$$

while for frequencies above 300 MHz, it is

$$\boldsymbol{a_{urbanHF}(h_{RX}) = 3.2 * [log_{10}(11.75 * h_{RX})]^2 - 4.97} \tag{24}$$

The path loss for suburban and rural/open areas are based on the urban model, so that

$$\boldsymbol{PL_{Suburban}^{Hata/COST\ 231} = PL_{Urban}^{Hata/COST\ 231} - 2 * \left[log_{10}\left(\frac{f_{C,MHz}}{28}\right)\right]^2 - 5.4,} \tag{25}$$

and for rural/open it is

$$\begin{aligned} \boldsymbol{PL_{Open}^{Hata/COST\ 231}} \\ \boldsymbol{= PL_{Urban}^{Hata/COST\ 231} - 4.78 * \left[log_{10}(f_{C,MHz})\right]^2 + 18.33} \\ \boldsymbol{* log_{10}(f_{C,MHz}) - 40.98.} \end{aligned} \tag{26}$$

4.1.4 Link Budgets

The values assumed for link budgeting are given in Table 12. These represent the author's choice and view of what are common values used in industry, as well as what is given in specifications and described in previous chapters.

Table 12. Uplink link budget parameters.

			NB-IoT	**LoRaWAN**	**TS-UNB**
Carrier (center) freq.			880.09 MHz	868.10 MHz	868.10 MHz
Carrier BW		1.	180 kHz	125 kHz	100 kHz
Subcarrier BW	$\boldsymbol{B_{SC}}$	2.	15 kHz	125 kHz	60.223 kHz
No. subcarriers	$\boldsymbol{n_{SC}}$	3.	12	1	24
Channel BW	$\boldsymbol{B}$	4.	$10\log_{10}(\mathbf{2}.*\mathbf{3}.)$ (dB)		$10\log_{10}(\mathbf{1}.)$ (dB)
End-Device ant. elevation	$\boldsymbol{h_{TX}}$		2 m		
BS ant. elevation	$\boldsymbol{h_{RX}}$		40 m		
TX Power	$\boldsymbol{P_{TX}}$	5.	23 dBm	14 dBm	14 dBm
TX Antenna Gain	$\boldsymbol{G_{TX}}$	6.	0 dBi		
	$\boldsymbol{EIRP}$	7.	$(\mathbf{4}.+\mathbf{5}.)$		
RX Antenna Gain	$\boldsymbol{G_{RX}}$	8.	17 dBi	6 dBi	6 dBi
Thermal Noise	$\boldsymbol{N_0}$	9.	$10\log_{10}(k*T*1000) = -174$ (dBm)		
Noise Power	$\boldsymbol{N}$	10.	$(\mathbf{4}.+\mathbf{9}.)$		
Noise Figure	$\boldsymbol{NF}$	11.	3 dB (eNB)	6 dB	6 dB
	$\boldsymbol{SNR_{Reqd}}$	12.	Table 13	Table 15	1 dB
RX sensitivity	$\boldsymbol{P_{RX,min}}$	13.	$(\mathbf{8}.+\mathbf{9}.+\mathbf{10}.)$		
Shadowing Margin	$\boldsymbol{M_{SF}}$	14.	7 dB		
Interference Margin	$\boldsymbol{M_I}$	15.	4 dB		
Total Margin	$\boldsymbol{M_{Total}}$	16.	$(\mathbf{12}.+\mathbf{13}.)$		
Cable Loss	$\boldsymbol{L_{C,TX}}$	17.	0 dB		
Cable Loss	$\boldsymbol{L_{C,RX}}$	18.	3 dB		
Total Loss	$\boldsymbol{L_{Total}}$	19.	$(\mathbf{15}.+\mathbf{16}.)$		

Path loss result by Hata/COST 231 model calculated using equations from (20) to (26) with values given in Table 12 is presented for all environments in Figure 22.

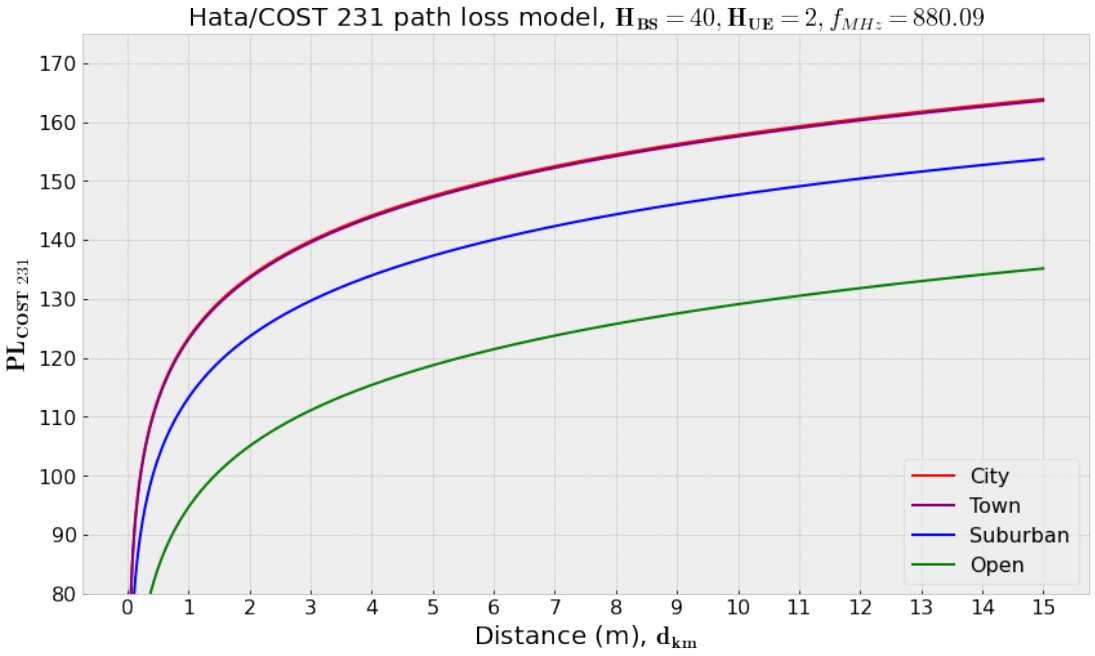

(a)

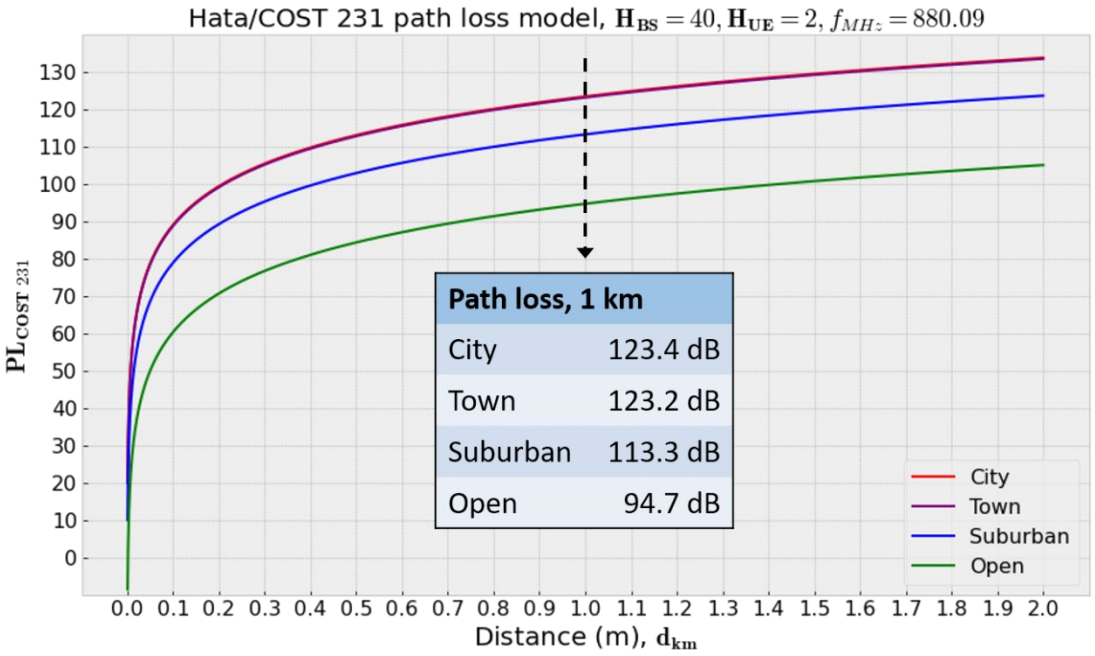

(b)

Figure 22. Path loss curves for different environment categories with Hata/COST 231 model with BS height at 40 meters and end-device at 2 meters, and carrier frequency 880.09 MHz (NB-IoT). Range up-to: a) 15 km and b) 2 km.

This analysis uses the rural / open environment model. The difference in Hata/COST 231 model path loss between the carrier frequencies of NB-IoT and LoRa / TS-UNB is only about 0.1% (~ 10 meters) in favor of LoRa / TS-UNB. This analysis thus applies Figure 22 for all technologies.

4.1.4.1 NB-IoT

As described in chapter 3.1.2, NB-IoT employs an adaptive resource allocation scheme, which optimizes the combination of MCS, repetitions, TBS and number of RUs. What is needed is the target SNR threshold, which corresponds to a target minimum BLER (as stated in [34]) of 10% for each combination of the scheme. One can think, that the cellular base station has a lookup-table for these thresholds, but the information is not public for most companies who manufacture base station equipment. Thus for this work, the lookup-table was derived using MatLab simulations. The used simulation code is provided as part of the MathWorks MatLab LTE Toolbox. Simulations were only performed for uplink using the code in the NB-IoT NPUSCH Block Error Rate Simulation.

The simulations allow to insert values for parameters corresponding to the items in Table 9 and Table 7, and graph BLER result over a range of SNR. Multi-tone operation with allocation of $\boldsymbol{n_{SC}^{RU} = 12}$ subcarriers was assumed, and no repetitions, but otherwise default parameters were used. Each run was performed with minimum of 200 simulated blocks. After setting the parameters, the simulation models the transmission channel effects through the following steps when run:

- Baseband waveform creation with random data by SC-FDMA modulation
- Passing the resulting passband waveform through channel of AWGN and frequency-selective fading
- Performing receiver operations, including block CRC checking
- Calculation of BLER against block CRC results.

Figure 23 provides an example of the resulting graph. [45]

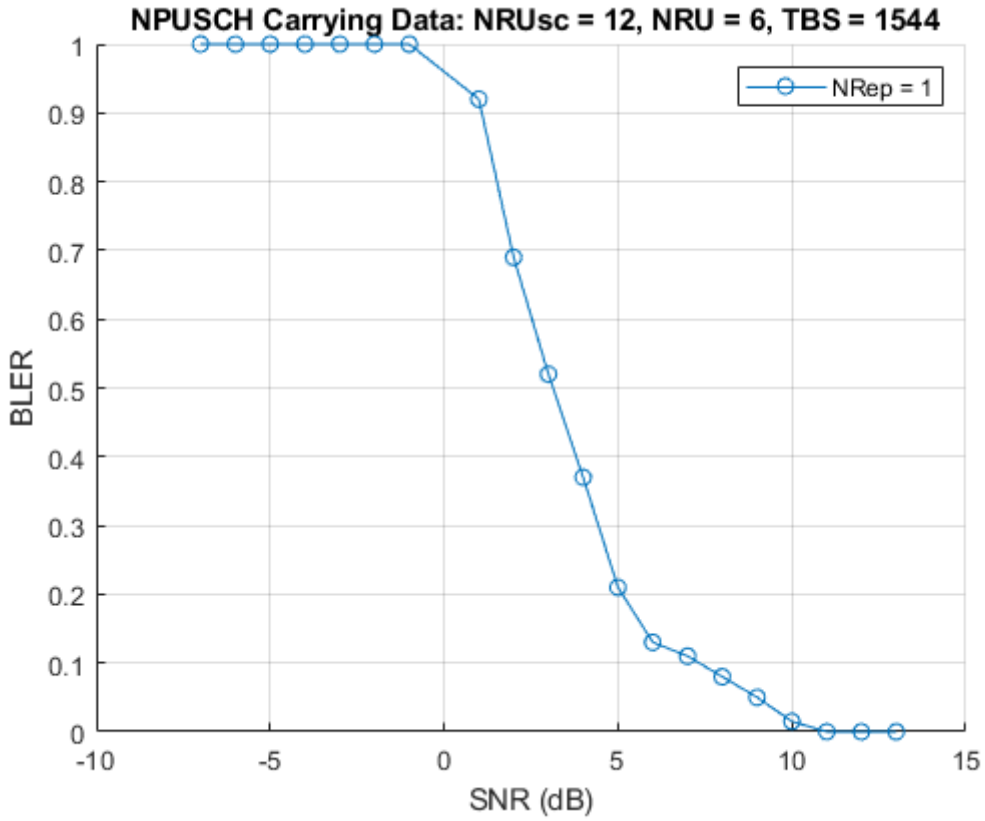

Figure 23. NB-IoT simulation result for NPUSCH for TBS=1544.

Table 13 represents the results of running the simulation for each $\boldsymbol{i_{MCS}}$ and $\boldsymbol{i_{TBS}}$ combination against each $\boldsymbol{i_{RU}}$ for a value of corresponding $\boldsymbol{SNR_{reqd}}$ to achieve a BLER of less than 10%. In other words, this value signifies the SNR required to be able to transmit using the associated TBS at target reliability.

Table 13. NB-IoT uplink TBS values with corresponding SNR requirement values (in dB).

SNR_{reqd}	i_{RU}								$min\{SNR_{reqd}\}$
i_{MCS}	0	1	2	3	4	5	6	7	
0	-3.3	-6.3	-7.2	-7.5	-5.9	-6.5	-7.0	-7.6	-7.6
1	-2.5	-3.2	-4.1	-3.8	-4.3	-4.0	-6.0	-6.4	-6.4
2	-0.9	-2.2	-2.1	-2.9	-4.0	-4.0	-5.2	-5.4	-5.4
3	0.0	-0.5	-1.2	-2.2	-3.1	-3.2	-4.2	-4.0	-4.2
4	0.9	-0.1	-0.5	-1.2	-1.7	-1.8	-3.2	-3.7	-3.7
5	1.6	0.5	-0.1	-0.4	-0.9	-1.4	-2.0	-2.6	-2.6
6	2.7	1.6	0.6	0.6	0.0	-0.6	-1.3	-2.0	-2.0
7	3.7	2.7	1.7	1.8	0.6	0.4	-0.1	-0.8	-0.8
8	4.2	3.6	2.8	2.4	2.1	1.2	0.7	-0.1	-0.1
9	5.1	4.5	3.7	3.3	2.8	2.2	1.6	0.7	0.7
10	5.5	5.2	4.6	4.0	4.0	2.9	2.1	1.7	1.7
11	6.8	6.5	6.0	5.5	4.9	3.9	3.4	2.8	3.4
12	8.4	7.8	7.2	8.0	5.7	5.3	4.4	3.8	3.8
13	9.5	9.3	8.5	8.8	7.0	6.9	5.8	5.2	5.2

For reference, the minimum value of SNR_{reqd} were also extracted for each MCS and these are further shown in Figure 24. As may be observed, in more favorable channel conditions, greater amounts of data may be transmitted without errors.

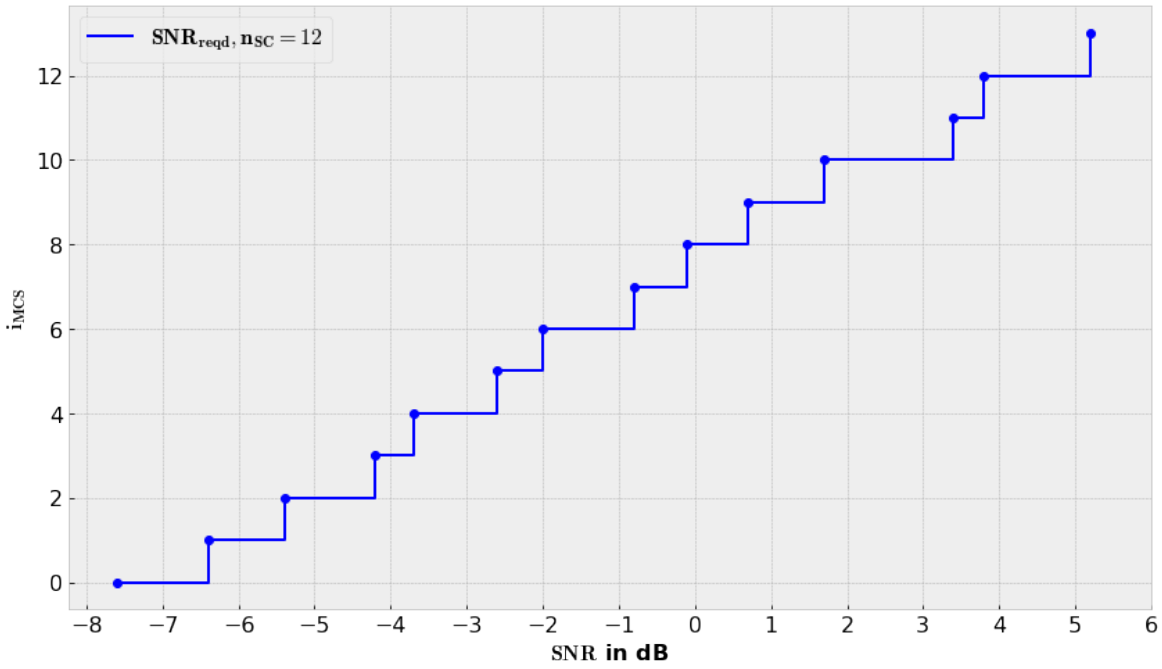

Figure 24. Indicative NB-IoT uplink SNR thresholds for each i_{MCS} level, while achieving BLER of 10 %.

Using equations (6), (7), (9) and link budget parameter values from Table 12, the APL can be calculated for each TBS index. These results are presented in Table 14.

Table 14. NB-IoT uplink TBS values with corresponding APL values (in dB).

APL	i_{RU}							
i_{MCS}	0	1	2	3	4	5	6	7
0	147.7	150.7	151.6	151.9	150.3	150.9	151.4	152.0
1	146.9	147.6	148.5	148.2	148.7	148.4	150.4	150.8
2	145.3	146.6	146.5	147.3	148.4	148.4	149.6	149.8
3	144.4	144.9	145.6	146.6	147.5	147.6	148.6	148.4
4	143.5	144.5	144.9	145.6	146.1	146.2	147.6	148.1
5	142.8	143.9	144.5	144.8	145.3	145.8	146.4	147.0
6	141.7	142.8	143.8	143.8	144.4	145.0	145.7	146.4
7	140.7	141.7	142.7	142.6	143.8	144.0	144.5	145.2
8	140.2	140.8	141.6	142.0	142.3	143.2	143.7	144.5
9	139.3	139.9	140.7	141.1	141.6	142.2	142.8	143.7
10	138.9	139.2	139.8	140.4	140.4	141.5	142.3	142.7
11	137.6	137.9	138.4	138.9	139.5	140.5	141.0	141.6
12	136.0	136.6	137.2	136.4	138.7	139.1	140.0	140.6
13	134.9	135.1	135.9	135.6	137.4	137.5	138.6	139.2

Cross-referencing between APL values of Table 14 and the path-loss curves in Figure 22 gives an indication of the TBS index and distance. This information may be used to evaluate, which i_{MCS} and n_{RU} combinations are available for a given distance between transmitter and receiver.

4.1.4.2 LoRaWAN

LoRa receiver sensitivity is commonly between -116 to -137 dBm depending on the bandwidth used. Greater bandwidth will increase throughput, but weaken sensitivity. The sensitivity value also depends on the SF used through the set requirement for level of SNR. Semtech specifies this in the datasheets of modules, i.e. in [54]. Table 15 gives an example listing for the SX1272 model, while sensitivity is calculated with equation (9). Similar results for BER 10^{-6} were also produced by authors in [19].

Table 15. LoRa sensitivity and SNR requirement values for corresponding SF for bandwidth of 125 kHz [54].

SF Config	2^{SF} Chips / symbol	LoRa Demod. SNR_{reqd} (dB)	Sensitivity $P_{RX,min}$ (dB)
6	64	-5	-122
7	128	-7.5	-124.5
8	256	-10	-127
9	512	-12.5	-129.5
10	1024	-15	-132
11	2048	-17.5	-134.5
12	4096	-20	-137

Using equations (6), (7), (9) and link budget parameter values from Table 12, the APL can be calculated for each SF index. The APL was further compared with the Hata/COST231 rural/open PL curve of Figure 22. These results are presented in Table 22 in Chapter 5.1.

4.1.4.3 TS-UNB

According to specification [20], TS-UNB shall use MSK modulation in the uplink. For MSK, there exists a well-established statistical formula in evaluating BER for an AWGN channel, as described in [52], which is

$$\boldsymbol{BER} = \frac{\mathbf{1}}{\mathbf{2}}\boldsymbol{erfc}\left(\sqrt{\frac{\boldsymbol{E_b}}{\boldsymbol{N_0}}}\right). \tag{27}$$

Here **efrc** is the complementary error function and $\boldsymbol{E_b/N_0}$ the energy per bit per noise power spectral density, as defined by eq. (8). In Figure 25, BER is graphed as a function of $\boldsymbol{E_b/N_0}$.

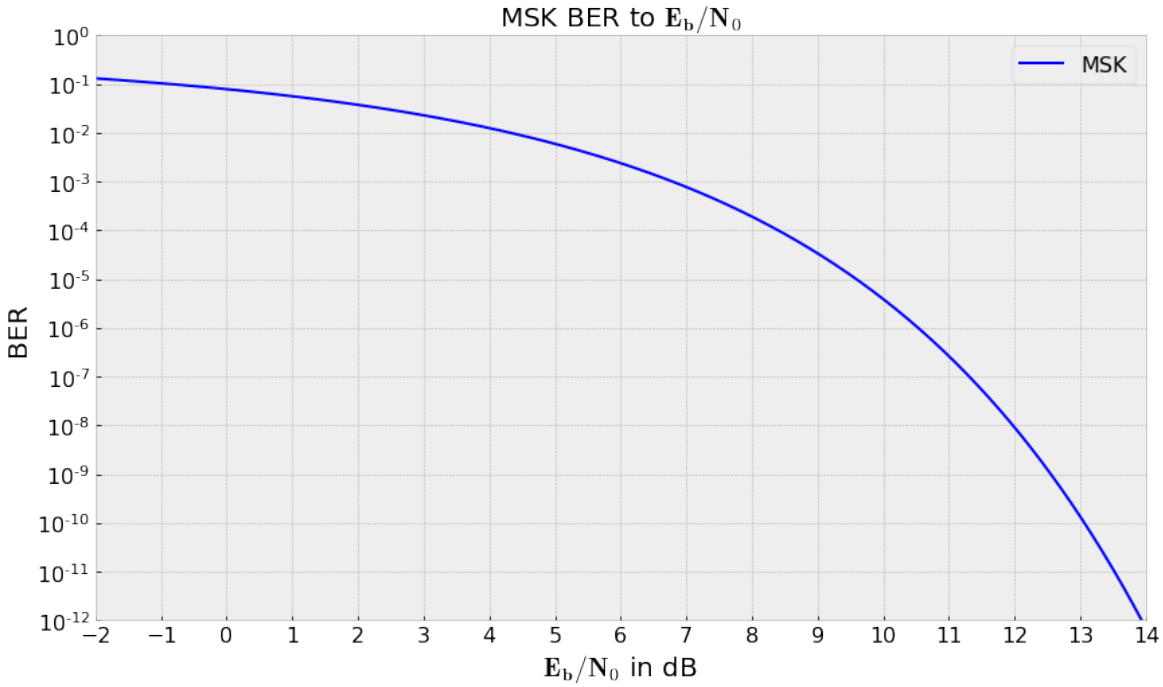

Figure 25. MSK modulation BER to $\mathbf{E_b/N_0}$.

It may be observed, that for our BER requirement of 10^{-6}, $\mathbf{E_b/N_0} = 10.5$ dB. As given in the specification [20], TS-UNB has a symbol rate of $\mathbf{R_S} = 2380.371$ sym/s. Furthermore, [20] states that, for TS-UNB, MSK modulation bit rate $\mathbf{R_b} = \mathbf{R_s}$. Bandwidth $\mathbf{B} = 100$ kHz, if the "Standard" bandwidth is used. The $\boldsymbol{SNR_{reqd}}$ given in Table 12 is derived with this information and equation (8). Using equations (6), (7), (9) and link budget parameter values from Table 12, the APL for TS-UNB may be calculated. Results are given in Chapter 5.1.

4.2 Duration of Activity States

This chapter will analyze the durations, which an end-device spends on five different states during message transmission event. These states are: TX, RX, Idle, Sleep and PSM. Time spent in each state is a required component in any further analysis of energy consumption. It can also be used for calculating data rate.

In general, a device is

- in TX-state when transmitting, for duration t_{TX}.
- in RX-state when receiving, for duration t_{RX}.

- in Sleep-state when it has suspended its operation. Generally after all other activity has ceased and before the next transmission event, for duration t_{Sleep}.
- in PSM-state when, similar to Sleep-state, it has powered down all internal components to the bare minimum, for duration t_{PSM}.
- in Idle-state at all other times, such as while waiting for a receive window, for duration t_{Idle}.

In real life, state transfers take a small amount of time, particularly in the case of returning to an active-state from Sleep- or PSM-state. The time taken to resume operation depends much on the hardware platform and operating system (OS). Generally, a lightweight OS or a Real Time OS takes a few milliseconds. However, using a general purpose embedded OS, i.e. Linux-based, resume process may take more than 10 seconds, even if the boot/resume process is optimized for the application. These transition times are generally not accounted for in the following analysis.

4.2.1 NB-IoT

As explained under Chapter 3.1, NB-IoT includes continuous information exchange between the end-device and eNB regarding the connection parameters, such as for resourcing and link adaption. The control information exchanges of SIBs and DCIs cause a highly complex scenario. Yet, for stationary end-devices, this information is not expected to change very often. Therefore, this analysis will simply focus on state durations of an uplink message transmission event. It is assumed, that the end-device has completed cell search and has received all the SIBs and DCIs from the eNB required for communication, including an uplink scheduling grant.

With NB-IoT, transmission and reception is measured in RUs and SFs, which correspond to a defined duration, as explained under Chapter 3.1. In short, for uplink, the duration was a result of the combination of subcarrier allocation and spacing, MCS and number of RUs and repetitions. TBS also plays a role in determining how many transmission events are required for the higher layer data payload. This analysis bases on the SCS of 15 kHz and subcarrier allocation ($\boldsymbol{n_{SC}^{RU} = 12}$) that were defined in Table 12 for link budget calculation. The MCS

is given by the coverage analysis of Chapter 4.1. Based on the results recorded in Chapter 5.1, this analysis sets $\boldsymbol{i_{MCS} = 13}$. Furthermore, we note that since $\boldsymbol{n_{SC}^{RU} > 1}$, $\boldsymbol{i_{MCS} = i_{TBS}}$ as given by Chapter 3.1.2. Then, according to Table 9, at the defined MCS level we get the TBS by selecting the minimum TBS able to accommodate the segment size handed down from RLC-protocol. The segmentation by RLC protocol with respect to the use-case profiles is further detailed under Chapter 4.4.1.

Finally, the number of RUs, denoted as $\boldsymbol{n_{RU,min}}$, required to transmit the transport block may be obtained again from Table 9. The number of repetitions $\boldsymbol{n_{rep}}$ are set to 1 for this analysis (no repetitions). For NPUSCH, the minimum time needed for transmission of a TB, denoted as $\boldsymbol{t_{TX,min}}$ is determined as

$$\boldsymbol{t_{TX,min} = n_{RU,min} * t_{RU} * n_{rep}} . \tag{28}$$

$\boldsymbol{t_{RU}}$ depends on SCS (3.75 or 15 kHz) and subcarrier allocation $\boldsymbol{n_{SC}^{RU}}$, which dictate the time to transmit one RU. This relation was shown in Figure 6. Finally, the value is multiplied for the amount of repetitions $\boldsymbol{n_{rep}}$ chosen.

On the downlink, this analysis only considers reception duration for the transmission acknowledgments (ACKs) as $\boldsymbol{t_{RX}}$. Given the same SCS and subcarrier allocation, this amounts to one subframe (1 ms). In addition to $\boldsymbol{t_{TX}}$ and $\boldsymbol{t_{RX}}$ there are two time gaps specified between states, which are counted as time in Idle-state $\boldsymbol{t_{Idle}}$. After receiving the DCI with scheduling info (minimum one sub-frame without repetitions, 1 ms), a time gap of 8 ms is required so that the end-device has time to decode the DCI and prepare the uplink transmission. After transmission is completed, another gap of minimum 3 ms is specified to allow the end-device to switch from transmission to receiving mode. [40]

A further segment in the analysis of duration of activity states for NB-IoT is the behavior inflicted by the, rather complex, power saving features, which were discussed in Chapter 3.1.3. Table 16 lists the assumed values for parameters such as timers set by the network or the end-device, along with other relevant information. The analysis is based on a simplified

model of the end-device's behavior. RRC Inactivity Timer is set to Immediate Release, thus disabling C-DRX. I-eDRX is used in RRC-Idle state. It is assumed, that the PO is an SF of index 9 (the last SF within an RF).

Table 16. Parameter values chosen for NB-IoT power saving features.

		Designation	**Value**
Radio Frame		$\boldsymbol{RF}$	$10\ ms$
Radio Subframe		$\boldsymbol{SF}$	$1\ ms$
RRC-Connected			
RRC Inactivity Timer	1.	$\boldsymbol{t_{RRC-IA}}$	$0\ s$
RRC-Idle			
PO Subframe index	2.	$\boldsymbol{i_{PO}}$	9
Number of I-DRX cycles	3.	$\boldsymbol{n_{IDRX}}$	4
I-DRX cycle	4.	$\boldsymbol{t_{IDRX}}$	$RF * 128$
Paging Window Timer	5.	$\boldsymbol{t_{PW}}$	$RF * 512$
Number of I-eDRX cycles	6.	$\boldsymbol{n_{IeDRX}}$	2
I-eDRX cycle	7.	$\boldsymbol{t_{IeDRX}}$	$RF * 2048$
Active Timer	8.	$\boldsymbol{t_{3324}}$	$6.* 7.$
TAU Timer	9.	$\boldsymbol{t_{3412}}$	$>= RF * 60000$

Time before expiry of Active timer T3324 is recorded to t_{Sleep}, while time after T3324 and before TAU timer expiry is recorded to t_{PSM}. TAU timer is expected to be set at 600 seconds or more, which has the effect that sole TAU transmissions are not expected and thus will not accumulate any time to t_{TX} and t_{RX} in this analysis.

4.2.2 LoRaWAN

Semtech provides the following equations in its LoRa chip datasheet [54] to calculate the number of payload symbols per transmission:

$$n_{payload} = 8 + max\left(\left\lceil \frac{8PLD - 4SF + 28 + 16CRC - 20H}{4(SF - 2DE)} \right\rceil * (CR_{ind} + 4), 0 \right). \quad (29)$$

$\boldsymbol{PLD}$ is the number of bytes in PHY Payload field (includes L2 headering). $\boldsymbol{CRC}$ is one, if payload CRC is enabled, and zero otherwise. $\boldsymbol{H}$ is one, if PHDR is included, and zero otherwise. $\boldsymbol{DE}$ is one, if a function called "low data rate optimization" is enabled, and zero otherwise. This function is mandatory for SFs 11 and 12 at 125 kHz bandwidth, but no further detail is provided of its effect. [6; 54]

TX-state duration is calculated as

$$t_{TX} = \left(n_{preamble} + 4.25 + n_{payload}\right) * \Delta t\,, \quad (30)$$

where

$$\Delta t = \frac{2^{SF}}{B} \quad (31)$$

This work expects the default settings, as given by Semtech in [54], regarding preamble length (12 symbols) and use of PHDR and CRCs (included). Additionally, a MAC overhead of 29 Bytes is expected, which allows for maximum FRM Payload size of 255 – 29 = 226. As explained in Chapter 3.2.2, LoRa messages omit L3-headering, but here we expect it to otherwise include other higher layers. Thus for P1, an application layer payload of 1025 is expected to be passed to the MAC layer, and as result it needs to be sent over several transmissions. After segmenting and adding the MAC overhead, the total PHY Payloads then result to:

- P1: 4 x 255 & 1 x 150 Bytes
- P2: 139 Bytes

All uplink messages are expected to be confirmed. An acknowledgement packet is a packet without payload and amounts to simply the overhead. Here the size of 29 bytes is assumed. The time intervals between TX- and RX-states is in LoRaWAN defined as RECEIVE_DELAY1, RECEIVE_DELAY2 etc. In this work only the first receive window with a delay of 1 second will be used, which the device spends in Idle-state. Also, a LoRaWAN device is expected to exclusively utilize PSM-state instead of Sleep-state.

4.2.3 TS-UNB

The total duration in TX-state can be obtained by applying the durations of core and extension frame radio bursts, as given in [19], with the total number of radio bursts for a transmission event. Repetitions are not considered in this analysis. The extension frame adds up to core frame RBs by one RB per each additional byte in the physical payload. The number of extension frame radio bursts may be calculated by deducting the minimum PSDU size of 20 bytes from the total application layer payload size. In short, as

$$\boldsymbol{n_{RB,ext} = PLD_{App} - PSDU_{min}}\,. \tag{32}$$

The duration in TX-state is then calculated as

$$\boldsymbol{t_{TX} = t_{core} - n_{RB,ext} * t_{ext}}\,, \tag{33}$$

where $\boldsymbol{t_{core}}$ and $\boldsymbol{t_{ext}}$ are the transmission times for the whole core frame and individual extension frame RBs, respectively.

As explained in Chapter 3.3.1, TS-UNB messages omit L3-headering, but here we expect it to otherwise include other higher layers. Given the payload sizes defined in Chapter 2.1 for P1, and the TS-UNB protocol details of Chapter 3.3, it can be concluded, that P1 requires more than one transmissions event (radio frame) and P2 manages with just one. Adding up the MAC- and physical layer overheads gives the size of the physical payload. Then through rules of the core- and extension frame formulation, the number radio frames and the number

of RBs for each extension frame may be obtained. The values used in the calculations are summarized in Table 17.

Table 17. Uplink OaT parameters per message.

Application layer payload	**Profile 1** 1045 Bytes	**Profile 2** 110 Bytes
Radio frame max. payload	245 Bytes	
Min. PSDU size	20 Bytes	
No. core frames	5	1
No. ext. RBs, $\boldsymbol{n_{RB,ext}}$	4 * 225 + 45	90
Core frame time, $\boldsymbol{t_{core}}$	362.97 ms	
Ext. frame time, $\boldsymbol{t_{ext}}$	15.14 ms per additional byte	
Full radio frame time, $\boldsymbol{t_{RF}}$	3769.5 ms	

As mentioned in Chapter 3.3, acknowledgements are sent as a bit in the MAC-headering, and thus require only the core-frame. Device is in Idle-state between RBs ($\boldsymbol{t_{OFF}}$) and while waiting for ACK in receive window. The time gap between UL and DL is given in [19] as 16384 symbol durations by default, or $\Delta\boldsymbol{t} * \boldsymbol{16384 = 0.42\ ms}$. Also, a TS-UNB device is expected to exclusively utilize PSM-state instead of Sleep-state between ACK and time of next message.

4.3 Duty Cycle

This chapter will look into capability with regards duty cycle regulation. For wireless links, duty cycle is defined as the ratio of the cumulated sum of time from all transmissions during an observation period $\boldsymbol{t_{obs}}$, this is expressed as:

$$\boldsymbol{DC_{MAX}} = \frac{\sum \boldsymbol{t_{TX}}}{\boldsymbol{t_{obs}}} . \tag{34}$$

Different regions in the world have their own regulations for the utilization of radio frequency resources. For most regions, duty cycle of transmission is one of the regulated parameters. Looking widely at the regulation, it may be observed that the rules are most strict in Europe and the US, and that many other regions follow their example or have more relaxed regulation. Authors in [10] gathered a good summary on technical constraints by regulations from top ten GDP countries worldwide, partly presented below in Table 18.

In Europe the regulation is dictated by the European Commission and is laid out by the commission decision in document 2006/771/EC [1]. In the US, the regulatory responsibility is with the Federal Communications Commission (FCC) and the relevant regulations are available in [17].

Table 18. Summary of Duty Cycle regulation of license-exempt spectrum in Europe and the US [10].

	US	**Europe**
General parameters		
Frequency Range (MHz)	902 - 928	863 - 875.6
Parameters for Medium Access based on Duty Cycle		
Band Duty Cycle (%)	-	0.1 (863-868) 1 (865-868) 0.1 (868.7-869.2) 10 (869.4-869.6) 1 (870-875.6)
Band Duty Cycle Period(s)	-	3600
Channel Duty Cycle (%)	2 (BW < 250 kHz) 4 (250 kHz < BW < 500 kHz)	-
Channel Duty Cycle Period(s)	20 (BW < 250 kHz) 10 (250 Hz < BW < 500 kHz)	-

Formally the Band Duty Cycle, applied in European regions means the percentage of time a device actively emits in the whole frequency band. Band Duty Cycle Period specifies the

observation period t_{obs} of one hour. To address frequency hopping access schemes, the US regulations specify Channel Duty Cycle, which specifies different duty cycles for each sub-channel. [10]

The following analysis is only valid for license-exempt technologies. It should also be noted, that individual countries may have their own regulation, which may differ from the regional norm. Particularly this is the case within the EU.

4.3.1 LoRaWAN

In LoRaWAN, each packet is sent continuously over a channel, although there are several channels available, region specifically. The channelization is given in the LoRaWAN specification [34], and for Europe there are six channels of 125 kHz of bandwidth, and for US, 64 channels of 125 kHz and 8 channels of 400 kHz. LoRaWAN has been designed to take into account duty cycle regulations by going even as far as encoding it to its specification. For example, it employs a scheme, where record is kept for each channels transmission time and duty cycle, which results in a time-off timer. A channel is blocked from further transmissions until its time-off timer has passed. [34]

Since P1 requires multiple transmission events or packets, this allows each packet to be sent over different channel. As result a faster interval may be used, than would be possible with just one channel. However, it makes the duty cycle calculation more complex, since it requires bookkeeping of t_{OFF} timer per channel.

For the analysis with LoRaWAN, a bookkeeping simulation was developed to derive the usability of each interval for each use-case profile. As explained above, the simulation enforces the duty cycle limit per channel by blocking used channels from further transmissions until each channel's t_{OFF} timer expires. The result is a Boolean determination whether the analyzed transmission interval is OK or NOK. Interval period is determined unfeasible, if there is an event, where no channels are available ($t_{OFF} \neq 0$) at start of packet transmission.

4.3.2 TS-UNB

As explained in Chapter 3.3.2, TS-UNB splits each message to RBs, which are transmitted over 24 subcarriers by way of a pseudo-random pattern. Using equation (34) the band DC may be calculated from the total $\boldsymbol{t_{TX}}$ of the message given in Table 24. Channel DC may be calculated by dividing the message $\boldsymbol{t_{TX}}$ with the amount of subcarriers. The transmission time per sub-channel for each profile is given in Table 17.

Table 19. Transmission time per subcarrier.

	P1	**P2**
$\boldsymbol{t_{TX}}$ per subcarrier	659.1 ms	71.9 ms

According to UPG1 carrier set table 6-49 in [19], the TSMA scheme frequency hops in a pseudo-random pattern and all subcarriers are treated with equal degree and of approximately 4.2% utilization per SC for the core-frame. With the extension frame the standard specifies a deterministic formula to select an SC for each consecutive RB. Yet, this analysis generalizes and expects, that the above mentioned SC utilization conforms to each consecutive set of 24 RBs of the extension frame. Although this is not clearly stated in the specification and thus not confirmed to be accurate, it is assumed.

4.4 Data Rate

This chapter presents data rate evaluation for both use-case profiles. At its basics, data rate $\boldsymbol{R_b}$ is defined as the amount of physical bits $\boldsymbol{D_{L0}}$ transferred over a communications channel in a unit of time $\boldsymbol{t_b}$ given in seconds. This is commonly called the "raw" physical layer bitrate, and is expressed as:

$$\boldsymbol{R_b = \frac{D_{L0}}{t_b}} \tag{35}$$

However, the raw bitrate is not a good measure for most applications from the designer's point of view, because it often times abstract any extra information or functions added to the

transmission by each layer in the protocol stack, such as packet headers, acknowledgement responses or retransmissions, all of which are generally referred to as "overhead". In practice, information bits are modulated to symbols, and only then transmitted. Depending on the modulation rate, a symbol can incorporate one or more data bits, making symbol rate less than or equal to raw bitrate. Furthermore, before modulation, information bits are commonly encoded with redundant bits for FEC, still reducing the actual information rate.

Thereof, for the same transmission, data rate gets different values depending on which protocol layer is under observation. As such, when discussing about data rate, it should be generally always also mentioned, that at which layer of the protocol stack it is "measured" at. When moving up the protocol stack, i.e. starting from the PHY-layer, the data rate of the next-above layer may generally be obtained with the following formula

$$\boldsymbol{R_{L(i)} = R_{L(i-1)} * \frac{D_{L(i)}}{D_{L(i)}^{OVH} + D_{L(i)}}} \tag{36}$$

Here $\boldsymbol{L(i)}$ represents the protocol layer of index $\boldsymbol{i}$, while $\boldsymbol{D_{L(i)}}$ is the data payload and $\boldsymbol{D_{L(i)}^{OVH}}$ the layer specific overhead. It may be observed, that data rate at $\boldsymbol{L(i)}$ (current layer) is simply data rate at $\boldsymbol{L(i-1)}$ (layer below) multiplied with the ratio of data payload and total payload. [39]

Regardless of which protocol layer is under examination, the layer specific data rate may be obtained also directly with equation (35) with assigning $\boldsymbol{D}$ as the sum of all data (payload + overhead) from the current and lower layers, and $\boldsymbol{t}$ as the total time it takes to transmit the data and perform all the necessary functions up to the current layer (i.e. reception acknowledgements and related waiting times, retransmissions). This method is used in this work, for example in Chapter 4.4.1 and equation (38).

4.4.1 NB-IoT

With NB-IoT, in literature it is common to read about data rate expressed as peak physical data rate, $\boldsymbol{R_{PeakPhy}}$. This is the raw bitrate derived from TBS including a 24-bit CRC, and

minimum transmission time as given by equation (28) from chapter 4.2.1. In short, the peak physical rate is calculated as

$$\boldsymbol{R_{PeakPhy}} = \frac{\boldsymbol{TBS + CRC}}{\boldsymbol{t_{RU}}} \ . \tag{37}$$

The peak physical data rate is not useful in evaluation of feasibility. For that, the MAC-layer data rate is better suited, which also acknowledges the signaling overhead of scheduling grant over the NPDCCH channel in the extra time required is also considered. Essentially, the time taken to receive or transmit control signaling, such as DCI. The payloads defined in Chapter 2.1 down to the Network-layer are further assumed to be added with the following protocol overheads when passed down to the Physical-layer for transmission, as given by [32]:

- PCDP: 1 Byte
- RLC: 2 Byte
- MAC: 2 Byte

The RLC headering depends on the payload and is included in every segmented part of the payload, while it may also be omitted if no segmentation is required (the whole payload fits to a single transport block) [29]. The ROHC function utilized by PCDP layer can compress the IP (v4) and UDP headers (20 and 8 Bytes) for the transmission between end-device and the eNB to a minimum size of 2 Bytes. MAC-headering is added to each TB. [24; 39]

Following these rules, P1 with a L3 payload of 1045 B is less than the maximum SDU size defined for the PCDP layer as given in Chapter 3.1.1. PCDP performs ROHC function and headering, resulting with a PCDP PDU of 1020 Bytes. This is too large to fit to any one transport block as given in Table 9 (max. is 317 B). Therefore, the PCDP PDU will get segmented by RLC to fit to a set of appropriately sized TBs.

P2 with 130 Bytes of payload results in a PCDP PDU of 105 Bytes after ROHC and headering, which can fit fully to a TB given high enough link quality. In a real life situation, segmentation by RLC may occur if link quality results with a combination of $\boldsymbol{i_{MCS}}$ and $\boldsymbol{n_{RU}}$

corresponding to a smaller TBS. Also, the selected transport block is dynamically fitted with segments from one or more payloads from higher layers, so that "wasted space" in the TB is kept at minimum. Segmentation and the amount of transmission events also affect control channel signaling. Every NPUSCH transmission requires receiving a DCI with scheduling info and/or (N)ACK signals from the eNB through NPDCCH. For this analysis, segmentation is minimized by fitting the PDCP PDU to the closest matching TBS.

As already mentioned in Chapter 4.2.1, there are two time gaps to also include in the L2 data rate analysis: at minimum, 8 ms from the reception of the DCI and before uplink transmission, and 3 ms after end of uplink transmission. Based on values used in Chapter 4.2.1 for SCS, number of SCs and no repetitions, the L2-data rate may be calculated with the following formula

$$\boldsymbol{R_{L2}} = \frac{(\mathbf{8} * (\mathbf{1}\boldsymbol{Byte} + \mathbf{2}\boldsymbol{Bytes} + \mathbf{2}\boldsymbol{Bytes}) + \boldsymbol{TBS} + \mathbf{24}\boldsymbol{bits})}{(\boldsymbol{n_{rep}} * \boldsymbol{n_{RU}} * \boldsymbol{t_{RU}} + \mathbf{1}\boldsymbol{ms} + \mathbf{8}\boldsymbol{ms} + \mathbf{3}\boldsymbol{ms})} \quad . \tag{38}$$

4.4.2 LoRaWAN

Physical layer bitrate calculation is clearly defined by equation (2) from Chapter 4.4. The LoRaWAN specification in [34] additionally gives transmission parameter configurations for different regions. These specify the frequency, bandwidth and coding rate for each spreading factor. The values given in Table 10 are used here. MAC-layer data rate is calculated by adapting equation (35) for L2 with activity durations from Table 24 and the derived total L2-payload from Chapter 4.2.2 calculations.

4.4.3 TS-UNB

The raw data rate may be calculated based on physical payload in bits and transmission time, as given by equation (35) in Chapter 4.4. For TS-UNB, the transmission time consists of periods of OaT of the radio bursts, followed by pseudo-random periods of idle-time between consecutive RBs, as explained in Chapter 3.3.2. The number of radio bursts ($\boldsymbol{n_{RB}}$) and the message transmission time $\boldsymbol{t_{TX}}$ required for each profile's transmissions are in provided by

Table 17 along with the payload sizes. The specification [19] tells that $t_{RB}(s,p)$ depends on the pattern p from set UPG1 used for each transmission event, which changes cyclically. For generality, the average value of 379 symbols given in chapter 3.3.2 for UPG1 is used here as $t_{RB,avg}$. The total duration of one transmission event in seconds is given by

$$\boldsymbol{t_{Total}} = \frac{\overbrace{\left(\boldsymbol{n_{RB,core} * t_{core} + n_{RB,ext} * t_{ext}}\right)}^{\boldsymbol{OaT}}}{\boldsymbol{1000}} + \underbrace{\left(\left(\boldsymbol{n_{RB,core} + n_{RB,ext} - 1}\right) * \left(\boldsymbol{t_{RB,avg} - 32}\right) * \boldsymbol{\Delta t}\right)}_{\boldsymbol{Idle-time}} \tag{39}$$

The total idle-time between RBs, T_{OFF} was described in Chapter 3.3.2 and equations (3) and (4). MAC-layer data rates for each profile are calculated adapting equation (35) so that:

$$\boldsymbol{R_{L2}} = \frac{\boldsymbol{D_{L2}}}{\left(\boldsymbol{t_{TX} + t_{Idle} + t_{RX}}\right)}, \tag{40}$$

Here $\boldsymbol{D_{L2}}$ is the total payload on L2 in bytes, which is divided by the total time in seconds of the transmission event ending in the reception of BS acknowledgement.

In the case of Profile 1, the data rate is calculated for one full radio frame (24 + 249 RBs) and max. higher layer payload of 245 Bytes. Results for P1 and P2 are given in Chapter 5.4. For reference, the physical layer bitrate is also calculated for the maximum sized radio frame and core-frame only. According to the specification [19] the maximum core-frame size is 576 bits and maximum total radio frame size is 6216 bits.

4.5 Energy Consumption

As has been a trend of this work, the overall energy consumption of a wireless module is a complex task to evaluate, because of the dynamic workings of each technology. Despite this, it is possible to find statements of energy consumption or battery lifetime in datasheets of devices. Such statements don't however hold much value, if the exact circumstances, device/connection configuration and use-case are not known.

In an attempt to abstract this analysis, a relatively simple model is used with a static scenario of a single transmission event. Its foundation is on the analysis of Chapter 4.2 and its results, including all assumptions made, and the definitions of activity states and their division. Furthermore, estimates of reasonable power consumption at each activity state are assumed to be common (except for $\boldsymbol{P_{TX}}$) between technologies analyzed here, and they are generally founded on information found in hardware module datasheets. By using common power consumption values with all technologies, we can still evaluate the differences between technologies in energy consumption, even if the original power consumption does not exactly reflect reality. An exception is made with transmit power, since different values for $\boldsymbol{P_{TX}}$ were used with previous link budget analysis, as given in Table 12. Any intermittent activities by the end-device, which take place before, after or between the four states are not included by the analysis. These could include activities such as wake-up, radio circuit powering, state-transfers, context-storing for suspend/sleep, and they may be distinguishable in actual power consumption measurements, as is mentioned by authors in [9].

Two terms appear in industry and academic literature, when discussing topics related to energy: power consumption and energy consumption. The first thing is to understand is what the difference between the two is. In short, power consumption $\boldsymbol{P}$ is the power drawn by a device, commonly in watts or milliwatts, at any given moment. This is expressed as the relation of voltage $\boldsymbol{U}$ in volts and current $\boldsymbol{I}$ in amperes, so that

$$\boldsymbol{P = U * I}\,. \tag{41}$$

From power, energy consumption $\boldsymbol{E}$ can be obtained by defining what period of time the device draws power, so that

$$\boldsymbol{E = P * t}\,. \tag{42}$$

Energy consumption is generally expressed in joules, which is defined as one watt of power per one second. Other common way to express energy is in different units of watt-hours. Energy consumption may also be expressed as consumption of current over time. This form

is often used when making current measurements of a device's operation, and is given in an appropriate unit of amperes per hour (Ah). Energy consumption from this form may be obtained with equations (41) and (42), when voltage is known.

In order to get a full picture of the energy consumption of one transmission event (time between two message transmissions) for a hardware module, the time component of equation (42) needs to be split apart to reflect the different activity states. The overall energy consumption becomes a sum of parts, so that

$$E_{total}^{module} = P_{TX} * t_{TX} + P_{RX} * t_{RX} + P_{Idle} * t_{Idle} + P_{Sleep} * t_{Sleep} + P_{PSM} * t_{PSM} . \quad (43)$$

Average power consumption can be obtained by dividing E_{total} with total time.

$$P_{avg}^{module} = \frac{E_{total}^{module}}{(t_{TX} + t_{RX} + t_{Idle} + t_{Sleep} + t_{PSM})} \quad (44)$$

Another unit of measure sometimes given in literature, regarding energy consumption of different technologies, is the average energy consumption per data byte $E_{byte}^{D_{L(i)}}$ in the transmission event. This may be obtained by dividing the total energy consumption with the amount of data $D_{L(i)}$ transmitted, so that

$$E_{byte}^{D_{L(i)}} = \frac{E_{total}^{module}}{D_{L(i)}} . \quad (45)$$

The specific protocol layer, to which $D_{L(i)}$ refers to as payload should be mentioned, as was the case in Chapter 4.4.

Table 20 summarizes the power consumption for each activity state. To get an idea of approximate power consumption, the values used here are derived from hardware module datasheets as worst-case averages and assumptions. With this information, as well as with

the results of analysis of Chapter 4.2 given in Table 23 and Table 24, the energy consumption may be calculated with equation (43).

Table 20. Power in milliwatts for each activity state.

	P_{TX}	P_{RX}	P_{Idle}	P_{Sleep}	P_{PSM}
NB-IoT	2747.000	47.454	51.870	6.365	0.017
LoRaWAN / TS-UNB	121.704				

4.6 Battery Lifetime Estimation

The most common types of markings on batteries is their capacity and nominal voltage. A battery's capacity is given in ampere-hours, which is measured by draining it at a known current load until the voltage drops to a minimum acceptable level and recording the time it took [6]. However, the load current on the battery is not always the same when the battery connected to different devices and is subject to change depending on the voltage. Therefore, a better unit of capacity $\boldsymbol{C_{bat}}$ is in watt-hours, which can be used directly to determine the life time of the battery, when power consumption is known. Capacity in watt-hours can be obtained with equation (41), while replacing current $\boldsymbol{I}$ with capacity in ampere-hours. Battery lifetime in hours can then be calculated by dividing the capacity with power consumption, as in the following formula

$$\boldsymbol{L_{bat}} = \frac{\boldsymbol{C_{bat} * SF_{bat}}}{\boldsymbol{P_{avg}^{module} + P_{avg}^{device} + P_{sd}^{bat} - P_{avg}^{charging}}}. \quad (46)$$

Here $\boldsymbol{C_{bat}}$ is the battery capacity reported in milliwatt-hours, $\boldsymbol{SF_{bat}}$ a safety factor, $\boldsymbol{P_{avg}^{device}}$ the average power consumption of the weather station, and $\boldsymbol{P_{sd}^{bat}}$ the average self-discharge power of the battery. The safety factor can be used to set the lifetime against a minimum remaining capacity instead of zero and is optional. In case the system has some means for energy harvesting, then in general any charging power $\boldsymbol{P_{avg}^{charging}}$ may be discounted from the denominator.

For this analysis, $\boldsymbol{P_{avg}^{module}}$ is obtained from results the analysis in Chapter 4.5, while the other values are given by Chapter 2.6. The average device power consumption and the battery self-discharge rate are calculated with a nominal voltage of 3.6 V. Safety factor is not used.

4.7 Costs

Costs are a major factor in deciding the choice of wireless technology. This chapter attempts to evaluate the costs involved with our use-case profiles when utilizing various technologies through a Life-Cycle Cost (LCC) –analysis. LLC includes all costs associated with the system through-out its lifetime. These are costs of purchase, deployment, operation, maintenance and eventual decommissioning at the end-of-life. LCC is expressed as:

$$\boldsymbol{LCC_{total} = LCC_{pur} + LCC_{depl} + LCC_{oper} + LCC_{maint} + LCC_{decom}} \quad (47)$$

Costs divide differently depending on technology. In the case of license-exempt technologies, the end-user/organization is also responsible for building the infrastructure, whereas with cellular technologies the infrastructure costs are embedded as part of the subscription with the cellular service operator.

Purchase cost consists of the cost of hardware and software and include items such as the cost ($\boldsymbol{C_{item}}$) of the communication modules, base station units, cost of additional hardware for fastenings and cabling. Any information property licenses would also fall under this category which may be charged at per unit basis. Purchase costs are given as

$$\boldsymbol{LCC_{pur} = nC_{mod} + mC_{BS} + mC_{BSkit}}, \quad (48)$$

where $\boldsymbol{n}$ is the number of end-devices and $\boldsymbol{m}$ the number of base stations.

Deployment costs encompass all labor costs of hardware installation, software setup and configuration work. In case of license-exempt technologies, these costs are multiplied by the number of base stations. Base stations may be installed to an existing mast. For example,

many telecom companies rent device space from their mobile masts. Purchase and deployment costs are generally thought of as one-time investments. Deployment costs are given as

$$\boldsymbol{LCC_{depl} = mC_{work}} \,. \tag{49}$$

Operational costs on the other hand accumulate over time. Cellular subscription data plans are clearly of this category and have potential to amount to the greatest share of lifetime costs. Still, license-exempt technologies are not without either, since the same costs bundled under the cellular data plan may exist individually for the base stations. Namely these include items such as mast/site rent, electricity and back-haul data connection costs. Costs from data subscriptions are often priced as megabyte per month. Operational costs are given as

$$\begin{aligned} \boldsymbol{LCC_{oper,mod}} &= \boldsymbol{tnDC_{msub}} \\ \boldsymbol{LCC_{oper,BS}} &= \boldsymbol{t(mC_{Mrent} + mC_{BSsub})} \,. \end{aligned} \tag{50}$$

Maintenance costs consist of replacement of faulty units over time. The items included here are cost of a new unit and the work cost of device replacement. The overall maintenance lifetime costs are dictated by the number of failed units over time $\boldsymbol{M(t)}$, which can be derived from the failure rate. The number of expected failures per end-device within a set of end-devices in the interval from $\boldsymbol{0}$ to $\boldsymbol{t}$ can be calculated using the renewal function, while expecting a constant failure rate of $\boldsymbol{\tau = 1/MTBF}$. [49]

$$\boldsymbol{M(t) = \tau t} \tag{51}$$

The renewal function assumes, that failed devices are repaired or replaced to become good-as-new versions of the device. Then expected number of failed devices for $\boldsymbol{n}$ units is then given by

$$\boldsymbol{F_{total} = nM(t)} \tag{52}$$

The overall maintenance costs are given as

$$\begin{aligned} \boldsymbol{LCC_{module\ maint}} &= \underbrace{\boldsymbol{F_n C_{mod}}}_{\boldsymbol{C_{repl}}} + \underbrace{\boldsymbol{F_n C_{work}}}_{\boldsymbol{C_{replwork}}} \\ \boldsymbol{LCC_{BS\ maint}} &= \underbrace{\boldsymbol{F_m C_{BS}}}_{\boldsymbol{C_{repl}}} + \underbrace{\boldsymbol{F_m C_{work}}}_{\boldsymbol{C_{replwork}}} \end{aligned} \tag{53}$$

Lastly, one must remember to include decommissioning costs relating to system, as electronic devices must be properly disposed of. These equal the deployment costs given by eq. (49).

4.7.1 LCC Cost Calculation

The purpose of this calculation is not to be all-encompassing, but to provide insight of the cost differences between technologies. Costs unrelated to technology choice, such as the LCC of the weather station itself, are omitted except for the communication module. Maintenance costs are calculated over number of modules and BSs, if applicable, and failed devices are replaced with new ones. Two scenarios are covered. In the first scenario (S1), the weather station is connected to a base station, which is installed to space rented from mobile mast operator. In the second scenario (S2), BS is installed to a private mast, and any data plan costs are not counted.

Table 21 presents the chosen cost items of the LCC calculation. The values are derived from various sources and aim to reflect the current market prices for the business customer. Some example prices are recorded in Appendix 2 from which averages are taken. The following is assumed:

- System life-time aimed at $\boldsymbol{t = 87\,600}$ hours (120 months or 10 years).
- A setup of $\boldsymbol{n = 100}$ weather stations.
- $\boldsymbol{m = 2}$ base stations are used with the license-exempt technologies to avoid a single point of failure.
- $\boldsymbol{MTBF = 340\,000}$ hours.
- Only one device expected to fail per day (regarding work cost calculation).

- The technician manages to install / replace / dismantle two BS per day with minimum of ½ day labor cost.
- Combined UL and DL monthly cumulative data amounts $\boldsymbol{D}$ as given by Table 3 of Chapter 2.3.
- Only dismantling work costs are applied for decommissioning.

Table 21. LCC cost items.

Cost Item (C_{item})	**No. (n, m)**	**LoRaWAN**	**TS-UNB**	**NB-IoT**
Purchase				
Module	100	12 €	14 €	14 €
Outdoor BS	2	800 €		-
BS Installation HW & Cabling Kit	2	150 € / BS		-
Deployment				
Installation work		550 € / day		-
Operative				
Data Subscription	100	-	-	0.2 €/MB
Mast Device Space Rent + Electricity	2	~120 € / Mast / Month		-
BS Data Subscription	2	~70 € / Month		-
Maintenance	No. given by eq. (52)			
Module / BS		As above		
Replacement work		550 € / day		
Decommission				
Dismantling work		550 € / day		

For overall clarification, below is a summary of all calculated items. For NB-IoT, the base station infrastructure is handled by the cellular operator, which means only S1 is applicable. Thus, in the calculation, deployment and decommissioning costs are not included. The formula $\boldsymbol{LCC}_{\boldsymbol{S1-P1/2}}^{\boldsymbol{NB-IoT}}$, where NB-IoT is used with P1 and P2, is given as:

$$LCC_{S1-P1/2}^{NB-IoT} = \overbrace{nC_{mod}}^{LCC_{pur}} + \overbrace{120nDC_{msub}}^{LCC_{oper,mod}} + \overbrace{\underbrace{F_n C_{mod}}_{repl} + \underbrace{F_n\left(\frac{1}{2}C_{work}\right)}_{repl\ work}}^{LCC_{maint}} \quad (54)$$

S1 for LoRaWAN and TS-UNB includes all cost items. A note here that the BS data subscription is a fixed monthly cost. The formula $LCC_{S1-P1/2}^{LoRaWAN/TS-UNB}$, where LoRaWAN and TS-UNB are used with P1 and P2, is given as:

$$\begin{aligned} LCC_{S1-P1/2}^{LoRaWAN/TS-UNB} &= \overbrace{(nC_{mod} + mC_{BS} + mC_{BSkit})}^{LCC_{pur}} + \overbrace{m\left(\frac{1}{2}C_{work}\right)}^{LCC_{depl}} \\ &+ \overbrace{120(mC_{Mrent} + mC_{BSsub})}^{LCC_{BS\ oper}} \\ &+ \overbrace{\underbrace{\underbrace{F_n C_{mod}}_{repl} + \underbrace{F_n\left(\frac{1}{2}C_{work}\right)}_{repl\ work}}_{module} + \underbrace{\underbrace{F_m C_{BS}}_{repl} + \underbrace{F_m\left(\frac{1}{2}C_{work}\right)}_{repl\ work}}_{base\ station}}^{LCC_{maint}} \\ &+ \overbrace{m\left(\frac{1}{2}C_{work}\right)}^{LCC_{decom}} \end{aligned} \quad (55)$$

Finally, S2 for LoRaWAN and TS-UNB includes no operational costs. The formula $\boldsymbol{LCC_{S2-P2}^{LoRaWAN/TS-UNB}}$, where LoRaWAN and TS-UNB are used only with P2, is given as:

$$\boldsymbol{LCC_{S2-P2}^{LoRaWAN/TS-UNB}} = \overbrace{\overbrace{(nC_{mod} + mC_{BS} + mC_{BSkit})}^{LCC_{pur}} + \overbrace{m\left(\frac{1}{2}C_{work}\right)}^{LCC_{depl}}}^{LCC_{maint}} + \underbrace{\underbrace{F_n C_{mod}}_{C_{repl}} + \underbrace{F_n\left(\frac{1}{2}C_{work}\right)}_{C_{work}}}_{module} + \underbrace{\underbrace{F_m C_{BS}}_{C_{repl}} + \underbrace{F_m\left(\frac{1}{2}C_{work}\right)}_{C_{work}}}_{base\ station} + \overbrace{m\left(\frac{1}{2}C_{work}\right)}^{LCC_{decom}} \quad (56)$$

5 RESULTS AND DISCUSSION

This chapter presents the results of each topic of the feasibility evaluation along with discussion of their implications. Further notes and considerations are also provided as support and reference.

5.1 Coverage

The communication range requirement set in Chapter 2.5 was 1000 meters, and for a Hata/COST 231 rural/open environment model this translates to a PL of 94.7 dB, as can be observed from Figure 22. For NB-IoT, given the information in Table 14, all TBS indexes ($\boldsymbol{i_{MCS}}$ and $\boldsymbol{n_{RU}}$ combinations) may be expected to be suitable for uplink transmission at BLER of less than 10%. In other words, NB-IoT may be expected to transmit at the highest data rate. If every TBS index in Table 14 is compared with Figure 22, and the distances are derived, we can observe that the maximum communication range is between 14.7 and 37.6 km.

As seen from Table 22, LoRaWAN is well within capability to operate at required range with SF config 6. The same is true for TS-UNB, given the APL of 129.7 dB, which in comparison with the path loss curve of Figure 22 results in an approximate coverage of 10.41 kilometers. This is also confirmed by measurements with a third party source in [32].

This is comparable with results of a study done by BehrTech in [32], which presents -126 dBm as the signal power at the receiver at which close to zero messages were lost during transmission. Their test setup consisted of a laboratory environment, where a transmitter was connected to a base station over wire. PL was simulated with a step attenuator, while the background noise was also expected as 10 dB higher than thermal noise floor. Using the signal power they provide, we can extend their study with an estimate of communication range by applying it to our link budget. The noise power given in Table 12 is -124 dB. If we then set $\mathbf{SNR_{reqd}} = -129 - (-124 - 10) = -15$ dB. Using this in our link budget results

in an APL of 119 dB. As to distance, in the Hata/COST 231 rural/open model, it represents approximately 5.1 kilometers.

Table 22. Calculated LoRa APL and corresponding Hata/COST 231 rural/open PL model distance values for each SF for bandwidth of 125 kHz.

SF config	APL (dB)	d_{km}
6	-122	19.4
7	-124.5	22.3
8	-127	25.4
9	-129.5	28.9
10	-132	32.6
11	-134.5	36.7
12	-137	41.1

It should be noted, that these analyses do not take into account the presence of interference, which has a degrading effect on coverage. Interference is caused by other transmitting devices around the receiver. For NB-IoT, in most studies on the matter, interference is mainly caused by transmissions from neighboring cells (in-band/guard-band deployment). Authors in [2] present, that the effect of inter-carrier interference is negligible.

With LoRa, much research has been done to understand the interfering effect of other LoRa transmissions with equal or different spreading factors to the decoding of received messages. For example, studies by [13] and [38] have shown that despite claims of orthogonality between SFs and that transmissions using different SF would not interfere with each other, this is not necessarily the case. A threshold for signal-to-interference-ratio (SIR) exists, where the decoding of a message is likely to fail due to errors caused by interfering transmissions. In real life, this may happen, when a transmitter using a high SF is placed far away from the receiver while the interfering transmitter is much closer. Performance of LoRa in multipath environments such as Raleigh and Rician fading channels is studied by authors in [25]. They point out significant range decrease in a heavily fading environments such as urban city centers.

TS-UNB, and its TSMA operation, is advertised by BehrTech to be resilient against interference. The study in [32], which was presented earlier, also includes PER evaluation under "dense" interference environment and claims nearly zero lost packets at $\boldsymbol{P_{RX}} = -126\ dB$.

5.2 Duration of Activity States

The analysis results for time spent in different activity states through the course of one message transmission event are presented in Table 23 for NB-IoT and Table 24 for LoRaWAN and TS-UNB. It should be noted, that in the case of Profile 1, one message is spread over several transmission events.

Table 23. State durations for NB-IoT.

NB-IoT			
State	**Interval**	**P1**	**P2**
TX		40 ms	4 ms
RX (ACK)	3 s	7 ms	4 ms
	15 s	6 ms	3 ms
	60 s	8 ms	5 ms
	600 s	8 ms	5 ms
Idle		3 ms	3 ms
Sleep	3 s	2950 ms	2989 ms
	15 s	12391 ms	12430 ms
	60 s	40956 ms	40956 ms
	600 s	40956 ms	40956 ms
PSM	3 s	0 ms	0 ms
	15 s	0 ms	0 ms
	60 s	18993 ms	19032 ms
	600 s	558993 ms	559032 ms

As explained in Chapter 3.1.3, the behavior of the end-device during and after a transmission event is dependent on the configuration imposed by the mobile network regarding the paging procedure and various timers. To add to the complexity, the different parameters and timers influencing the behavior are also commonly configurable through an API for most hardware modules, as explained by [38]. It is also a choice between optimizing energy consumption and minimum latency downlink access. For very long transmission intervals, it should be kept in mind, that once the T3324 timer expires, the end-device is not reachable until the next UL event or TAU. If the network allows, the Active Timer T3324 may fine-tuned to desired end-device reachability. Essentially, in combination with the TAU timer T3412 and message interval, the chosen value has an effect to the maximum delay that exists when trying to reach the end-device.

Of course, the downlink traffic imposed by higher layers plays a major role in the end-device's behavior. As described in Chapter 3.1, if any new DL data is received during paging in RRC-Idle state, the end-device is transferred again back to RRC-Connected state and the Active Timer T3324 is reset. If this happens, and depending on message transmission interval, the device may not reach PSM-state for the message cycle. This should be kept in mind, when designing any data collection systems to which the weather station connects to.

Results in Table 23 base solely on the author's choice of parameter values and the choice has an effect on the results. Further optimization is highly recommended, if possible, with for example:

- The Active Timer T3324, TAU timer T3412
- Usage of DRX/eDRX in Connected, Idle or both RRC states
- Usage of DRX or eDRX paging cycles.

Given the choice by the network, the values of the timers may be adjusted to accommodate the use-case and transmission patterns.

Furthermore, it must be mentioned, that in practice hardware modules and chipsets functionality regarding their state transfers may not strictly follow to the expected behavior conveyed by the specification. In other words, one should verify through testing, that a chosen hardware module does in fact, in example, power down unnecessary processes and

components of its radio stack when entering to Sleep-state. In addition, as previously mentioned in Chapter 4.2, the time required for state transitions must be taken to account in real-life.

Table 24. State durations for LoRaWAN and TS-UNB.

	State		**P1**	**P2**
LoRaWAN SF 6	TX		1502 ms (4 * 324.9 + 226.6)	190 ms
	RX (ACK)		314 ms (4 * 62.7 + 62.7)	63 ms
	Idle		1000 ms	
	PSM	3s	0 ms	1748 ms
		15s	8185 ms	13748 ms
		60s	53185 ms	58748 ms
		600s	593185 ms	598748 ms
TS-UNB	TX		15819 ms (4 * 3769.5 + 1 044.3)	1726 ms
	RX (ACK)		529 ms (4 * 105.8 + 105.8)	105 ms
	Idle		158490 ms	23356 ms
	PSM	3s	0 ms	0 ms
		15s	0 ms	0 ms
		60s	0 ms	41802 ms
		600s	432574 ms	581802 ms

At SF6 LoRaWAN is at the high line of performance, but could cope with all message intervals. If each transmission is expected to be acknowledged by the BS, a further 1314 ms for P1 and 1063 ms for P2 are required ($\boldsymbol{t_{Idle} + t_{RX}}$). For P1 this extends the total transaction time for one message close to three seconds, essentially making PSM-state unusable for that interval.

The operation of TS-UNB results with a too low data rate to be suitable to transmit such large payloads in short enough amount of time. The problem is, that there is a relatively large amount of time spent in Idle-state between transmissions of RBs, as well as between transmission and RX-window. Combining that Idle-time with TX- and RX-time, it can be seen that for both profiles the three and 15 second intervals are too fast and will result in congestion. Profile 1 is only conceivable with 10 minute interval.

5.3 Duty Cycle

LoRaWAN duty cycle results, which base on derived SF6 in Chapter 5.1 and OaT times derived in Chapter 5.2, are given in Table 25. In theory, from duty cycle point of view, P1 and P2 may be used at any transmission interval. For Profile 1, intervals 3s and 15s are not achievable in the European region, but may be achieved in the US.

Table 25. LoRaWAN SF6 uplink message interval feasibility against duty cycle limits.

	P1	**P2**
8 Channels, BW 125 kHz, EU865-868 & EU870-875.6 MHz – DC 1 %		
3 s	NOK	OK
15 s	NOK	OK
60 s	OK	OK
600 s	OK	OK
64 Channels, BW 125 kHz, US902-928 MHz – DC 2 %		
3 s	OK	OK
15 s	OK	OK
60 s	OK	OK
600 s	OK	OK

It needs to be noted, as given in Chapter 3.2.1, that choosing a higher spreading factor has an increasing impact on OaT. Therefore, minimum feasible interval increases at higher SFs. Additionally, this simulation looks at the best case from duty cycle regulatory perspective and naively assumes, that all channels were always free from other transmissions. In real

life, collisions with other transmission can cause retransmission requests, and force a dynamically changing environment for the bookkeeping of t_{OFF} timers. In other words, delays occur in the transmissions and the strict message intervals may not be achieved.

For TS-UNB, Table 26 presents the result of the duty cycle analysis. It can be clearly seen, that reaching the European regulatory limit for band duty cycle of 1 % is only achievable for P2 at 10 minute transmission interval. The faster 60 second interval could be used for the frequency band 869.4 - 869.6 MHz, which allows for 10% band duty cycle. At this band, P11 at 10 minute interval may also be usable.

Table 26. Uplink duty cycle results.

	P1		P2	
Interval	Band DC	Ch. DC	Band DC	Ch. DC
3 s	527.3 %	22.0 %	57.5 %	2.4 %
15 s	105.5 %	4.4 %	11.5 %	0.5 %
60 s	26.4 %	1.1 %	2.9 %	0.1 %
600 s	2.6 %	0.1 %	0.3 %	0.0 %

The US regulations are more allowing for a large portion of spectrum. Since duty cycle is per subcarrier, the limit is 2% if Standard TS-UNB bandwidth of 100 kHz is used. At best, this allows the use of 15 second interval for P2, while for P1 intervals down-to 60 seconds are possible.

5.4 Data Rate

Table 27 gives the results for the calculated L2 data rates for each technology and use-case profile. These are very much theoretical values and only indicate capability in ideal circumstances, and are subject to choices and assumptions made by the author. As previously explained, in NB-IoT the achieved rate is dependent on the channel conditions and resource assigned by the BS, therefore the relevant parameters of i_{MCS} and n_{RU} are given. The MCS

i_{MCS} is based on results in Chapter 5.1 and n_{RU} was determined based on i_{MCS} and the minimum TBS to accommodate the RLC segment.

Table 27. L2 data rates.

	Rate	**Max.**	**P1**	**P2**
NB-IoT	i_{MCS}	13	13	13
	n_{RU}	10	10	4
	L2	114.5 kbps	114.5 kbps	63.5 kbps
LoRaWAN SF6	L2	695.7 bps	695.7 bps	562.0 bps
TS-UNB	L2	40.6 bps	40.6 bps	32.3 bps

With LoRaWAN and TS-UNB, channel and interference conditions ultimately dictate the realized rate.

5.5 Energy Consumption and Battery Lifetime

This chapter presents the results of energy consumption and battery lifetime calculations. Values were only calculated for intervals, which were deemed applicable by analyses of Chapters 4.2 and 4.3.

Authors in [4] put it succinctly on how it comes to wireless transmission: power gives you range and energy drains your battery. In short, if you can have high transmit power, while keeping transmission time very short, then you are on the right track in terms of energy efficiency. This may be clearly seen from the average power consumption per message interval given in Figure 26, which is used to derive the battery lifetime results in Table 28.

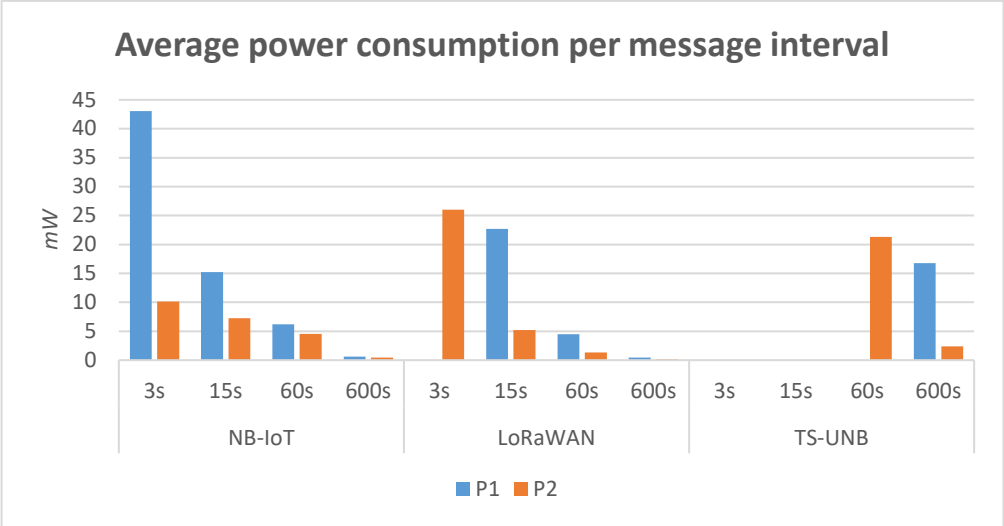

Figure 26. Average power consumption for each message interval.

The differences in reception behavior may also be observed, in particular when looking at the energy consumption per payload byte in Figure 27. NB-IoT's paging cycle and its use of the more consuming Sleep-state instead of PSM-state starts to have a noticeable effect with longer message intervals. In contrast, the energy consumption of LoRaWAN and TS-UNB does not differ much between applicable message intervals, since much of the time between transmissions is spent in the very low power PSM-state. In general, TS-UNB energy consumption is a degree of magnitude higher due to the very long transmission time.

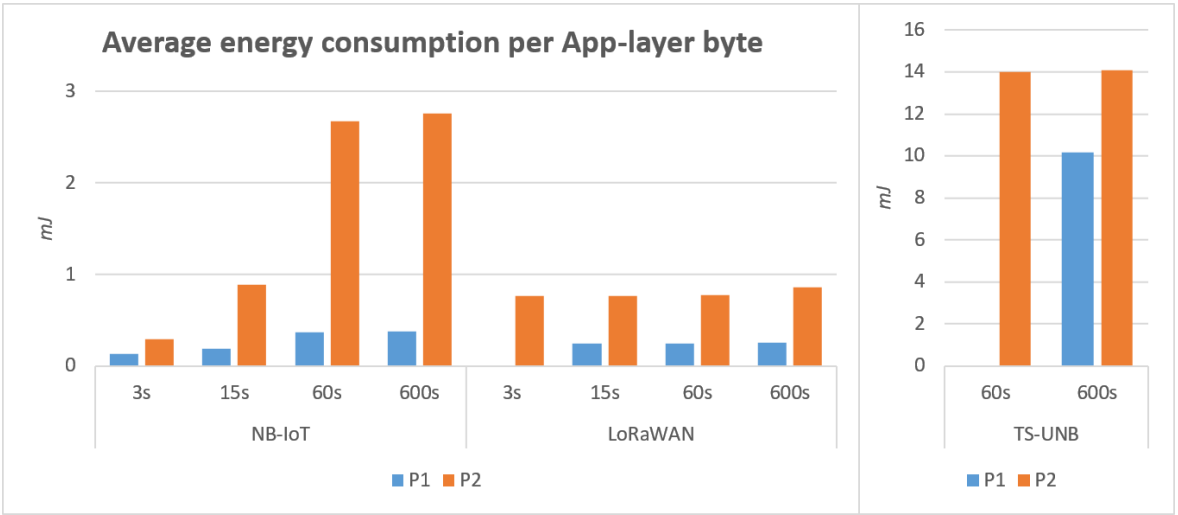

Figure 27. Average energy consumption of one byte of App-layer payload from Chapter 2.1.

The battery lifetime calculation results in days are presented in Table 28.

Table 28. Battery lifetime estimation in days for each technology and message interval.

	Int.	**P1**		**P2**	
Weather Station base		20.7		9.3	
		Module portion	Total	Module portion	Total
With NB-IoT	3 s	8.8	11.9	1.4	7.9
	15 s	4.3	16.4	1.0	8.3
	60 s	2.0	18.7	0.7	8.7
	600 s	0.2	20.5	0.1	9.3
With LoRaWAN	3 s	NA	0.0	2.9	6.4
	15 s	5.8	14.9	0.8	8.6
	60 s	1.5	19.2	0.2	9.1
	600 s	0.2	20.6	0.0	9.3
With TS-UNB	3 s	NA	0.0	NA	0.0
	15 s	NA	0.0	NA	0.0
	60 s	NA	0.0	2.5	6.8
	600 s	4.6	16.1	0.4	9.0

For reference, the battery life of the (base) weather station without any communication module was also calculated and is given on the first line. Then follow battery lifetime results per technology and message interval, itemized to total battery life and portion the module is uses up of the total. The modules share is further illustrated in Figure 28 in percentages of the total battery life.

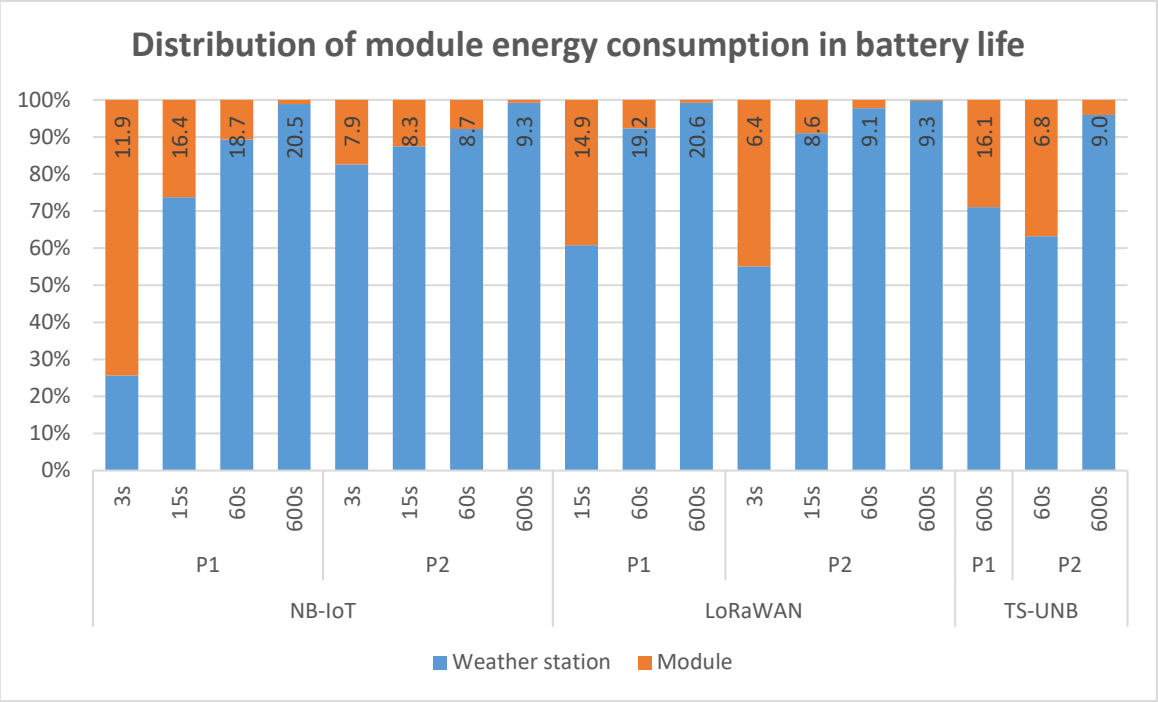

Figure 28. Share of module's energy consumption in total battery life.

Obviously, the effect of transmission interval on battery life is dramatic. Comparing NB-IoT at three and 600 second intervals, the battery life almost doubles. What is also noticeable with the results is, that higher transmission power and shorter TX-duration in fact do provide longer battery life than low-power alternatives. This may be seen particularly with P1 on 15 second interval, and P2 with 3 s interval. In short, the larger the message payload, the greater the effect. In example, with P2 and 60 seconds it is no longer noticeable and other factors have become more prominent.

We can conclude that for the message intervals applicable for comparison, NB-IoT allows for the longest battery life at the faster intervals, while LoRaWAN takes over when interval becomes longer. TS-UNB is worst performer of the bunch due to the slow transmission rate and the time spent in the higher consuming Idle-state accumulating between each RB. However, the absolute values of battery lifetime are subject to rather high degree of variability due to the previously mentioned dynamic behavior of the technologies, which is subject to channel conditions. In example, as stated by authors in [31], for NB-IoT significant variations are observed in the transmission power depending on channel conditions. This is due to power control mechanism explained in Chapter 3.1.3, and the end-device has no

control over it. To account for this, this analysis was conducted with maximum transmission power in mind. Additionally, considerable differences in consumption may also be witnessed between modules from different hardware manufacturers. [31]

5.6 Costs

The results of the LCC calculations are shown in Figure 29 and Figure 30, while Table 29 gives the totals over the span of the specified time of 10 years. Noting that Figure 29 is in logarithmic scale, it can be clearly seen that the most significant factor is the operational costs. These costs are highly dependent on how much data is transmitted (payload size $*$ interval) and the price per megabyte of the data subscription with the cellular operator.

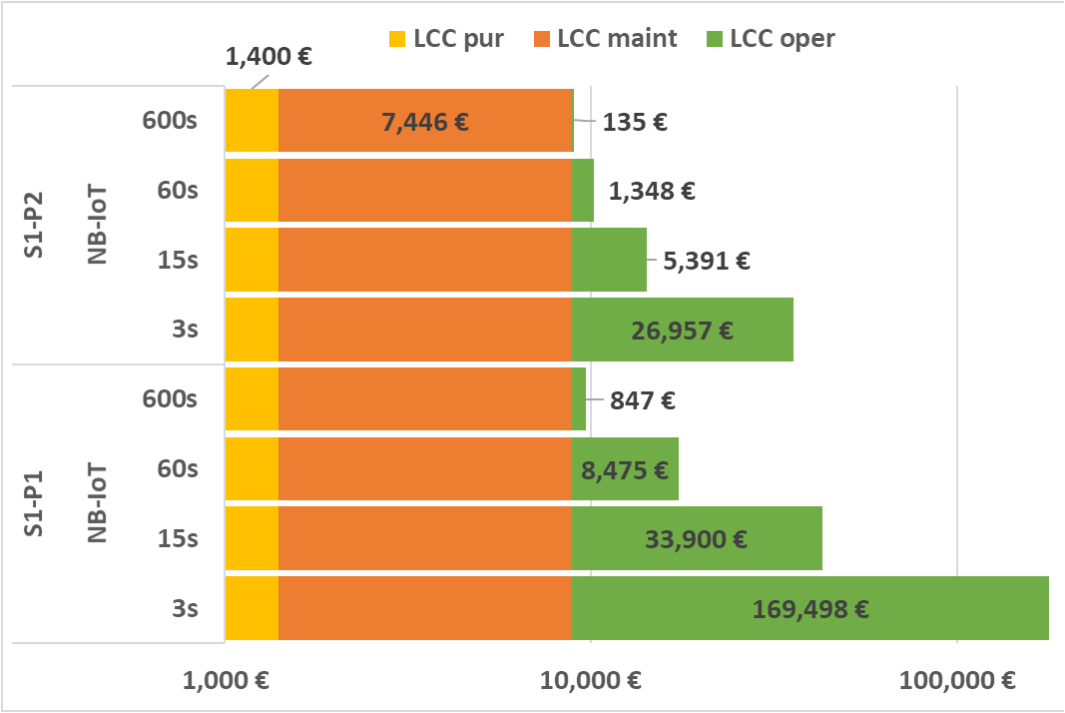

Figure 29. LCC breakdown for NB-IoT.

Given a system of 100 weather stations, already with the 0.02 € per MB price is an NB-IoT based solution cheaper than the unlicensed alternatives for all intervals except for P1 at the most frequent 3 second interval. The costs of operating the BS with device space rented from a telecom mast adds the most significant costs for LoRaWAN and TS-UNB. Furthermore,

with respect to costs related to data transfer between the weather station and BS, the transmission interval plays no role with unlicensed technologies.

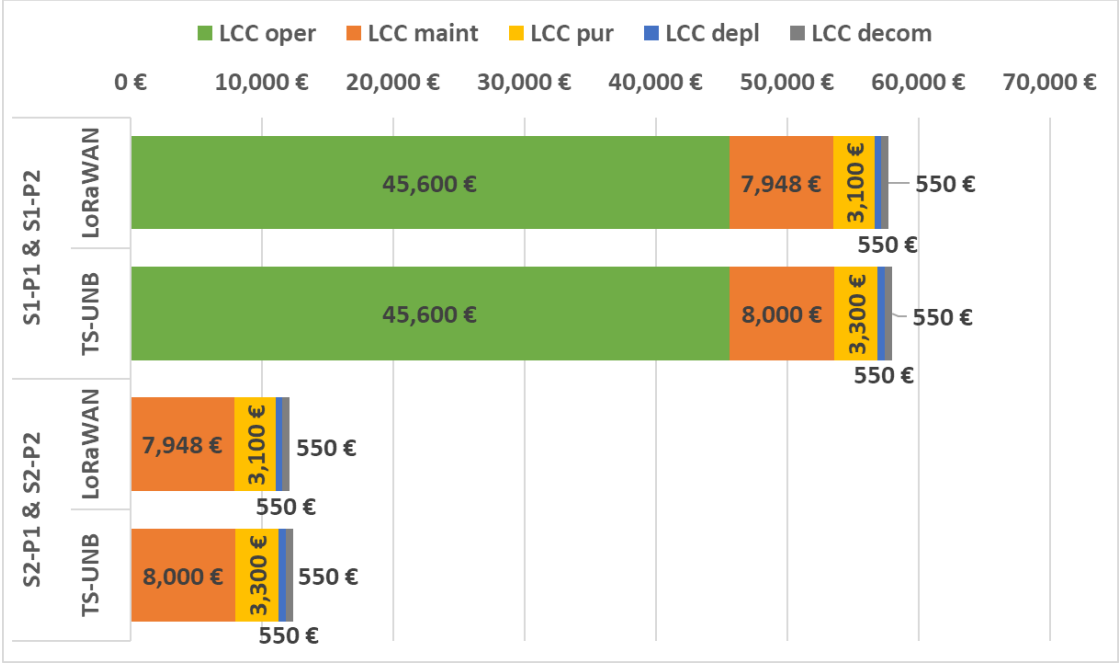

Figure 30. LCC breakdown for LoRaWAN and TS-UNB.

S2 represents the case, where the cost of operating the base stations is entirely local, and thus the costs device space rent, electricity or backhaul data subscription are not considered. In this situation, there is not much difference in costs between technologies. It is mainly a matter of module price, which in also affects expected maintenance costs.

Table 29. LCC results for 100 weather stations.

	Total LCC cost					
	S1-P1	S1-P2	S1-P1 & S1-P2		S2-P1 & S2-P2	
	NB-IoT	NB-IoT	LoRaWAN	TS-UNB	LoRaWAN	TS-UNB
3s	178344 €	35803 €	57748 €	58000 €	12148 €	12400 €
15s	42746 €	14237 €				
60s	17321 €	10194 €				
600s	9693 €	8981 €				

It should be noted that prices may vary significantly for a real life case and direct business-to-business sales and large bulk. For example, as explained by sales representative of Telia Towers Oy, renting space from a mobile mast is a sum of three components: antenna as in height and wind load, equipment floor space in m^2, and electricity. With a large number of end-devices, even small changes in price per unit of measure can have major impact in total LCCs. As in this example calculation, getting a better deal with the cellular operator (i.e. 0.01 € per MB) may even result in the reduction of one third from original costs. Generally, the most significant factors for cost optimization is with data plans and BS operating costs. Selecting the proper data plan according to measured cumulative transmitted data amount can give significant reductions in costs. In this calculation the BS backhaul data plan price was based on accumulation by 3 second interval as given in Table 3.

Based on Table 29, cost-wise for a large system the choice is clear. Overall, NB-IoT is the cheapest choice. Giving the analysis another angle, NB-IoT's rule becomes even more pronounced if the considered number of modules is set to two and with just one BS. In this situation, as shown by Table 30, NB-IoT is cheapest of all for S1 by an order of magnitude.

Table 30. LCC results for 2 weather stations (and 1 BS).

	Total LCC cost					
	S1-P1	S1-P2	S1-P1 & S1-P2		S2-P1 & S2-P2	
	NB-IoT	NB-IoT	LoRaWAN	TS-UNB	LoRaWAN	TS-UNB
3s	3,567 €	716 €	24,749 €	24,754 €	1,949 €	1,954 €
15s	855 €	285 €				
60s	346 €	204 €				
600s	194 €	180 €				

6 CONCLUSIONS

This chapter concludes the findings of each factor in the feasibility study and sets the final verdict. The findings are summarized in a table in Appendix 3 in terms of ranking or whether requirements set in Chapter 2 were reached. Results of Chapters 4.2 and 4.3 are combined as the capability to utilize a given message transmission interval.

The required communication range set in Chapter 2.5 can be reached with all technologies, while retaining the required reliability of message delivery. In terms of range, for the Hata/COST 231 open/rural environment model, the greatest range of 19 km was given by LoRaWAN, while TS-UNB performed worse at 8 km. Out of the three, only NB-IoT has the capability to guarantee message delivery, since for LoRaWAN and TS-UNB, the duty cycle limits will prevent retransmissions for shorter message intervals. Essentially, use-cases which are sensitive about lost messages may consider NB-IoT as the best option. TS-UNB is advertised with good resilience against noise and interference and thus may be ranked higher than LoRaWAN in terms of reliability.

The feasibility of each message interval is either limited by the sum of time taken to perform all required activity states (TX, RX and any obligatory waiting times) for one message transmission, or the duty cycle restrictions put in place by a regulator. NB-IoT can cope with any of the message intervals defined in Chapter 2.2 due to having high capacity and not being bound by duty cycle limits. As such, NB-IoT is the only option, if real-time wind gust reporting capability is a requirement, as specified in Chapter 2.2. With LoRaWAN, reaching the three second interval could potentially be possible under US-specific duty cycle regulation, but only by relinquishing reception feedback (RX-ACKs). TS-UNB on the other hand struggles with high messaging frequency. For TS-UNB it simply takes too long to transmit P1 or even P2 messages to consider three or 15 second intervals. In addition, the duty cycle limits further restrict interval period more or less to intervals greater than 60 seconds. TS-UNB is clearly aimed to be used with much smaller payloads than what were analyzed here.

The information value of MAC-layer data rate is more or less complimentary to message interval analysis and reflects the results of the examination of duration of activity states. Never the less, the requirements are reached by all technologies for P1 only with 600 second interval, and for P2 only up to 60 second intervals.

Different battery sizes, as specified in Chapter 2.6, were given for P1 and P2 to represent the real life case, where profile specific messaging is expected to be used. Here we find a kink in the otherwise perfect score of NB-IoT so far. At the longer message intervals, the greater energy efficiency in TX- and RX-states is no longer enough to counter the greater energy consumption spent in Sleep-state during the I-eDRX cycles in comparison with PSM-state, which LoRaWAN utilizes for the whole of the remaining interval period after RX-state finishes. TS-UNB is worst performer here.

Cost-wise it is not straight forward to compare all technologies side-by-side due to the difference in the nature of their deployment options. However, generally it may be pointed out, that the shorter the message interval or the larger the number of weather stations in the network, the more costly NB-IoT becomes. LoRaWAN and TS-UNB, which utilize the "free", unlicensed radio spectrum, have to bear the cost of deploying the network infrastructure, at least to some degree, but the transmission interval (and cumulative amount of data transmitted) does not affect costs as with NB-IoT. Still, on smaller networks, NB-IoT remains cheapest.

All in all, based on the results of all factors, NB-IoT lands as the most feasible choice. Figure 31 attempts to visualize the ranking of technologies by presenting the results of each factor through min-max normalized scaling. The minimum value for each factor is adapted to a suitable value based on the author's judgement.

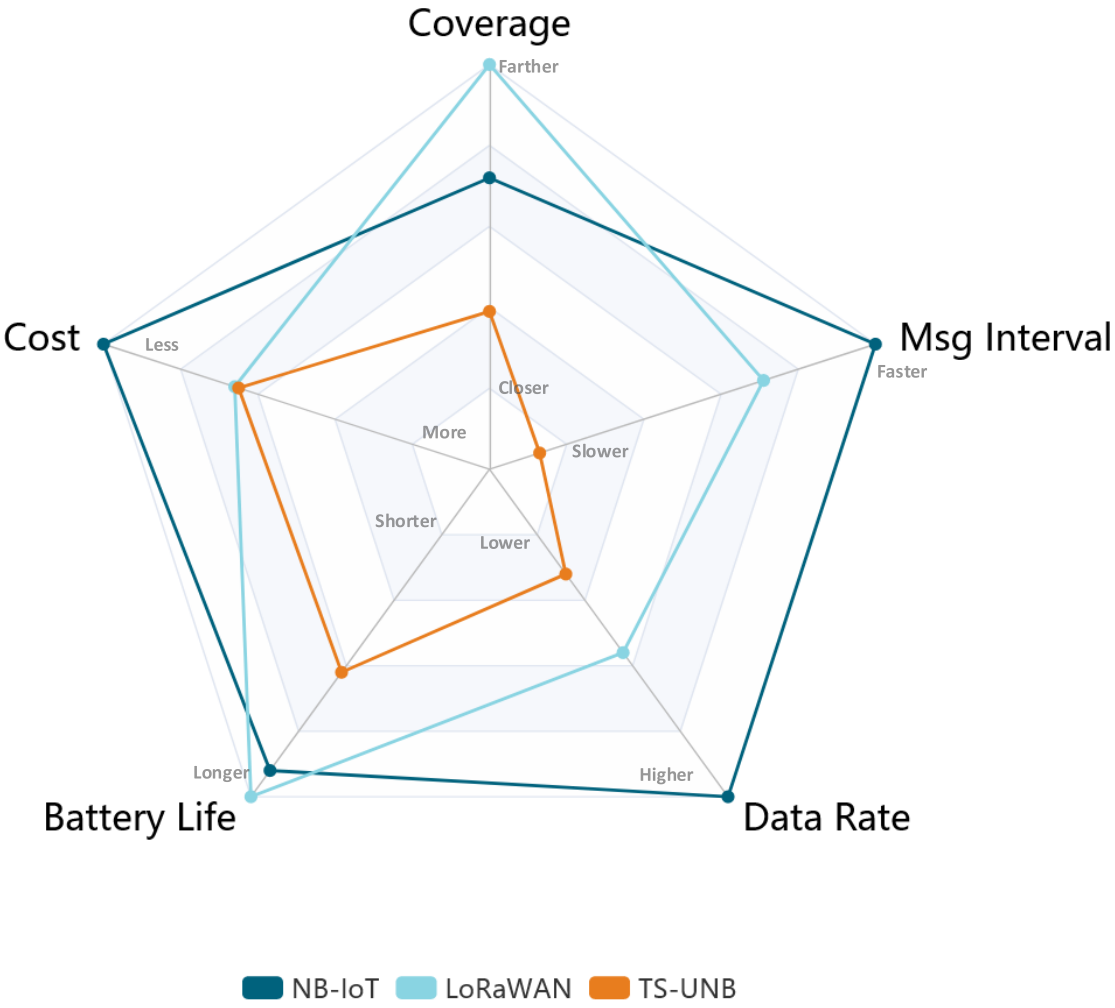

Figure 31. Performance visualized.

6.1 Closing Remarks and Future Work

This thesis provided a literary view and theoretical analysis on feasibility of selected wireless technologies in this specific use-case. It provides a starting point for anyone considering the use of wireless technology to transmit data from a Vaisala weather station and the results give concrete information for decision making. However, the weakness of the study is in that it is a static analysis, much like a best case slice, of the characteristics of the evaluated technologies. The analysis touches only little on what effect changes in channel conditions and presence of interference has on the capabilities of each technology.

The work could be improved by a more thorough analysis on the effect that channel conditions and presence of interference has on the capability of each technology. In addition, if making business decisions, these generalizations may only point the reader towards the right direction. A thorough prototype testing with hardware would be the obvious next step. As indicated by [31], the choice of hardware platform has impact on the behavior of the wireless module and thus performance of energy consumption. Therefore, it is imperative to perform trials on different modules before committing to a choice.

Since the messaging interval has such an impacting effect on the feasibility, one angle is to research the effect of a method called event-based sampling. For human time scales, weather appears to be in constant shift. However, machines regard time differently. Looking at the data sent by the weather station, most measurements may not change even by one digit from message to message, except for wind measurements. This observation may present an opportunity to decrease transmission time, because one may argue that it brings no informational value to transmit the same values in multiple consecutive messages. The sensor could instead transmit a message only when the measured values change, for example over a specified threshold, leaving it up to the receiver side to fill in the time series based on previously received data. It may allow savings in consumed energy and subscription based data transmission costs, but this would need to be verified for example with time series of real life data.

REFERENCES

1. 2006/771/EC: Commission Decision of 9 November 2006 on harmonisation of the radio spectrum for use by short-range devices, *Official Journal of the European Union*. Available: https://eur-lex.europa.eu/legal-content/EN/TXT/?uri=CELEX%3A02006D0771%2801%29-20190813.
2. Adhikary, A., Lin, X., Wang, Y.-P. E., Performance Evaluation of NB-IoT Coverage, *2016 IEEE 84th Vehicular Technology Conference (VTC-Fall)*, September 2016. Available: https://ieeexplore.ieee.org/document/7881160.
3. Alani, M. M., Guide to OSI and TCP/IP Models, *Springer*, 2014.
4. AN1200.22 LoRa Modulation Basics, Revision 2, *Semtech*, May 2015.
5. Andreev, S., Galinina, O., Pyattaev, A., Gerasimenko, M., Tirronen, T., Torsner, J., Sachs, J., Dohler, M., Koucheravy, Y., Understanding the IoT connectivity landscape: a contemporary M2M radio technology roadmap, *IEEE Communications Magazine*, Vol. 53, No. 9, September 2015, pp. 32-40. Available: https://ieeexplore.ieee.org/document/7263370.
6. Andres-Maldonado, P., Ameigeiras, P., Prados-Garzon, J., Ramoz-Munoz, J. J., Navarro-Ortiz, J., Lopez-Soler, J., Analytic Analysis of Narrowband IoT Coverage Enhancement Approaches, *2018 Global IoT Summit (GIoTS) Conference*, March 2019. Available: https://ieeexplore.ieee.org/document/8534539.
7. Barsukov, Y., Jinrong, Q., Battery Power Management for Portable Devices, *Artech House*, 2013.
8. Blackman, J., What is MIOTY? All about telegram splitting and LoRaWAN bashing, *Enterprise IoT Insights*, September 2019. Available: https://enterpriseiotinsights.com/20190926/channels/fundamentals/all-about-mioty-telegram-splitting-for-iiot. Retrieved: 27.10.2020.
9. Bor, M., Roedig, U., LoRa Transmission Parameter Selection, *2017 13th International Conference on Distributed Computing in Sensor Systems (DCOSS)*, June 2017. Available: https://ieeexplore.ieee.org/document/8271941.

10. Casals, L., Mir, B., Vidal, R., Gomes, C., Modeling the Energy Performance of LoRaWAN, *MDPI Sensors*, Vol. 17, No. 10, October 2017, Art. 2364. Available: https://www.mdpi.com/1424-8220/17/10/2364.
11. Castells-Rufas, D., Galin-Pons, A., Carrabina, J., The Regulation of Unlicensed Sub-GHz bands: Are Stronger Restrictions Required for LPWAN-based IoT Success?, *arXiv.org*, November 2018. Available: https://arxiv.org/abs/1812.00031. Retrieved: 19.8.2020.
12. Chaudhari, B. S., Zennaro, M., Borkar, S., LPWAN Technologies: Emerging Application Characteristics, Requirements, and Design Considerations, *MDPI Future Internet*, Vol. 12, No. 3, March 2020, Art. 46. Available: https://www.mdpi.com/1999-5903/12/3/46/.
13. Chew, D., The Wireless Internet of Things: A Guide to the Lower Layers, *Wiley-IEEE Standards Association*, 2019.
14. Croce, D., Gucciardo, M., Mangione, S., Santaromita, G., Tinnirello, I., Impact of LoRa Imperfect Orthogonality: Analysis of Link-Level Performance, *IEEE Communications Letters*, Vol. 22, No. 4, April 2018, pp. 796-799. Available: https://ieeexplore.ieee.org/document/8267219.
15. De la Roche, G., Glazunov, A. A., Allen, B., LTE-Advanced and Next Generation Wireless Networks – Channel Modelling and Propagation, *John Wiley & Sons*, 2013.
16. The Future of Connectivity in IoT Deployments, *Deloitte*, March 2018. Available: https://www2.deloitte.com/content/dam/Deloitte/de/Documents/technology/Connectivity-in-IoT-deployments-Deloitte.pdf. Retrieved 14.8.2020.
17. El-Aasser, M., Gasser, A., Ashour, M., Elshabrawy, T., Performance Analysis Comparison between LoRa and Frequency Hopping-based LPWAN, *2019 IEEE Global Conference on Internet of Things (GCIoT)*, December 2019. Available: https://ieeexplore.ieee.org/document/9058411.
18. Electronic Code of Federal Regulations, Title 47, Chapter I, Subchapter A, Part 15 – Radio Frequency Devices, February 2021. Available: https://www.ecfr.gov/cgi-bin/text-idx?SID=7abc89590df38dc1442edd5e4369519f&mc=true&node=pt47.1.15&rgn=div5.

19. Elshabrawy, T., Robert, J., Closed-Form Approximation of LoRa Modulation BER Performance, *IEEE Communications Letters*, Vol. 22, No. 9, September 2018, pp. 1778-1781. Available: https://ieeexplore.ieee.org/document/8392707.
20. ETSI TS 103 357 V1.1.1, Short Range Devices; Low Throughput Networks (LTN); Protocols for radio interface A. *European Telecommunications Standards Institute*, June 2018. Available: https://www.etsi.org/deliver/etsi_ts/103300_103399/103357/01.01.01_60/ts_103357v010101p.pdf.
21. ETSI TS 136 211 V16.2.0, Technical Specification, E-UTRA - Physical channels and modulation, 3GPP Release 16, *European Telecommunications Standards Institute*. September 2020. Available: https://www.etsi.org/deliver/etsi_ts/136200_136299/136211/16.02.00_60/ts_136211v160200p.pdf.
22. ETSI TS 136 212 V16.2.0, Technical Specification, E-UTRA – Multiplexing and channel coding, 3GPP Release 16, *European Telecommunications Standards Institute*. July 2020 Available: https://www.etsi.org/deliver/etsi_ts/136200_136299/136212/16.02.00_60/ts_136212v160200p.pdf.
23. ETSI TS 136 213 V14.16.0, Technical Specification, E-UTRA – Physical layer procedures, 3GPP Release 16, *European Telecommunications Standards Institute*. September 2020. Available: https://www.etsi.org/deliver/etsi_ts/136200_136299/136213/16.02.00_60/ts_136213v160200p.pdf.
24. ETSI TS 136 322 V16.0.0, Technical Specification, E-UTRA – Radio Link Control (RLC) protocol specification, 3GPP Release 16, *European Telecommunications Standards Institute*, July 2020. Available: https://www.etsi.org/deliver/etsi_ts/136300_136399/136322/16.00.00_60/ts_136322v160000p.pdf.
25. ETSI TS 136 323 V16.1.0, Technical Specification, E-UTRA – Packet Data Convergence Protocol (PDCP) specification, 3GPP Release 16, *European Telecommunications Standards Institute*, September 2020. Available:

https://www.etsi.org/deliver/etsi_ts/136300_136399/136323/16.01.00_60/ts_136323v160100p.pdf.

26. Ferreira Dias, C., Rodrigues de Lima, E., Fraidenraich, G., Bit Error Rate Closed-Form Expressions for LoRa Systems under Nakagami and Rice Fading Channels, *MDPI Sensors*, Vol. 19, No. 20, October 2019, Art. 4412. Available: https://www.mdpi.com/1424-8220/19/20/4412.
27. Foubert, B., Mitton, N., Long-Range Wireless Radio Technologies: A Survey, *MDPI Future Internet*, Vol. 12, No. 1, January 2020, Art. 13. Available: https://www.mdpi.com/1999-5903/12/1/13/pdf.
28. Goldsmith, A., Wireless Communications, *Cambridge University Press*, 2005.
29. Gravina, R., Palau, C.E., Manso, M., Liotta, A., Fortino, G., Integration, Interconnection, and Interoperability of IoT Systems, *Springer International Publishing*, 2018.
30. Holma, H., Toskala, A., Nakamura, T., 5G Technology – 3GPP New Radio, 1st edition, *John Wiley & Sons Ltd.*, 2020.
31. Hämäläinen, J., Course Material, Long Term Evolution – Part 5: Radio Link Budget, ELEC-E7230 – Mobile Communication Systems, *Aalto University*, 2016.
32. Khan, S., Alam, M. M., LeMoullec, Y., Kussik, A., Parand, S., Verikoukis, C., An Empirical Modelling for the Baseline Energy Consumption of an NB-IoT Radio Transceiver, *TechRxiv*, Aug 2020. Available: https://www.techrxiv.org/articles/preprint/An_Empirical_Modelling_for_the_Baseline_Energy_Consumption_of_an_NB-IoT_Radio_Transceiver/12738725.
33. Lauterbach, T., MYTHINGSTM vs. LoRa – A Comparative Study of Quality-of-Service Under External Interference, BehrTech Inc. Available: https://behrtech.com/resources/lora-vs-mythings/. Retrieved: 29.11.2020.
34. Liberg, O., Sundberg, M., Wang, Y.-P. E., Bergman, J., Sachs, J., Wikström, G., Cellular Internet of Things – From Massive Deployments to Critical 5G Applications, 2nd edition, *Academic Press*, 2020.
35. LoRaWAN Specification v.1.0, *LoRa Alliance*, January 2015. Available: https://lora-alliance.org/resource_hub/lorawan-specification-v1-0/.
36. LoRaWAN Specification v1.1, *LoRa Alliance*, October 2017. Available: https://lora-alliance.org/resource-hub/lorawanr-specification-v11.

37. Malik, H., Pervaiz, H., Alam, M. M., Le Moullec, Y., Kuusik, A., Radio Resource Management Scheme for NB-IoT Systems, *IEEE Access*, Vol. 6, Mach 2018, pp. 15051-15064. Available: https://ieeexplore.ieee.org/document/8306882.

38. Margelis, G., Piechocki, R., Kaleshi, D., Thomas, P., Low Throughput Networks for the IoT: Lessons learned from industrial implementations, *2015 IEEE 2nd World Forum on Internet of Things (WF-IoT)*, December 2015. Available: https://ieeexplore.ieee.org/document/7389049.

39. Markkula, J., Mikhaylov, K., Haapola, J., Simulating LoRaWAN: On Importance of Inter Spreading Factor Interference and Collision Effect, *CC 2019 - 2019 IEEE International Conference on Communications (ICC)*, May 2019. Available: https://ieeexplore.ieee.org/document/8761055.

40. Matz, A. P., Fernandez-Prieto, J-A., Cañada-Bago, J., Birkel, U., A systematic Analysis of Narrowband IoT Quality of Service. *MDPI Sensors*, Vol. 20, No. 6, March 2020, Art. 1636. Available: https://www.mdpi.com/1424-8220/20/6/1636.

41. Mesh Profile v1.0.1, Bluetooth Specification, *Bluetooth Special Interest Group*, January 2019. Available: https://www.bluetooth.com/specifications/mesh-specifications/ Retrieved: 15.7.2020.

42. Michelinakis, F., Al-selvi, A. S., Capuzzo, M., Zanella, A., Mahmood, K., Elmokashfi, A., Dissecting Energy Consumption of NB-IoT Devices Empirically., *IEEE Internet of Things Journal*, Vol. 8, No. 2, Aug 2020, pp. 1224-1242. Available: https://ieeexplore.ieee.org/document/9159902.

43. Narayanan, A., Sousa De Sena, A., Gutierrez-Rojas, D., Carrillo Melgarejo, D., Hussain, H. M., Ullah, M., Bayhan, S., Nardelli, P.H.J., Key Advances in Pervasive Edge Computing for Industrial Internet of Things in 5G and Beyond, *IEEE Access*, Vol. 8, November 2020, pp. 206734-206754. Available: https://ieeexplore.ieee.org/document/9257390.

44. Narrowband Internet of Things, Whitepaper, *Rohde & Schwarz*. Available: https://cdn.rohde-schwarz.com/pws/dl_downloads/dl_application/application_notes/1ma266/1MA266_0e_NB_IoT.pdf. Retrieved: 4.9.2020.

45. NB-IoT Channels – Examples, MathWorks LTE Toolbox R2020b, *The MathWorks Inc.* 2020. Available:

https://se.mathworks.com/help/lte/examples.html?category=nb-iot-channels&s_tid=CRUX_topnav.

46. Oliveira, L., Rodrigues, J. J. P. C., Kozlov, S. A., Rabêlo, R. L., de Albuquerque, V. H. C., MAC Layer Protocols for Internet of Things: A Survey, *MDPI Future Internet 2019*, Vol. 11, No. 1, January 2019, Art. 16. Available: https://www.mdpi.com/1999-5903/11/1/16.
47. Pahl, J., Interference Analysis – Modelling Radio Systems for Spectrum Management, *John Wiley & Sons Ltd*., 2016.
48. Popovski, P., Wireless Connectivity: An Intuitive and Fundamental Guide, *John Wiley & Sons*, May 2020.
49. Power saving methods for LTE-M and NB-IoT devices, White Paper, v.01.00, *Rohde & Schwarz*. Available: https://www.rohde-schwarz.com/fi/solutions/test-and-measurement/wireless-communication/iot-m2m/whitepaper-power-saving-lte-m-nb-iot-register_251417.html. Retrieved: 10.12.2020.
50. Rzepecki, W., Ryba, P., IoTSP: Thread Mesh vs Other Widely used Wireless Protocols – Comparison and use Cases Study, *2019 7th International Conference on Future Internet of Things and Cloud (FiCloud), IEEE*, January 2020. Available: https://ieeexplore.ieee.org/document/8972835.
51. Saelens, M., Hoebeke, J., Shahid, A., De Poorter, E., Impact of EU duty cycle and transmission power limitations for sub-GHz LPWAN SRDs: an overview and future challenges, *EURASIP Journal on Wireless Communications and Networking*, September 2019, Art. 219. Available: https://doi.org/10.1186/s13638-019-1502-5.
52. Sheikh, A. U. H., Wireless Communications – Theory and Techniques, 1st edition, *Springer Scrience+Business Media LLC*, New York, 2004.
53. Specification TR 21.916 version 0.5.0, Release 16, *3GPP*, July 2020. Available: https://portal.3gpp.org/desktopmodules/Specifications/SpecificationDetails.aspx?specificationId=3493. Retrieved 20.8.2020.
54. SX1272/73, Datasheet, Semtech Corporation, January 2019. Available: https://www.semtech.com/products/wireless-rf/lora-transceivers/sx1272#download-resources. Retrieved: 19.11.2020.
55. Tikhvinskiy, V., Bochechka, G., Gryazev, A. and Aitmagambetov, A., Comparative analysis of QoS management and technical requirements in 3GPP standards for

cellular IoT technologies, *Journal of Telecommunications and Information Technology*, Vol. 2, July 2018, pp. 41-47. Available: https://www.itl.waw.pl/czasopisma/JTIT/2018/2/41.pdf.

56. Wang, W., Capitaneanu, S. L., Marinca, D., Lohan, E.-L., Comparative Analysis of Channel Models for Industrial IoT Wireless Communication, *IEEE Access*, Vol. 7, July 2019, pp. 91627-91640. Available: https://ieeexplore.ieee.org/document/8756193.
57. Weather Transmitter WXT530 Series Datasheet. *Vaisala* Available: https://www.vaisala.com/sites/default/files/documents/WXT530-Datasheet-%20B211500EN.pdf. Retrieved 10.6.2020.
58. Weather Transmitter WXT530 Series User's Guide. *Vaisala* Available: https://www.vaisala.com/sites/default/files/documents/WXT530-Users-Guide-M211840EN.pdf. Retrieved 10.6.2020.

APPENDIX 1. Comparison table of wireless technologies

This table summarizes the comparison factors with typical values for each technology including use-case requirements from Chapter 2.

Table 31. Full list of comparison factors.

Variable	SigFox	LoRaWAN	BLE	IEEE 802.15.4 (ZigBee, Thread)	IEEE 802.11ah	TS-UNB	LTE-M	NB-IoT	EC-GSM-IoT
Typical Max Range	< 50 km	< 15 km	< 150 m	< 150 m	< 1 km	< 20 km	< 11 km	< 15 km	< 15 km
Max MAC-layer Data Rate	100 bps	< 50 kbps	236.7 Kbps	< 250 kbps	100 kbps – 7.8 Mbps	< 50 bps	< 1 Mbps	< 200 kbps	< 70 kbps
Max Payload	12 B	243 B	23 B	102 B	511 B @ 1 MHz	245 B (U) 250 B (D)	8188 B	1600 B	unknown
Modulation	DBPSK	GFSK CSS	GFSK	DSSS BPSK O-QPSK	M-PSK M-QAM	MSK, GMSK	QPSK, 16QAM	BPSK, QPSK	GMSK 8PSK
Channelization / Media Access	UNB/FHSS (ALOHA)	ALOHA	TDMA	CSMA/CA	RAW	TSMA	OFDMA	OFDMA (D) SC-FDMA (U)	TDMA
Directionality	Limited Bi	Bi	Bi	Bi	Bi	Bi	Bi	Bi	Bi
Duplicity & Mode	Half	Half	Half	Half	Half	Half	Full or Half FDD / TDD	Half FDD / TDD	Half
Energy Consumption	Very Low	Very Low	Low	Low	Low	Very Low	Low	Low	Medium

(continues)

APPENDIX 1. (continues)

Variable	SigFox	LoRaWAN	BLE	IEEE 802.15.4	IEEE 802.11ah	TS-UNB	LTE-M	NB-IoT	EC-GSM-IoT
RF Band	Unlicensed Sub-1 GHz 900 MHz	Unlicensed Sub-1 GHz	Unlicensed 2.4 GHz	Unlicensed Sub-1 GHz, 2.4 GHz	Unlicensed Sub-1 GHz	Unlicensed Sub-1 GHz	Licensed LTE	Licensed LTE	Licensed GSM
Standardization	SigFox Proprietary	LoRa-Alliance Proprietary	Bluetooth SIG Bluetooth 5.0	IEEE Std 802.15.4-2020	IEEE Std 802.11ah-2016	ETSI TS 103 357	3GPP Rel. 13	3GPP Rel. 13	3GPP Rel. 13

(1) Bluetooth and IEEE 802.15.4 may reach over greater coverage are through meshing.

(2) Meshing-topologies may experience higher latencies

APPENDIX 2. Link to original calculations and simulations

The many different calculations and simulations used in this work are available on the Author's GitHub –page:
https://github.com/vesamaki/MastersThesisSupplementaries

APPENDIX 3. Summary of feasibility evaluation

This table summarizes the results of the analyzed factors against requirements from Chapter 2 or in terms of rank in capability.

Table 32. Summary table of feasibility study.

			NB-IoT	LoRaWAN	TS-UNB
Coverage			✓	✓	✓
Interval	P1	3s	✓	×	×
		15s	✓	×	×
		60s	✓	✓	×
		600s	✓	✓	×
	P2	3s	✓	✓	×
		15s	✓	✓	×
		60s	✓	✓	×
		600s	✓	✓	✓
Data Rate	P1	3s	✓	×	×
		15s	✓	✓	×
		60s	✓	✓	×
		600s	✓	✓	✓
	P2	3s	✓	✓	×
		15s	✓	✓	×
		60s	✓	✓	✓
		600s	✓	✓	✓
Battery Lifetime	P1	3s	1st	×	×
		15s	1st	2nd	×
		60s	2nd	1st	×
		600s	2nd	1st	3rd
	P2	3s	1st	2nd	×
		15s	2nd	1st	×
		60s	2nd	1st	3rd
		600s	2nd	1st	3rd
Cost – S1	P1	3s	1st	×	×
		15s	1st	×	×
		60s	1st	2nd	×
		600s	1st	2nd	×
	P2	3s	1st	2nd	×
		15s	1st	2nd	×
		60s	1st	2nd	×
		600s	1st	2nd	3rd
Overall Ranking			1st	2nd	3rd